1974

Reduction Of Iron Ore In A Fluidized Bed By Hydrogen: The Problem Of Defluidization

John Frederick Gransden

REDUCTION OF IRON ORE IN A FLUIDIZED BED BY HYDROGEN: THE PROBLEM OF DEFLUIDIZATION

by

John Frederick Gransden

Faculty of Engineering Science

Submitted in partial fulfillment
of the requirements for the degree of
Doctor of Philosophy

Faculty of Graduate Studies
The University of Western Ontario
London, Canada
September 1973

ABSTRACT

The search for an economical method to reduce iron ores has often led to the consideration of a fluidized bed technique. In this process the reducing gas is passed upwards through a bed of finely divided ore at temperatures in the range 450-850°C. A major problem encountered is the tendency of the ore particles to stick to one another and cause defluidization (bogging) of the bed.

The work presented in this thesis investigates on a laboratory scale the reduction of iron ore in a fluidized bed, and in particular the cause of defluidization and some methods of prevention.

Reduction proceeds in a stepwise manner. The hematite particles are reduced to magnetite which in turn are reduced to wustite, then to iron. The iron phase alone was found responsible for bogging. With the experimental conditions used defluidization was observed at temperatures as low as 595°C when the bed was fully reduced. Nucleation of iron at the surface of particles and their growth into nodules (whiskers) of iron under certain reduction conditions led to defluidization shortly after the beginning of metallization.

The specular hematite ore used in the bulk of this work proved less susceptible to defluidization than an apparently similar hematite ore and reagent grade Fe_2O_3 particles. This was found to be due to a slime film on the particles which prevented iron-iron contact and changed the reduction morphology, preventing the growth of nodular iron. The active constituent of the slime film was shown to be silica, and the application of silica coatings to other ores ameliorated their defluidization properties, allowing complete reduction at temperatures as high as 840°C. The role of silica is discussed.

Other artificial coatings did not modify the reduction morphology and only produced, in general, a small improvement in the defluidization characteristics.

A solid state cell was used to monitor the gas phase composition in the bed during reduction. An anomaly in the gas utilization curves as iron nucleates was detected and is discussed.

ACKNOWLEDGEMENTS

I would like to express my deepest sense of appreciation to Professor J.S. Sheasby, my chief adviser, for his continued guidance and inspiration throughout this work. I also wish to thank the other members of the Material Science Group, Professors J.D. Brown, C. Roy, G.A. Geach, and I. Duerden for their encouragement.

Special thanks are due to Professor M.A. Bergougnou for continued advice.

The financial support of the National Research Council of Canada is gratefully acknowledged.

TABLE OF CONTENTS

LIST OF FIGURES

LIST OF TABLES

CHAPTER 1

INTRODUCTION

The blast furnace produces by far the greatest portion of iron ore reduction capacity in the world. The reasons for its prime position include its ability to produce large quantities of metal at low cost and to handle a wide range of iron ore compositions and its dependability. Research and development has improved tremendously and continues to improve the furnaces efficiency.

In certain situations other processes may be economical or desirable. For example, a large capital cost is required for a single blast furnace and its auxilliary equipment, and high grade coking coal must be available. A local market may not be great enough to utilize the large amount of iron produced from a single blast furnace, or coking coal may not be available while other forms of energy - gas, oil or electricity - are plentiful.

Processes other than the blast furnace are termed "direct reduction" processes and include reduction of iron ore in kilns, retorts, shaft and electric furnaces, and fluidized beds.

During benefication of ores (especially low grade ores) fine grinding is often necessary to liberate the iron

oxide from the gangue. The fluidized bed technique of reduction requires such small particle sizes. A reducing gas (e.g. H_2, CO, CH_4) is passed upwards through beds of finely divided ore imparting a circulatory motion to the particles. Some gas passes through the bed as bubbles and the general appearance is similar to that of a boiling liquid. Other processes including the blast furnace often required the extra step of agglomerating the fine grind by sintering or pelletizing before reduction.

Fluidized bed reduction is therefore attractive, but has its own limitations. A major difficulty has been the tendency for the ore particles to stick to one another causing defluidization or, as it is often called, bogging of the bed during reduction. When this occurs a major shut-down of the process is usually required to remove the bogged bed.

An early successful operation overcame this difficulty by operating at low temperature (500°C) and to increase the reduction rate to an economic level, high pressure (35 atmospheres). A high pressure operation has obvious cost penalties and in addition the product is pyrophoric. This has led a number of interested companies to seek ways of overcoming the defluidization tendency during reduction at high temperatures.

A literature survey indicated disagreement on the cause of bogging, a marked difference in the susceptability of ores of different origins to defluidize, and a number of patented techniques to curb this phenomena.

The object of the work reported in this thesis was to characterize the mode of reduction of iron ore in a fluidized bed, to determine the cause of defluidization and possible reasons why various ores behave differently, and to investigate some methods of prevention.

CHAPTER 2

REVIEW

2.1 The Iron-Oxygen and Iron-Oxygen-Hydrogen Systems

The Fe-O[1] and Fe-O-H[2] systems are shown in Figure 2.01 and 2.02 respectively. Iron forms three stable solid compounds with oxygen, $Fe_{1-y}O$ (wustite), Fe_3O_4 (magnetite) and Fe_2O_3 (hematite).

Wustite has a cubic lattice of NaCl type and may contain between 23.1 and 25.6% oxygen. This range does not contain the stoichiometric composition, FeO, and wustite always contains iron ion vacancies, electric neutrality being obtained by the formation of trivalent iron ions. Wustite is unstable below 570°C, where it decomposes eutectoidally into α-Fe and Fe_3O_4.

Magnetite also has a cubic lattice. The iron ions are distributed in the interstices of the close-packed cubic lattice of the larger oxygen ions. The unit cell contains 32 oxygen ions and 24 iron ions and has 64 tetrahedral and 32 octahedral interstices. Eight Fe^{3+} ions occupy tetrahedral and 8 Fe^{3+} and 8 Fe^{2+} occupy octahedral interstices. The magnetite lattice is similar to the wustite lattice in that the oxygen lattices correspond, but the arrangement and

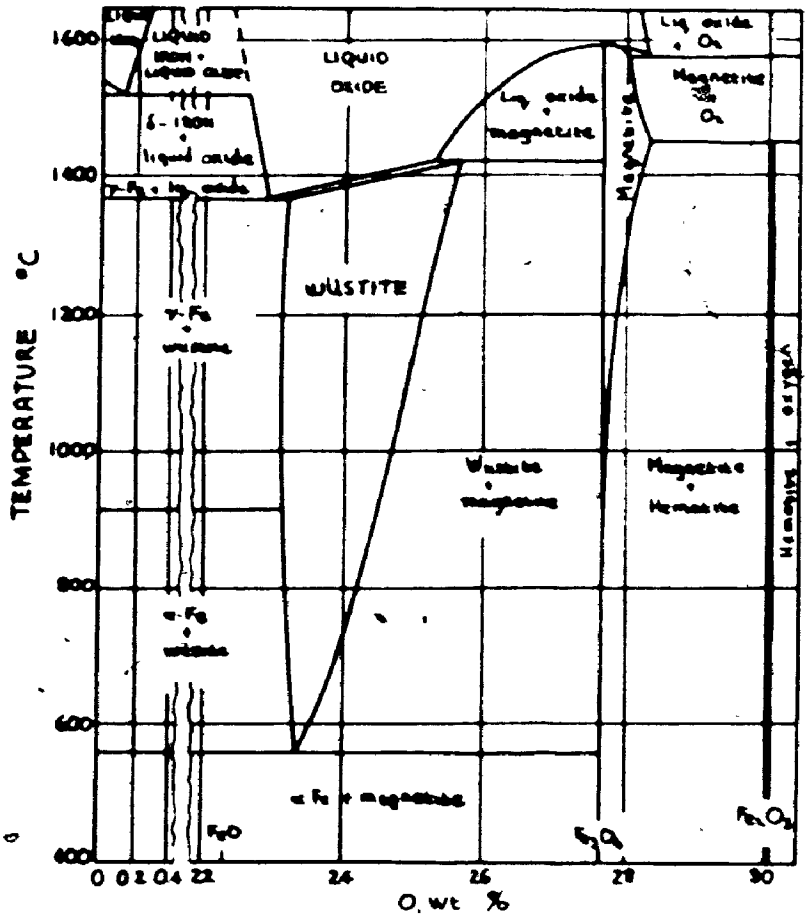

Figure 2.01 Iron-Oxygen Phase Diagram

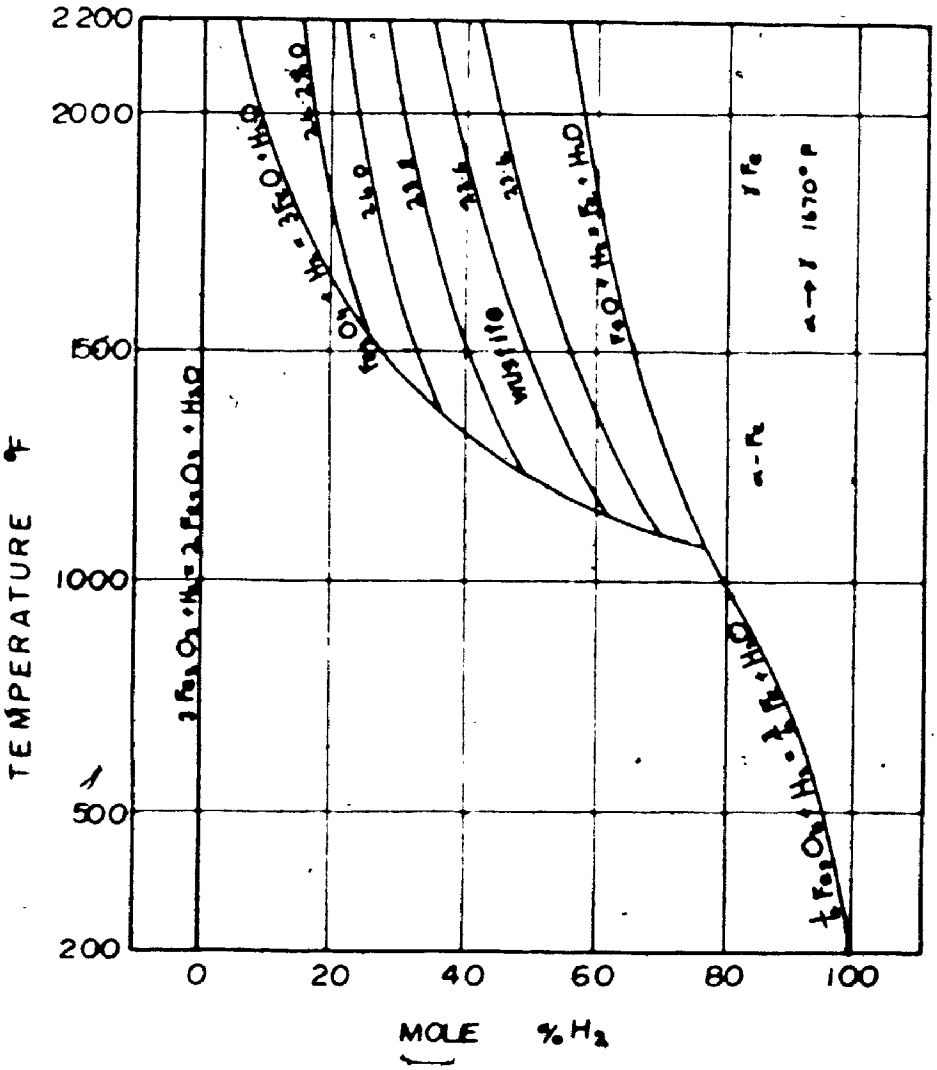

Figure 2.02 Iron-Oxygen-Hydrogen Equilibrium Diagram

number of iron ions differ. This similarity has been used to explain the observation that no or very little porosity develops when magnetite is reduced to wustite[3]. Magnetite is essentially stoichiometric at lower temperatures but at high temperatures, the lattice parameter decreases, with increasing oxygen content, indicating the presence of vacant positive lattice points, probably in octahedral positions[4].

Hematite may exist in two modifications. The most common form is α-Fe_2O_3 which has a rhombohedral corundum type lattice and a small oxygen deficit. The modification γ-Fe_2O_3 has a cubic spinel type lattice and is formed only under certain conditions, e.g. on oxidation of Fe_3O_4 below 400°C.

The equilibrium diagram for the iron-oxygen-hydrogen system shows that it is theoretically possible to reduce hematite and magnetite to iron at any temperature and that below 570°C wustite will not be formed.

2.2 Mechanism of Reduction of Iron Oxides

During the gaseous reduction of hematite, hematite, magnetite, wustite (above 570°C) and iron often co-exist. The excellent work and photomicrographs of Edstrom[4] clearly show this. The hematite core is surrounded by successive concentric layers of magnetite, wustite and iron. This reduction morphology is termed topochemical and, as discussed later, forms only under certain conditions. Its occurrence is believed due to the gas-solid reaction taking

place primarily at the iron/wustite interface, the other oxides being formed by the inward migration of iron ions due to the iron activity gradient.

2.2.1 Reduction Mechanism of Iron Oxide Pellets

It has long been recognized, as the review of Themlis and Gauvin[5] shows, that the gaseous reduction of iron ore may be controlled either by a transport process or by chemical reaction at a phase boundary. The complexity of the reduction process has led many workers to investigate experimentally and mathematically the reduction of a single pellet in a stream of reducing gas.

In experiments of this nature the loss in weight of a pellet while undergoing reduction is monitored at different temperatures, pressures and reducing gas compositions. In addition the size and porosity of the pellet may be varied. The gas flow rate is chosen to be greater than the "critical flow rate", above which the overall reaction is not limited by the supply of reducing gas.

Lu[6,7], Levenspiel[8], St. Clair[9], Seth and Ross[10] and Spitzer, Manning and Philbrook[11] amongst others have formulated equations describing the chemical and mass transport processes. In the "dense" pellet model of Spitzer et al[11] the resistance to the reduction of a single pellet is considered to be due to the following five steps:

1. transport of gaseous reactant from the bulk gas phase through the boundary layer to the outer surface of the particle.

2. diffusion of hydrogen or carbon monoxide through the porous iron layer to the iron/wustite interface.

3. chemical reaction of the gas with the oxide to form iron and a gaseous product.

4. outward diffusion of the gaseous product through the iron layer.

5. transfer of the gaseous product from the outer surface to the bulk gas phase.

Steps one and five are termed the gas film resistance, 2 and 4, the shell-layer resistance and 3, the interface resistance. The chemical reaction is envisaged as only taking place at the iron/wustite interface, the wustite and magnetite phases being formed by the inward solid state diffusion of iron. If either step is wholly rate controlling then differing reaction rate versus time plots result, so in theory it should be possible to distinguish the rate controlling mechanism. If step 3, the chemical reaction is the rate determining step, then it can be shown that the rate of advance of the iron/wustite interface should be linear with time. This led McKewan[12-17] to postulate that the chemical

reaction was the slowest step as his data for the most part, showed this relationship. Themelis and Gauvin[18] and Quets, Wadsworth and Lewis[19], amongst others supported this belief. On the other hand, Udy and Lorig[20], Bogdandy and Janke[21], and Kawasaki et al[22] found their results best fitted the postulate that the shell resistance is the rate controlling step. Lu and Bitsianes[23] reduced cylinders to hematite from one end only and found the iron grew according to a parabolic relationship, so showing the importance of gaseous diffusion. A similar result has been obtained by Turkdogan and Vinters[24] who reduced unidirectionally, hematite packed in silica tubes.

Warner[25] has demonstrated the importance of diffusion across the boundary layer by suspending a pellet asymetrically in the reduction tube, whereupon the reaction proceeded asymetrically. He suggested that the establishment of a "critical" gas velocity only assures that the reduction is not being "starved" of reducing gas by a significant concentration of the gaseous product in the bulk gas phase.

Spitzer et al[11] considered all three resistances and showed how a nearly linear advance of the iron/wustite interface, as observed by McKewan could occur if all three resistances assumed some importance. In a later paper[125], the same authors considered the gaseous reduction of a porous pellet the reaction then occurring at all the advancing interfaces (iron/wustite, wustite/magnetite, magnetite/hematite). In

this model the reaction occurs through a series-parallel combination of transport and chemical steps. They found that this model predicted more accurately the movement of the magnetite/wustite interface than the dense pellet model in which this interface is formed by the solid state diffusion of iron.

Seth and Ross[10] and Seth[26] formulated a general rate equation neglecting the boundary layer resistance. They showed that in the limiting cases of chemical and transport control the time to reach a certain degree of reduction R should be proportional to

$$[1 - (1 - R)^{1/3}] \quad \text{and} \quad [1/2 - R/3 - (1 - R)^{2/3}/2]$$

respectively

By reducing hematite pellets of varying diameter they were able to estimate the relative importance of the chemical and shell resistance. The results show that for hydrogen reduction at one atmosphere pressure the relative contribution of gaseous diffusion increases with increasing particle size, degree of reduction and temperature.

Gray and Henderson[27] investigated the reduction of natural and synthetic hematite pellets of diameter 10 mm and less from a number of sources and found that above 570°C, when wustite is stable, reduction is not completely topochemical. The magnetite forms a concentric layer around the hematite core followed by a layer of dense wustite, then

porous wustite with iron lining the pores. Eventually the magnetite and hematite layers are consumed leaving porous wustite and iron, the iron completely surrounding the wustite. The reduction of these "islands of wustite" leads to a lower reduction rate. The authors suggest that complete topochemical reduction only occurs in artificially made pellets and that a generalized rate equation based on this mode of reduction is therefore incorrect.

The occurrence of "islands of wustite" as described above has been observed by Strangway and Ross[28] when reducing magnetite pellets. In a later paper Lien, El-Mehairy and Ross[29] suggest that the occurrence of this morphology is responsible for the rate minimum often observed around 700°C when reducing iron oxide. Their argument includes the experimental fact that the onset of the rate minimum occours when substantial "islands of wustite" are retained in the iron layer and that their reduction, which must proceed by solid state diffusion through the nonporous iron surrounding them, noticeably slows the overall reaction rate.

2.2.2 Reduction of Small Particles

Themelis and Gauvin[18] analysed the reduction data of their own work on Canadian ores and other workers data for particle sizes 5 cm down to 200 μm and concluded that if the diffusional resistance through the gaseous boundary layer is not rate controlling, then the reduction may be considered

to be governed by the reaction rate at the interface between the reduced and unreduced layers. In a later paper the same authors[30] showed this was also true for particle sizes down to about 50 μm. Below this size they considered a two dimensional surface phenomenon was rate controlling.

More recently Turkdogan and Vinters[24,31] studied the reduction of a high grade hematite ore in pure hydrogen at temperatures between 200° and 1200°C, and particle size between 300 μm and 1.5 cm. The sample was spread flat on a platinum basket to prevent gas starvation. They found the rate of reduction passed through a minimum between 500° and 800°C, which was more pronounced the smaller the particle size and the greater the amount of reduction. On the basis of their rate data and metallographic examinations the authors believe there are three possible rate controlling processes applicable over the range of variables studied.

At low temperatures and with small particle sizes, porous wustite particles were produced with "rosettes" of iron occurring throughout the particle. This was called internal reduction and considered to be a limiting case when gas diffusion in the pores of the oxide is rapid and the rate is controlled primarily by the reaction of hydrogen on the pore walls. In this case the rate of reduction is independent of particle size.

With large and dense particles and particularly at high temperatures gas diffusion is comparatively slow and the

reaction takes place essentially at pore mouths only on the outer surface of the particle. The reduction morphology is then topochemical, i.e. a porous layer of iron is formed around the unreacted core. If the iron layer is sufficiently thin the gas diffusion through it is rapid and the rate of reduction is controlled jointly by the gas diffusion in the pores and the reaction on the pore walls. In this case there will be partial internal reduction slightly ahead of the nominal iron/wustite interface and the time for reduction will be proportional to the particle radius.

The third rate controlling process occurs when the iron has reached a substantial thickness and the gas diffusion within the pores of this layer assumes control of the reduction process. If the reduction is controlled solely by this process then the time for reduction will be proportional to the square of the particle radius.

The last mentioned process fitted well the data of Turkdogan and Vinters for particle sizes larger than 7 mm between 50 and 95 or 99% reduction.

2.2.3 Nucleation of Iron

In theory, and of considerable importance under some experimental conditions, the steps through which the reaction proceeds may be further broken down. A step of importance in the present work, and included in the analysis of Engell[32] is the formation of nuclei of the next phase in the reduction

sequence, in particular nuclei of iron forming in porous wustite. Ions of iron formed by the chemical reaction and electrons must migrate to the iron nucleus where the following reaction takes place:

$$Fe^{++} + 2e \rightarrow Fe$$

Wagner[33,34] has discussed the reduction and formation of nuclei in various non-stoichiometric oxides and sulphides. In the case of wustite, as reduction proceeds an increase of the metal/oxygen ratio occurs by filling cation vacancies and decreasing the number of cations in higher valence states. Eventually the outside phase becomes supersaturated with respect to the metal and nucleation occurs.

Using a potentiostat Schmalzried and Wagner[35] were able to measure the supersaturation that occurs before nucleation in silver sulphide. They observed that the nuclei grew up from the surface of the AgS pellet to form whiskers. The reduction of wustite may be considered analogous to AgS.

Sasabe[36] et al found "point-like irons" grew from dense wustite reduced in a slow stream of hydrogen in the temperature range 600 to 1,000°C. The number of "point-like irons" or nodules grew with time until the surface was covered after which the reduction rate decreased.

Theoretically the treatment of nucleation originally developed by Volmer et al[37] for formation of nuclei from a

vapour, may be applied to nucleation in the solid state. In this theory the energy liberated by the new phase forming from the supersaturated phase balances the phase boundary energy created by its growth at some critical nucleus size. Below this size the nucleus is unstable while above it can freely increase further in size as the energy liberated is greater than that expended in creating an increase in phase boundary area. Engell[38] has discussed the application of nucleation theory to the problem of nucleus formation in iron oxides.

Qualitatively we may expect nuclei formation to take place preferentially at any areas of strain in the lattice (line or point defects for example), as the energy released aids stable nucleus formation[39]. This is called heterogeneous nucleation.

Many investigators have reported incubation times before the onset of reduction when reducing magnetite to iron at low temperatures (200 to 500°C). Perhaps the most extensive study concerning the influence of iron nucleation on the reduction rate of hematite, magnetite and wustite at low temperatures is that of Morawietz and Schaefer[40]. These authors reduced very porous specimens, and for hematite reduction by hydrogen above 350°C found the rate of reduction passed through a minimum when the oxygen to iron ratio was about 1.33. Analysis showed that before the minimum no metallic iron was present while after no hematite was present,

suggesting that while hematite is reducing the gases inside the pellet are too oxidising to produce the supersaturation of iron needed for nucleation of the iron phase. After the minimum the reaction rate increased slowly and this was believed to reflect the slow growth of the number of nuclei.

If the reducing gas contained additions of water vapour the reaction rate was further slowed and when the water vapour hydrogen ratio reached about 80% of the equilibrium value (for reduction at 350°C) the reaction was completely stopped, that is iron was unable to form.

At higher temperatures Botticher, Bogdandy, Forster and Schierloh[41] have studied the significance of iron nucleation in the reduction of wustite. Their experimental technique involved reducing 40-60 μm hematite particles to wustite of constant defect structure (i.e. concentration of iron vacancies) in the temperature range 700-900°C. The wustite was then further reduced at 700°C after annealing for various times in the temperature range 700-900°C.

They considered that when the phase boundary reaction is rate controlling the reduction rate, after allowing for the change in reaction area, should be independent of time. Any deviation at the beginning of reduction was thought to be due to the formation and initial growth of nuclei and the time taken before a straight line relationship was realized (t_k) was taken as a measure of the nucleation hindrance. The reduction to wustite produced a distorted lattice which

was changed by annealing before the reduction to iron at 700°C and measured using a technique based on the half height width of the peaks of the wustite diffraction pattern. The authors found a good correlation between the "apparent lattice distortion" measured in this way and t_k. They also showed that as the oxygen potential of the reduction mixture approached the equilibrium oxygen potential of the iron/wustite, t_k increased and the number of nuclei, observed after 25% reduction, decreased. It was found that the rate constant of the phase boundary reaction was approximately independent of the lattice distortion.

Using a similar experimental technique Forster, Schierloh and Smeets[42] have shown that the nature of the reducing gas effects the nucleation hindrance probably by changing the surface free energy through adsorption. They found that using a reducing gas of fixed oxygen potential but varying the hydrogen/carbon monoxide ratio, t_k decreased as the hydrogen concentration increased. In addition t_k was larger if nitrogen was used as a diluent instead of argon, all other parameters remaining constant.

At still higher temperatures Stotz[43] determined, by measuring the variation of the electrical conductivity of wustite specimens during reduction by CO/CO_2 mixtures at 900°C, that the iron activity in the oxide before nuclei begin to form does not exceed 1.015. This corresponds to a CO/CO_2 ratio about 97% of the equilibrium value.

2.2.4 Effect of Impurities On Iron Oxide Reduction

The effect of impurities or additives on the reduction of iron ores has been of constant interest to investigators as all ores contain foreign elements to varying extents. Recently the possibility that the presence of certain elements may influence the swelling characteristics of iron ore pellets during reduction (leading to degradation of the burden in the blast furnace) has led to increased interest.

Calcium compound additions have long been known to increase the rate of reduction of iron oxide sinters[44,45]. Doi and Kasai[46] considered that lime helps to break up hard-to-reduce compounds such as fayalite and illmenite. Schenck et al[47] suggested that the increased rate could be due to the instability of wustite in the presence of calcium oxide:

$$2CaO + 3FeO \rightarrow Fe + Fe_2O_3 \cdot 2CaO$$

Seth and Ross used this mechanism to explain their experimental results[48]. The dicalcium ferrite formed has a reducibility similar to hematite[49] and on reduction yields iron and calcium oxide which is free to dissociate more wustite. Strangway and Ross[50] found calcium carbonate additions increased the reduction rate and attributed this finding to the above mentioned mechanism and to the increased porosity formed during the sintering and reduction of the pellets.

Khalafalla and Weston[51] investigated the effect of Li, Na, K, B, Mg, Ca, S, and B compound additions on the reduction kinetics of wustite by CO at 1,000°C. The results showed additions of 0.69 atomic % accelerated the reduction rate to an extent proportional to the ionic radius and electronic charge of the added metal iron. These authors explained the result as being due to lattice disturbances (created by the foreign metal irons occupying interstitial positions in the wustite lattice) increasing the number of active centers for the surface reaction by providing new adsorption sites. The divalent ions produced a greater enchancement of the rate than singly ionized atoms as more vacancies are present in the lattice (to conserve electroneutrality). They further found that increasing the impurity concentration accelerated the reaction up to a maximum point beyond which further increases exerted a deleterious effect on the reaction rate which may be attributed to slag formation.

Lahiri[52] criticized the interpretation of Khalafalla and Weston in that, among other inconsistencies, the added metal ion would be expected to substitute for Fe, rather than going to interstitial sites. He shows the increase rate of reduction with additives of groups I and II oxides may be explained by a lowering of the Permi level in the crystals while group III additions should raise the Fermi level and decrease the reduction rate. This later result was found by Levin and Wagner[53] using Cr_2O_3 additions, who attributed the decreasing rate to either an increase in vacancy concentration

which slows the vacancy diffusion rate or an accumulation of Cr at the surface due to its diffusion rate being slower than that of Fe ions.

Lien, El-mehairy and Ross[54] and Strangway et al[55] found that 3 mole % additions of alumina or lime in magnetite eliminated the rate minimum mentioned previously and thus the reaction rate was increased. Similar additions of silica decreased the reaction rate significantly (about 40% at 25% reduction at 700°C), as did titania, to a lesser extent, while magnesia did not have any noticeable effect.

Geiger and Wagner[56] also observed a decrease in the reduction rate when reducing hematite to magnetite with additions of titania and an increase with additions of lime.

In a previous section evidence that the reduction rate of wustite might be slowed by the nucleation and growth of iron was presented. Morawietz and Schaefer[57] proposed that the addition of nucleating agents may accelerate the reaction rate and showed that the additions of small amounts of copper iron, nickel oxide and cobalt oxide powders had such an effect.

2.3 The Fluidized Bed Reduction of Iron Ore

2.3.1 The Fluidized Bed

When a gas is passed upwards through a bed of particles the bed expands as the flow is increased. At a certain flow rate, when approximately the pressure drop across the bed is

equal to the bed weight per unit area, the particles become agitated and adopt a circulatory motion. Increasing the flow rate further brings about more rapid motion of the particles while the pressure drop across the bed increases only slightly. Bubbles of gas are observed rising through the bed giving the appearance of a boiling liquid. This phenomenon is termed aggregative fluidization. In particulate fluidization, which occurs mostly with water-solid systems no bubbles are formed.

The domain of existence of a fluidized bed is small. The solid particles must not be so large that unrealistic flow rates are required for fluidization nor too small (10 μm) when balling is observed. Balling occurs when the free surface area and therefore the interparticle attractions are large. Particles of size between 1 μm and 64 mm may be fluidized but the optimum size is around 10-250 μm[59]. The gas velocity must be above the minimum fluidization velocity but below a value that transports the particles upward continuously, a value that can be identified as the free fall velocity of the particles in that particular gas. Singh and Bhat[58] have reported on the minimum fluidizing velocity for hematite air systems and V. Bogdandy[59] has defined the domains of existence of a fluidized bed at 700°C for hydrogen and carbon monoxide gases and hematite particles of various sizes.

Slugging occurs in the fluidized bed when bubbles grow to the size of the containing vessel before bursting at the free surface. In a poorly fluidized bed channeling may occur, that is the gas passes through the bed along preferred paths. Bubbles, slugging and channeling give rise to poor gas-solid contact and therefore conversion rates and hence reactors are designed and operated to suppress the last two mentioned phenomena.

Fluidized beds operate close to isothermal conditions as the turbulence of the particles disperses hot and cold spots, the solids have a high heat capacity relative to the gas, and the heat transfer rates are high due to the large transfer surface per unit volume[60]. In addition the turbulence assures good mixing of the particles.

A major disadvantage of the fluidized bed is that the particles have a circulatory motion in the bed and counter flow of gas and solid, necessary for optimum yield, does not occur (unlike for example the blast furnace). This difficulty can be partially solved by arranging a number of fluidized beds on top of one another, the topmost discharging into the one beneath it and so on. Meissner and Schora[61] have shown theoretically the advantage of such a system.

The first major industrial application of the fluidized bed principle was the Winkler generator for gasification of coal. Perhaps the most important application today is its use for the catalytic cracking of petroleum where it has been employed since 1942. Other uses include the roasting

of ores, calcination of limestone, the drying of solids and the coating of metals with plastic to name only a few. The International Nickel Company of Canada makes use of fluidized beds to roast nickel sulphide to oxide, to volatilize and remove copper and other impurities from the oxide by contact with chlorine, and finally to reduce the oxide to nickel by hydrogen gas[62].

2.3.2 Laboratory Investigations of Reduction of Iron Ore in Fluidized Beds

Considering the reduction of hematite in a single bed reactor, the amount of ore is large compared to the instantaneous volume of gas in a reactor. The H_2/H_2O ratio would then be expected to approach the equilibrium concentration for the particular iron oxide-gas system at some point in the bed. The higher the temperature and bed height and the lower the gas velocity or particle size the closer the approach to equilibrium to be expected. Expressed differently the rate controlling step is the rate of supply of gas and the reduction rate increases as the flow rate increases. Bhat and Whitehead[63] showed the percentage instantaneous hydrogen utilization varied in a stepwise manner with time, the steps corresponding to the reduction of Fe_2O_3 to Fe_3O_4, Fe_3O_4 to FeO and FeO to iron. For each step the value of the gas ratio (H_2/H_2O) was nearer to the equilibrium value the higher the temperature.

As the gas flow is rate controlling, and the range of particle sizes that can be employed is relatively small, the rate of reduction is practically independent of particle size[63-65] and porosity[66]. In addition the increase in reduction rate with increasing temperature observed, mainly reflects the increase in the concentration of water in equilibrium with the various oxides at higher temperatures and such increases are relatively small compared to those expected for single particles in gas streams[67] (when the gas flow rate is not usually rate controlling).

In practice, the nearer equilibrium is approached the more efficient the operation. The formation of bubbles leads to bad solid/gas contact and the possibility that a substantial fraction of hydrogen passes through the bed without reacting. Osberg and Tweddle[68] have shown that wire mesh cylinders help break up and control the growth of bubbles and that the reduction rate is increased most noticeably at low temperatures (575°C). Agarwal and Davis[69] have experimented with horizontal and vertical baffles to achieve the same end. Using a different approach Okura and Lu[70] studied the reduction rate in a fluidized bed with intermittent gas flow. The on-off cycle was varied between 1/8 and 1 second (with equal on-off duration), and an enchanced gas utilization realized (especially at low temperatures) due to the more particulate nature of the fluidization.

Feinman and Drexler[71] have proposed a model for reduction in a steady state fluidized bed and analyzed their data accordingly. Feinman[64] has obtained kinetic data from simulations of two and three bed reactor systems and shown the three bed system is more productive and has reported the effects of mass flow and pressure on the reduction rate.

The tendency of particles to stick to one another during reduction was made use of by Langston and Stephens[72] who added fine hematite (100% below 40 μm) to a fluidized bed of iron particles 300-840 μm in size. The fine particles were reduced and stuck to the larger particles which gradually grew in size.

Ezz[73] has described the development of a small five bed pilot plant for reducing iron ore in which a certain portion of the reducing gas is burned to supply the necessary heat.

2.3.3 Commercial Processes

Only a few of the many proposals for iron ore reduction in fluidized beds have been developed industrially.

The H-iron process[74-77] (developed by Hydrocarbon Research Inc., and Bethlehem Steel Co.), operates at high pressure (36 atmospheres) and low temperature (500°C). The iron ore is reduced in two beds (a third preheats the ore) by hydrogen. Carbon monoxide is not used as a reducing agent

as carbon would be formed at this low temperature according to the Boudouard reaction. The high pressure employed somewhat increases, the reduction rate which is slow at 500°C and one atmosphere pressure, and allows a greater mass flow rate of gas, so increasing the conversion per pass. Lubker and Bruland[74] have described 20, 50, and 120 tons/day plants which have operated. Traub[75] has reported on the 50 tons/day installation in more detail.

The Nu-iron process[69,78,79] (developed by the United States Steel Corp.) employs three beds, hydrogen, a reaction temperature between 600 and 700°C and moderate pressure (2 atmospheres). Reed et al[79] have described the development of a pilot plant, and Agwarwal and Davis[69] have reported on the fluidization and reduction characteristics of an 18" reactor. This process is the only one that has been used on a significant industrial scale - it is the heart of an installation dubbed H.I.B: (High Iron Briquettes) in Venezuela which produces one million tons of iron briquettes annually[80]. The beds are 22 feet in diameter and the product is 86.5% iron[81].

The Esso Research - Little Process[82], later renamed Fior[83], operates at high temperature (870°C) and low pressure (1-2 atmospheres). Hyde[82] has described the operation of a 5 ton/day pilot plant and a 300 ton/day unit operated for some time in Nova Scotia but is now shut down[84].

Little information is available on the Novalfer-Onia process. Bogdandy[85] has described a 60 tons/day plant that operates with two stages each having two fluidized beds.

2.3.4 The Problem of Defluidization

The occurrence of defluidization, (commonly termed 'bogging'), in a commercial reactor is to be considered a gross malfunction necessitating shut down, cooling and probably the manual removal of the defluidized bed. A knowledge of the variables effecting the tendency of a bed to defluidize is therefore essential. The results of previous investigations on these variables is presented below under separate headings.

1. Temperature: In general, authors agree that if other conditions are held constant, increasing temperature increases the tendency towards defluidization. Ezz[66] using a one inch diameter bed investigated a number of different ores and found that none defluidized during reduction at 500°C. At 700°C bogging occurred in each ore at a different degree of reduction.

Osberg and Tweddle[68], using a Labrador iron ore, encountered sticking only above 650°C. Winzer[86], using a hematite of particle size 60-100 μm found that complete defluidization occurred at all temperatures above 450°C and was only dependent upon time. At 450°C the time for defluidization was about 24 hours, while at 700°C only a few minutes was

required. Yamamichi[87], when operating a 35 cm reactor at 700°C encountered bogging but fluidization was uninterrupted at 600°C. Agarwal and Davis[69] report that there was little tendency for defluidization to occur below 620°C, that between 620°C and 730°C the susceptability to defluidization was the highest, while above 730°C the tendency to stick is diminished.

2. Flow Rate: All authors agree that increasing flow rate diminishes the tendency for a bed to defluidize. For example, Ezz[66] determined that the percentage reduction at which bogging occurs, which was different for different ores at the same flow rate and temperature, increased with increasing flow rate.

3. Particle Size: The literature agrees that increasing the particle size diminishes the tendency of the ore to bog. Jolley[88] was awarded a patent which was concerned with controlling the particle size in the fluidized bed with a view to increasing the gas efficiency and preventing defluidization. He claimed that too many fines or too few fines increase the possibility of defluidization. In another patent, Mayer and Roberts[89] claimed a process in which large particles - at least twice as large as is present in the bed at the start - be added to the bed, to prevent a "maximum density aggregate" (i.e. a wide particle size distribution in which the voidage is low) from forming which increases the tendency of the bed to bog. In addition they claimed these large particles also tended to break up

agglomerates.

4. Composition: A number of workers have found that impure ores are less susceptible to bogging than high grade ores. However the susceptibility to defluidization cannot be determined by a simple chemical analysis and is shown by the results of Brown et al[83] who list ten different ores and their sticking tendencies. Gray and Maak[90] claim that defluidization is most severe when reducing specular hematite ores for example, Carol Lake concentrate.

5. Extent of Reduction: Some authors have found that sticking and defluidization occur when the material in the bed is highly reduced, i.e. mostly iron. Others have encountered it at various stages of reduction. For instance, Hyde[82] and Whalley[91] concluded that sticking occurs in the 20-50% metalization range and that excessive temperatures should be avoided in this range, while Ezz[66] found that bogging of a particular ore occurred at various degrees of reduction which depended upon temperature and gas velocity.

6. Reducing Gas: Whalley[91] and Gray and Maak[90] found that defluidization was more acute when using pure hydrogen than when a hydrogen-carbon monoxide mixture was employed.

The reasons for defluidization of a bed of iron ore undergoing reduction put forward by authors are usually vague.

Ezz[66] believes that iron at elevated temperatures is inherently sticky and that the more iron on the surface of the particles the higher is the likelihood of defluidization. He considers this explains the effect of temperature, particle size, gas velocity and the "smoothness" of particles that he observed. Whalley[91] attributes bogging to a transient phase of low softening temperature but gives no further details. Mayer et al[89], Gray and Maak[90] and Bailey[92] consider that defluidization occurs due to the growth of iron whiskers or nodules which stick to other particles forming agglomerates.

2.3.5 Prevention of Defluidization

Bhat and Whitehead[63] diluted beds of ore with silica sand of similar particle size and found that a sand :: ore ratio of 2:1 prevented defluidization at 800°C. Ezz[66] found that covering the ore particles with carbon and calcium oxide of particle size less than 1 micron stopped bogging at lower temperatures but was ineffective at 800°C. Osberg and Tweddle[68] who encountered sticking above 650°C found that a five weight percent addition of brucitic limestone overcame defluidization between 700 and 800°C, while similar additions of coke and silica were not fully effective. Johnson and Engle[93] were awarded a patent concerned with preventing defluidization by adding 0.15-3.0% graphite to the ore. Schenck et al[94] investigated the possibility of reducing

fine iron ore suspended in a fluidized bed of coke and was able to operate at a temperature of 1,000°C without any sticking problems. Sterling[95] claimed a process in which the iron ore is soaked in a solution of a compound which after drying, leaves the particles coated by the compound. Compounds are chosen which decompose while the ore is being reduced to give a metal oxide coating. A similar method patented by Bailey[92] involves applying such a coating by means of a slurry.

In a patent awarded to Gray and Maak[90], the authors considered that the growth of whiskers or nodules of iron are the prime cause of defluidization and found that their growth could be stopped by partially reducing the ore at low temperatures (485-560°C) when an iron layer is formed on the outside of the particles. They found that after pre-reduction, the reduction temperature could be as high as 770°C without defluidization occurring while without pre-reduction defluidization occurred in 11 minutes at this temperature.

The methods of preventing defluidization of Jolley[88] and Mayer and Roberts[89] which involve controlling the particle size distribution in the fluidized bed have already been mentioned.

CHAPTER 3

EXPERIMENTAL METHODS

3.1 Ores Investigated

The ore used for most of this study was a high grade specular hematite concentrate supplied by Imperial Oil Enterprises Limited, Halifax, Nova Scotia. It assayed (dry basis) 66.5% Fe with 4% insolubles. After sieving to obtain the required particle size the ore was washed in a water fluidized bed to remove small particles clinging to the large particles.

The reduction of Carol Lake concentrate (specular hematite) and an Australian goethtite ore were also investigated.

For comparison "pure" Fe_2O_3 particles were prepared in the following manner and reduced. "Fisher" reagent grade Fe_2O_3 was pressed into pellets 1/4 of an inch high in a 1 inch die at a pressure of 15,000 psi. The green pellets were sintered for 12 hours at 1200°C in air and then crushed to the required particle size.

3.2 Reduction Apparatus and Procedure

3.2.1 The Reactor

The fluidized bed reactor (Figure 3.01) was a silica tube 2.5 cm. internal diameter and 100 cm. long. The distributor plate was a silica frit of porosity 50-60 μm situated about 30 cm. from the lower end of the tube. Gas tight connections to the tube consisted of brass caps each with two "O" rings. The bed was heated externally by a vertical tube furnace, wound non-inductively, with an observation port level with the top of the bed. Two gas trains, one for hydrogen and one for nitrogen containing flow regulators and flowmeters met at the entrance of the reactor. The pressure was monitored at this point by a manometer containing dibutyl phthalate. The gases were dried with anhydrite but not further purified.

Two chromel-alumel thermocouples were positioned 2 cm. from the frit. One controlled the input of current to the furnace through a proportional controller and power supply and the other was used to measure the bed temperature.

3.2.2 Fluidization Meter

To obtain a constant measure of the degree or quality of fluidization of the bed, a fluidization meter was developed. This consisted of a fine silica rod about 300 μm in diameter suspended from an induction force transducer (Sanborn Model

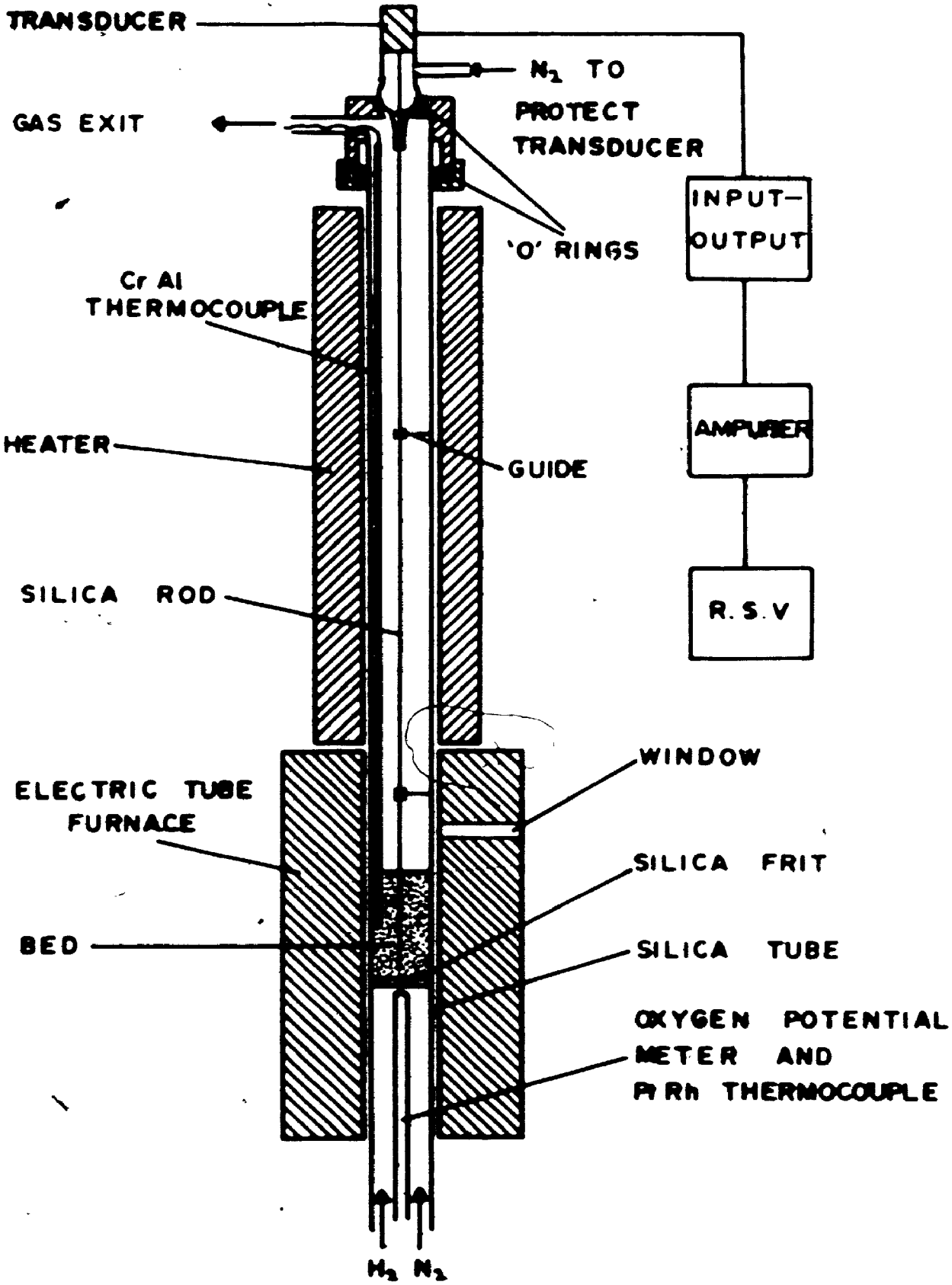

Figure 3.01 Schematic Diagram of Fluidized Bed Reactor

FTA-1-1) capable of measuring forces in the range ± 1000 dynes. The transducer was attached to a ball joint and the silica rod passed through a small diameter nozzle through two guides in the silica tube and extended through the bed to within 2 mm of the distributor plate. The transducer was protected from small particles by passing a small flow of nitrogen through the nozzle. The bubbles formed in the bed and the general movement of the particles created fluctuating forces on the silica rod which were measured on the transducer output indicator. A spectral analysis indicated that most of the bed energy was in the frequency range 0.5-1 Hertz.

During a reduction run the transducer output was amplified and measured on a random signal voltmeter which had a time constant of 4 seconds. This produced a steady reading on the r.s.v. related to the degree of fluidization.

In addition to providing a measure of the degree of fluidization during reduction, the fluidization meter proved useful in the following ways.

1. In the selection of a flow rate for reduction, a suitable degree of fluidization was obtained at room temperature when the entire bed could be observed. At the reduction temperature the flow of hydrogen was then adjusted until the same degree of fluidization was indicated by the meter.

2. If a fixed mass flow rate of gas is used the degree of fluidization will vary with temperature. Using the fluidization meter the degree of fluidization could be adjusted to a standard value by increasing or decreasing the flow.

In practice it was found that this adjustment did not alter the defluidization phenomena significantly so that a flow of 20 ml/second of hydrogen at S.T.P. was used in all the runs reported. This gave an empty tube velocity of 14 cm./second at 700°C.

3. When nitrogen and hydrogen mixtures were used the flows could be adjusted to the same degree of fluidization as that used for the reduction by pure hydrogen.

Defluidization was also followed by observing the pressure difference across the bed on the manometer.

3.2.3 Procedure

Batches of 80 grams of iron ore of particle size 210-250, 105-140 and 74-140 μm were used, giving a static bed height of about 6.2 cm. The apparatus was heated with the bed fluidized by nitrogen until the stable required temperature was achieved, whereupon the flow was changed to hydrogen.

The water produced by the reaction was collected in a measuring cylinder held beneath a condenser, containing an ice/water mixture, in the exhaust line. The upper half of

the apparatus was maintained a little above 100°C to avoid water vapour condensation before the condenser.

At the end of a run the bed was quickly cooled by raising the furnace.

3.2.4 Metallographic Examination

Particles were placed on a glass slide and a short length of acrylic tube placed around them. "Bioplastic" was poured into the mould and after the resin had set at room temperature and cured for 2 hours at 65°C, the slide was removed. The sample was then ground on 600 silicon carbide paper, polished on a napless cloth (to diminish relief polishing) with 6 and 3 μm diamond paste and finally polished with 0.3 μm alumina.

Specimens for scanning electron microscopy (S.E.M.) examination were mounted on copper blocks with "Dag" dispersion No. 420 (Acheson Colloids) - a water base colloidal silver. A conducting film of carbon on the particles was found to be necessary only when they consisted primarily of hematite or Fe_3O_4.

3.3 Reduction Apparatus with Solid State Cell and Sampler

The interesting morphology of reduction of the particles found by stopping the reduction during runs in the previous apparatus, led to the construction of a modification

of the apparatus in which small samples could be withdrawn during reduction at well defined points in the reduction.

Basically the apparatus consisted of a device to withdraw samples from the bed and a zirconia solid state cell to monitor the oxygen potential of the gas in the bed. The reactor was essentially unchanged except its length above the frit was shorter so the cell could be immersed in the bed. The apparatus is shown diagrammatically in Figure 3.02.

Sampler

A diagram of the sampler is shown in Figure 3.03. Two short rods about 2 mm. in diameter and 2 cm. long were silver-soldered, one at the end, the other 8 inches from the same end to a long rod of slightly smaller diameter. The rod was made of push-pull fit inside a tube silver-soldered to the top copper end cap of the apparatus. A 1 mm. diameter hole half an inch from the end of the rod filled with particles when the rod was lowered into the bed. On raising the rod the samples were quenched in the off gas and were then extracted through a hole in the tube by the sample getter. This consisted of a squeeze bulb which sucked air through a piece of cotton wool on which the sample was caught. In this way, a sample consisting of a few hundred particles could be obtained at any time during a reduction run.

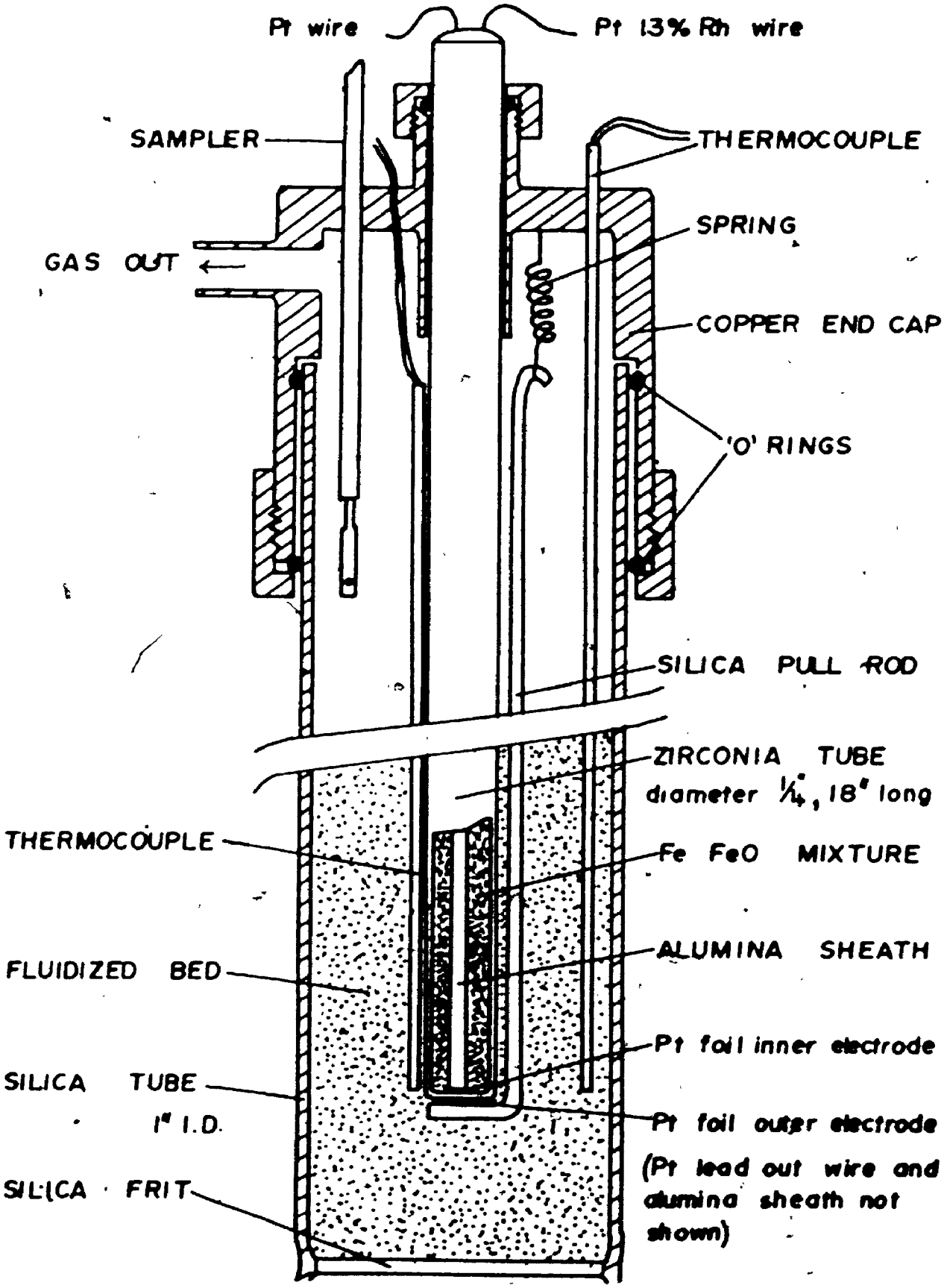

Figure 3.02 Schematic Diagram of Solid State Cell and Sampler

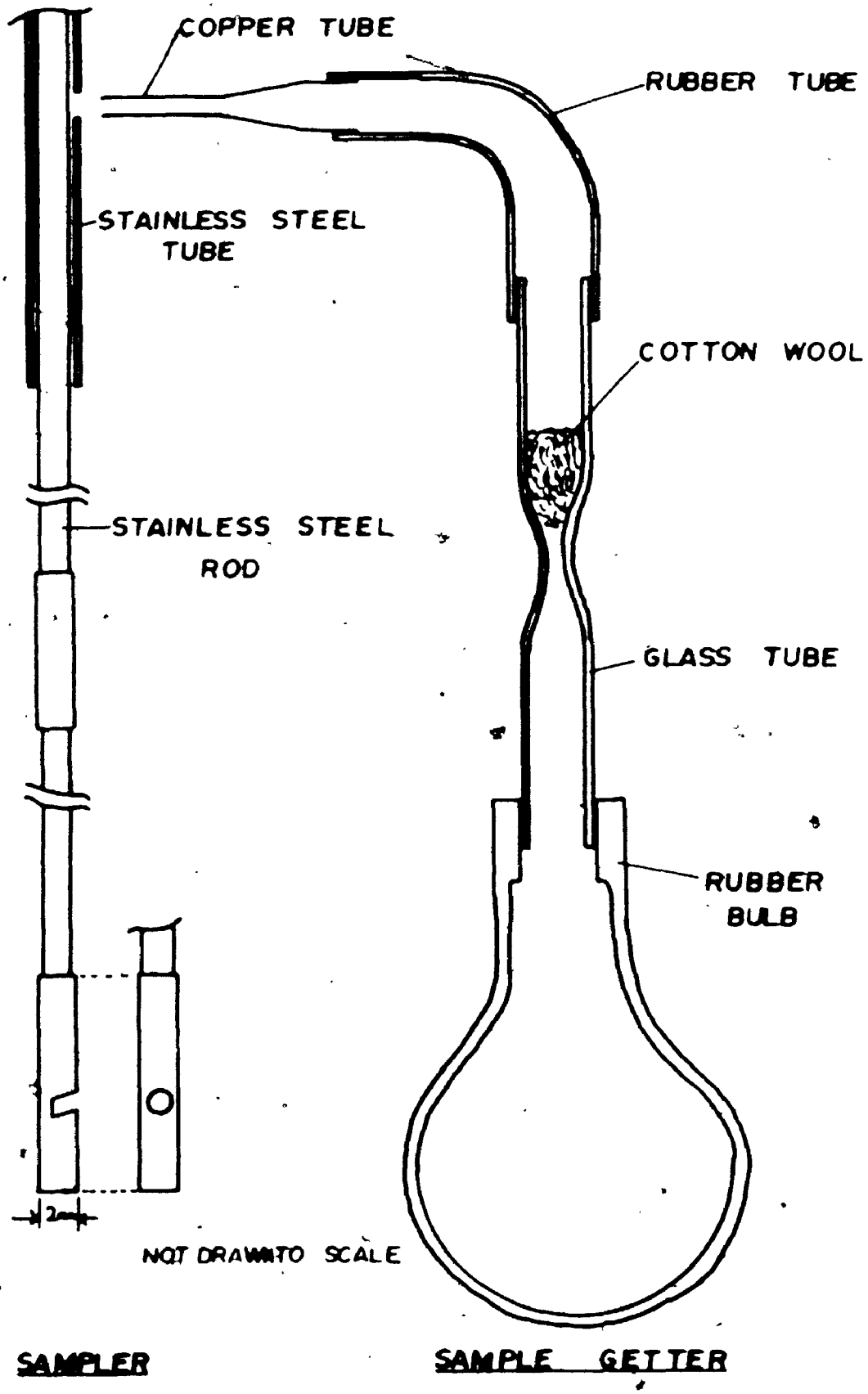

Figure 3.03 Sampler and Sample Getter

Solid State Cell

A solid state electrolytic cell was used to measure the oxygen potential of the gas phase in the fluidized bed during the reduction reaction. The use and theory of operation of cells of this type has been recently reviewed by Rapp and Shores[96].

The cell electrolyte consisted of a CaO stabilized (10 mole %) zirconia tube 1/4" O.D., 18" long, closed at one end (flat) supplied by the Zirconium Corporation of America. As the reaction wustite to iron was of prime interest, the oxygen potential inside the cell was fixed at the Fe/FeO equilibrium by filling it with "Fisher" reagent grade Fe_2O_3 and Fe in the proportion about 1 to 2. A double bore alumina tube carrying a platinum and a platinum 13% rhodium wire (see Figure 3.02) each welded to a piece of platinum foil extended to the end of the closed tube. The alumina rod was pushed hard against the end of the zirconia tube as the tube was packed with the Fe_2O_3/Fe mixture. After filling the tube, the open end was filled with epoxy cement. The exterior electrode consisted of a piece of platinum foil held against the flat end by a silica pull rod, and a platinum lead out wire sheathed in a alumina tube.

The cell was used with its flat end immersed in the fluidized bed at three different positions 1.5, 2.5 and 6.4 cm. from the frit. The voltage generated by the cell was

measured with a Keithly Model 602 electrometer and the output recorded on a Philips PM 8100 flat bed recorder.

Five different cells were used during the course of this study.

3.4 Static Reduction Experiments

To determine if the observed reduction morphology of the particles taken from the fluidized bed was due to their cyclic exposure to severe and then mild reducing conditions, studies were undertaken using 10 to 20 particles in platinum boats. The apparatus is shown diagrammatically in Figure 3.04. The three platinum boats (only 2 are shown in Figure 3.04) could be raised and lowered by means of magnets. In the raised position they were directly under the zirconia cell which was used to monitor the reducing gas, so that a reduction cycle similar to that in a fluidized bed reduction could be simulated.

To obtain the required H_2/H_2O ratios, hydrogen was bubbled successively through three 350 ml. capacity gas washing bottles containing distilled water immersed in a water bath. A fourth bottle was left empty to trap entrained water droplets. The temperature of the water bath was controlled using a Haake "Unitherm" with auxillary heating and stirring by another unit. Temperature control was better than ±0.1 C.

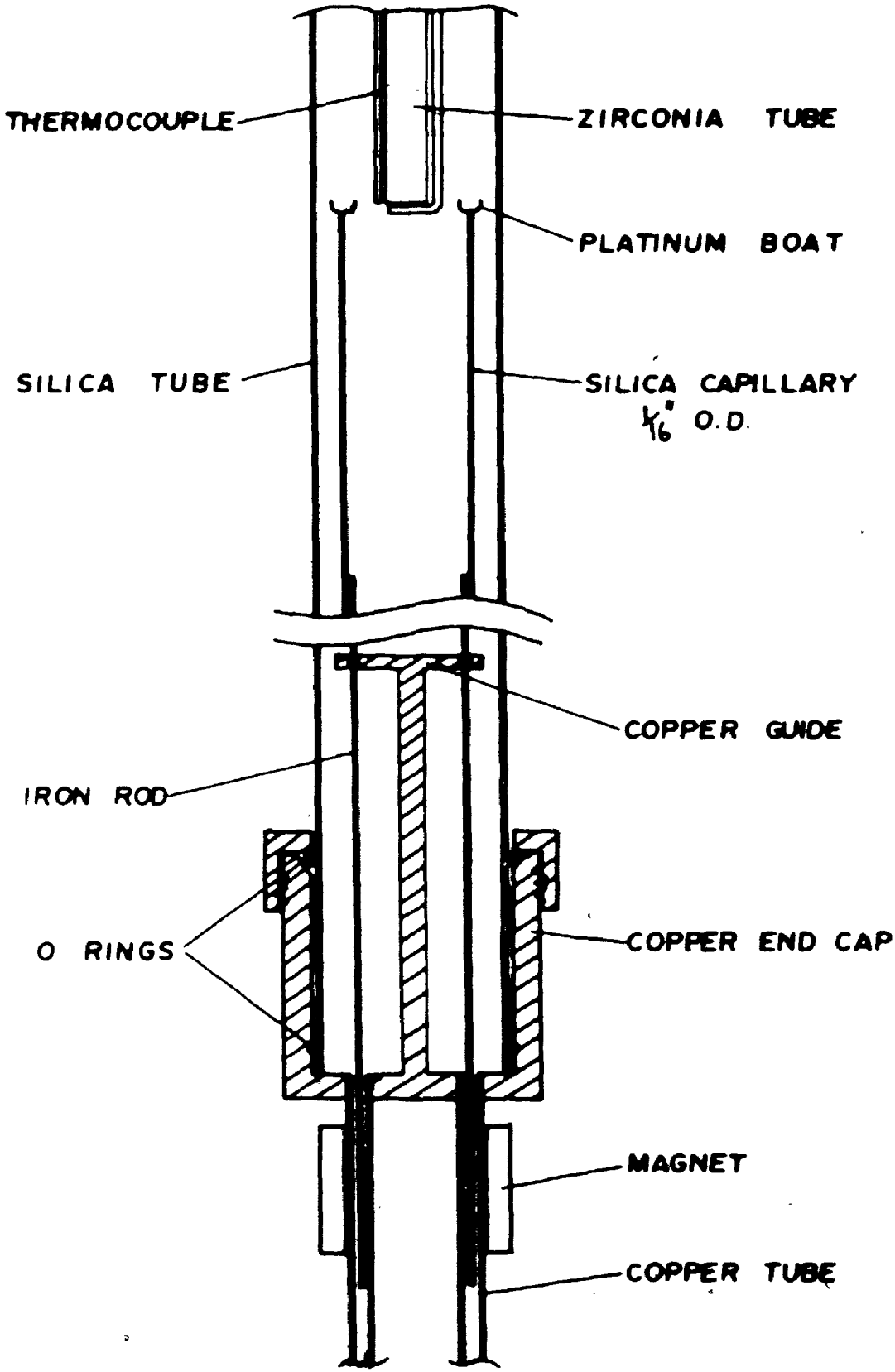

Figure 3.04 Schematic Diagram of Apparatus Used to Reduce Small Samples of Ore

The particles were heated in a nitrogen atmosphere to temperature and then the gas flow switched to the required H_2/H_2O mixture. At the end of the run the boats were lowered to quench the particles, which were then examined metallographically.

3.5 Particle Coatings

The possibility of preventing defluidization by coating the particles with various inorganic substances was investigated. Experiments showed that for successful results the coverage had to be very good. Sterlings'[95] method of soaking the ore in a solution containing a metal compound then evaporating did not give, in general, good coverage. The slurry technique reported by Bailey[92] gave better results.

In general the coating substance with particle size as small as possible, was mixed into the ore to which had previously been added 2% by weight of water. However the process was optimized for each coating substance.

CHAPTER 4

EXPERIMENTAL RESULTS

4.1 Reduction of As-received Ore

4.1.1 Defluidization Phenomena of As-received Ore

The defluidization characteristics of the washed as-received ore were defined using the fluidization meter. A bed weight of 80 g of ore of particle size 105-140 μm was used and isothermal reduction investigated in the temperature range 640-903°C.

Figure 4.01 shows graphically the data obtained from a typical run when bogging occurred. This illustrates that defluidization can be followed either by the pressure drop across the bed or by using the fluidization meter. However the latter technique was found more useful when defluidization was slow or occurred only to a limited extent.

The data obtained from the fluidization meter for all the experiments at different temperatures can conveniently be classified into three groups, Figure 4.02. Below about 710°C, Figure 4.02 curve I, the ore reduced to iron particles without sticking or defluidization taking place. However the degree of fluidization decreased slowly throughout the reduction, reaching a constant value after the reaction had practically ceased.

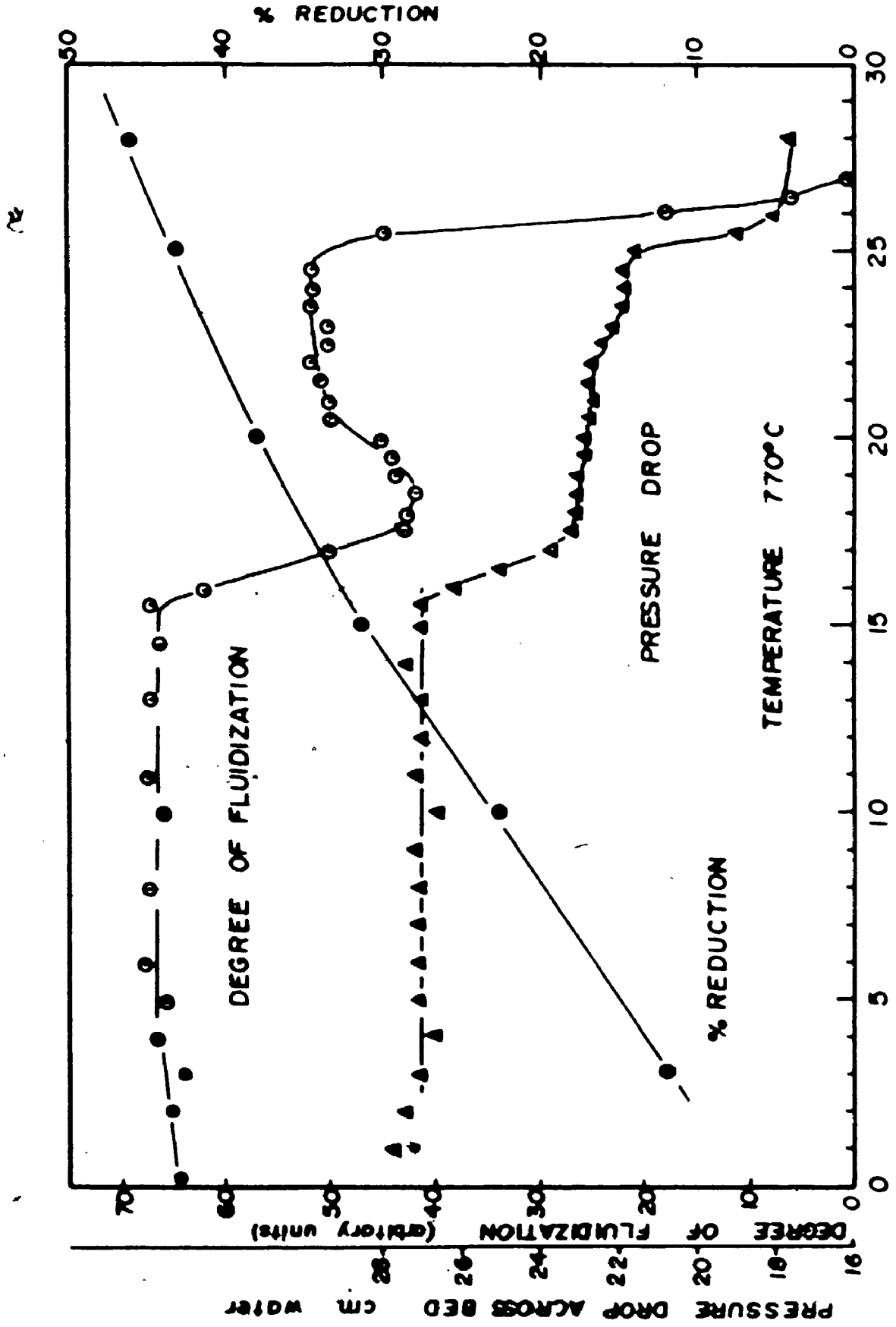

Figure 4.01 The Variation of the Degree of Fluidization, Pressure Drop Across the Bed and the % Reduction With Time at 770°C

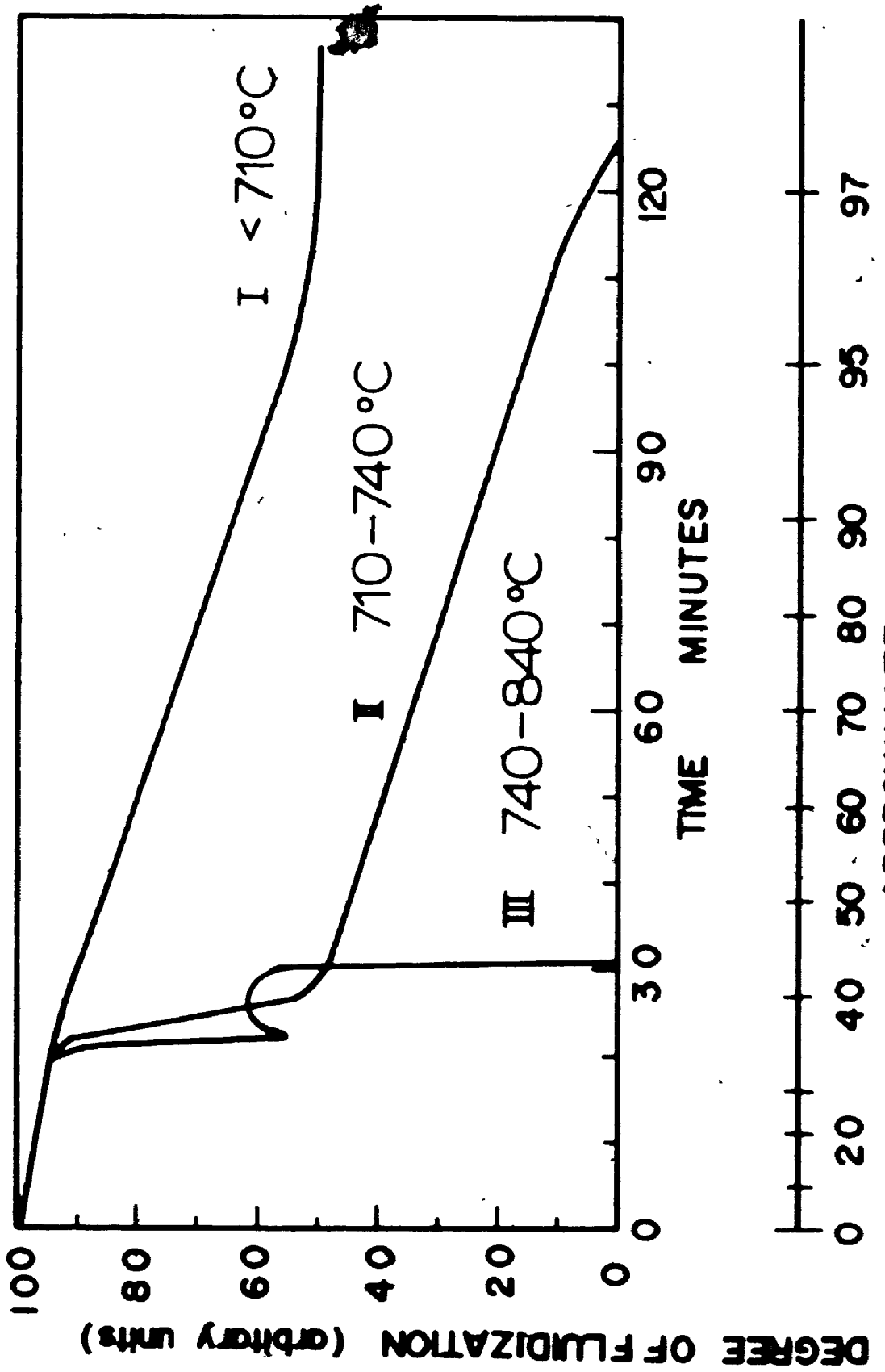

Figure 4.02 Relation Between the Degree of Fluidization and Time for Ore Reduced at Different Temperatures

Above 710°C the reduction proceeded smoothly until the beginning of the formation of the iron phase, i.e. 33% reduction, when the bed showed a marked tendency to defluidize. Between about 710 and 740°C, after the sudden drop in the quality of fluidization at 33% reduction, the bed continued to defluidize more slowly (curve II). Between 740°C and about 840°C the bed defluidized suddenly as iron began to form and then defluidized completely a few minutes later (curve III). At 903°C the highest temperature investigated the bed defluidized in just one step at about 33% reduction.

The results for the reduction of ore of particle size 74-104 μm and 210-250 μm were essentially identical.

The fixed (i.e. no gas flow) bed height before reduction was 6.2 cm. If no defluidization occurred the completely reduced ore had a fixed bed height of 4.8 cm. When the reaction was stopped after defluidization occurred, the fixed bed height was greater than the latter value and often larger than the former. Thus the final fixed bed height is a useful indicator of any defluidization that has occurred. In Figure 4.03 the final fixed bed height is plotted against the reduction temperature and shows that defluidization first occurs at approximately 710°C.

When a bed defluidized, increasing the flowrate substantially (by say 30-40%), just after bogging had occurred would usually re-fluidize the bed but for only a short time. The defluidized bed height after increasing the flowrate was

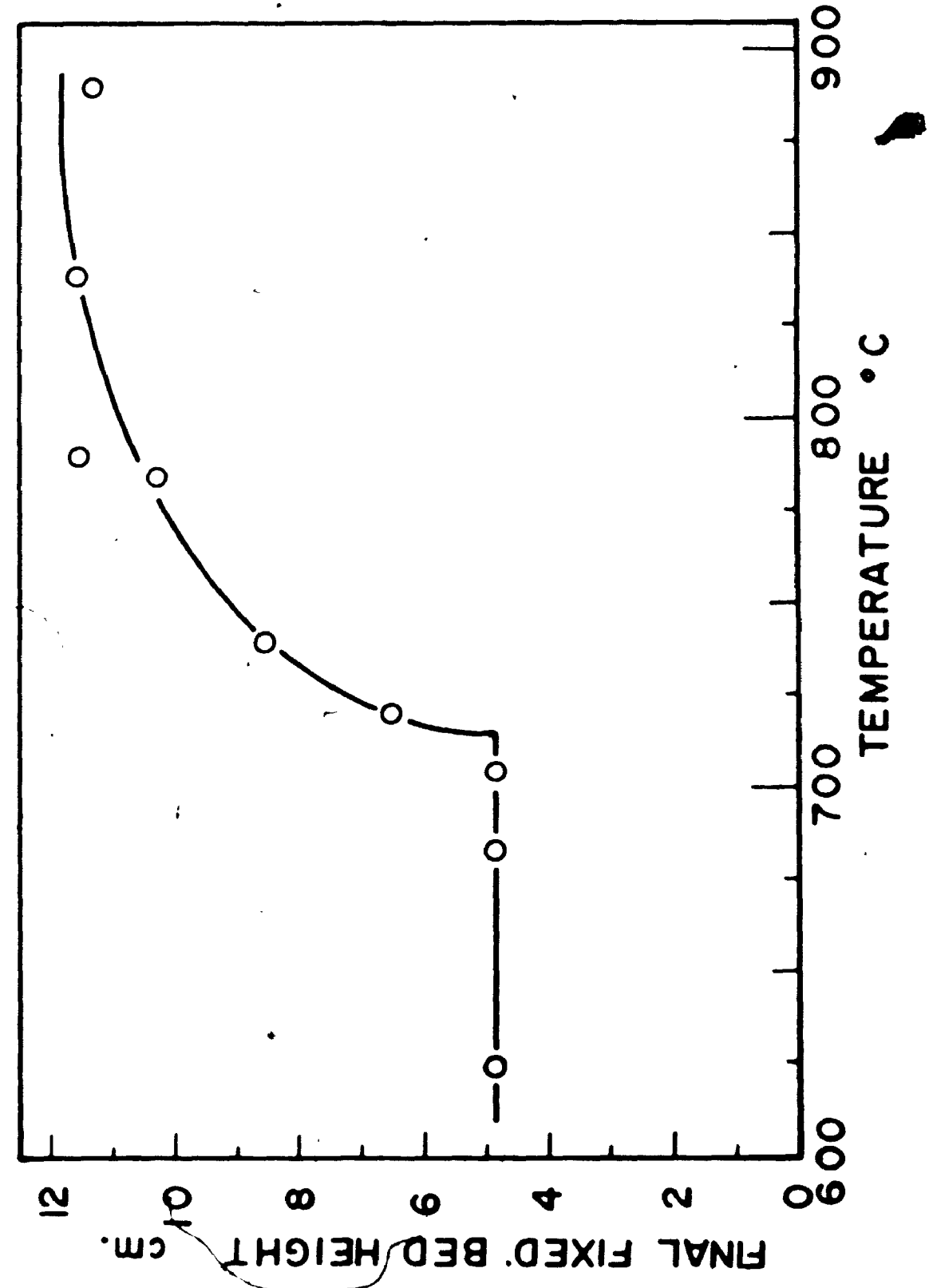

Figure 4.03 Relation Between the Final Bed Height and the Reduction Temperature

observed to be larger than the original defluidized bed height. It thus appears that increasing the gas velocity overcomes the sticking forces between some or all of the particles, but then the particles stick in a configuration of greater porosity, which again allows the passage of gas through the bed without fluidization.

On cooling bogged beds it was found that the particles were only lightly fritted together and beds were substantially broken up while extracting the product from the tube.

It appears that defluidization occurs when the inter-particle adhesive forces, cannot be overcome by the hydro-dynamic forces.

4.1.2 Two Temperature Reduction

To ascertain if the observed defluidization was just a sticking phenomenon which would be expected to be more severe the higher the temperature, two further series of runs were performed. In these experiments ore of a particle size range 105-140 μm was pre-reduced various amounts at 630°C and the reduction continued, in the first series of runs at 790°C and in the second series at 870°C.

In these experiments the bed sometimes only partly defluidized at the higher temperature. The particles for a certain distance above the bottom of the bed were stationary while the rest of the bed remained fluidized. The final fixed bed height is therefore a useful measure of the amount

of defluidization that took place after complete reduction. Figure 4.04 shows the final bed height plotted against the percentage pre-reduction.

In the first series of runs when the final reduction temperature was 790°C, little defluidization occurred for ore pre-reduced beyond the iron formation stage, i.e. 33% reduction. The second series with a final reduction temperature of 870°C did not show a similar drop in fixed bed height (i.e. amount of defluidization) around 33% reduction.

Ore fully reduced at 630°C could be kept fluidized at 790°C for five hours without any drop in the degree of fluidization and at 870°C with only a small drop.

The results presented in this section show that defluidization is not simply dependent on temperature only. The reasons will become apparent only after further work is described.

4.1.3 Preliminary Studies of the Reduction Morphology

The reduction morphology was initially studied by stopping the reaction after varying periods of time, cooling the bed, and examining cross-sections of the particles. This lengthy procedure was used only for isothermal reduction at four temperatures, 650°, 690°, 840° and 900°C.

The reduction of hematite particles to magnetite proceeded topochemically at all four temperatures (Figure 4.05).

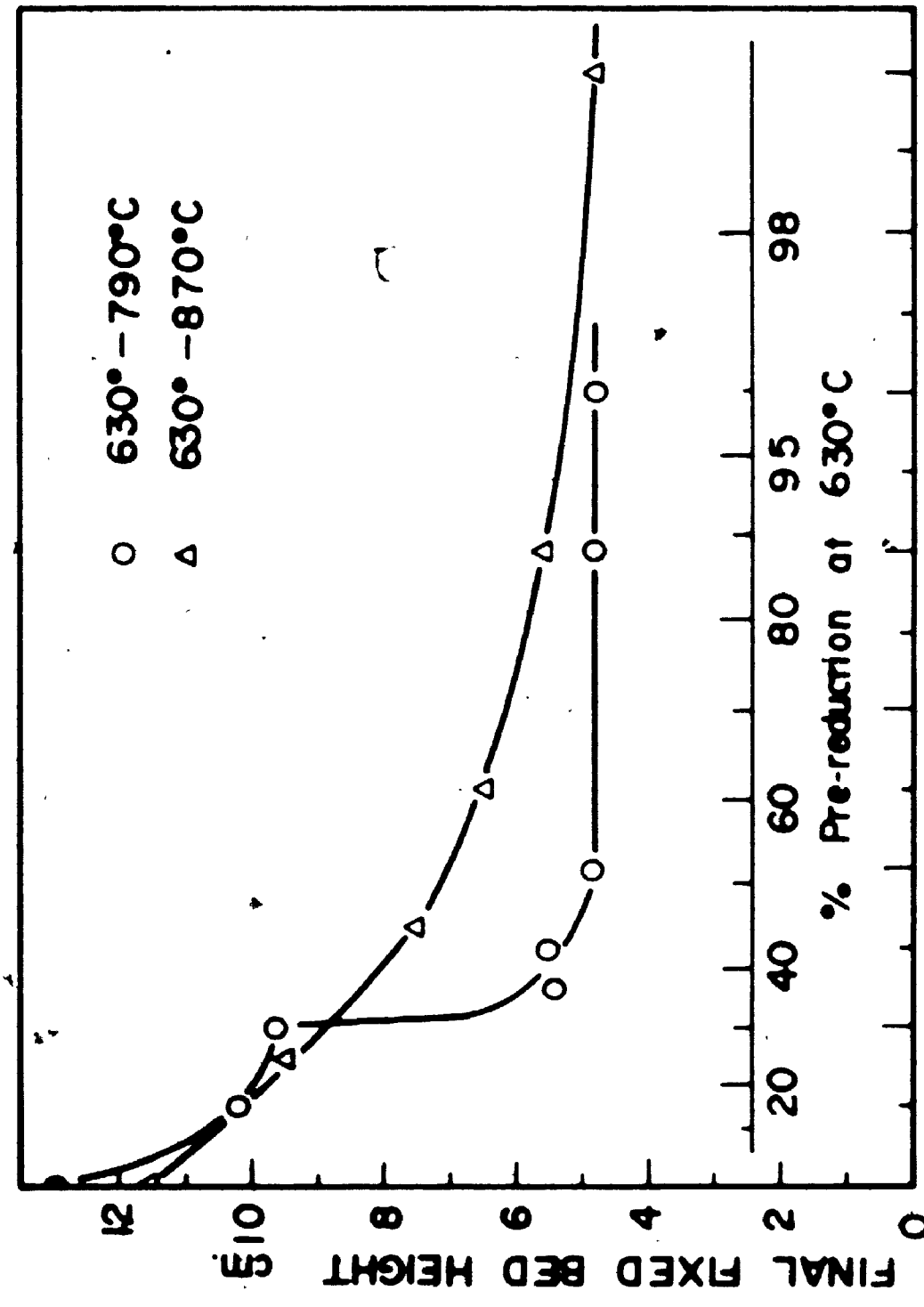

Figure 4.04 Relation Between the Final Bed Height and the Amount of Pre-Reduction at 630°C for Ore Reduced at 790°C and 870°C

On further reduction, Fe_3O_4 was reduced to FeO. The usual etchants (HCl in alcohol or acid stannous chloride solutions[66]) failed to reveal the Fe_3O_4/FeO phase boundary in detail. The reaction appeared to take place throughout the porous particles. Before nucleation of iron it was determined that the bed consisted wholly of porous wustite at all temperatures. The pores were fewer but larger the higher the reduction temperature.

At 650° and 690°C continued reduction caused nucleation of iron inside the wustite phase, none being observed at the exterior surface/gas interface. Figures 4.06, 4.07, 4.08 show polished sections of particles at increasing degrees of reduction at 650°C. In Figure 4.06 iron has started to nucleate and grow within the particle (bed reduced 40%). In Figure 4.07 more of the iron phase is present (bed reduced 70%) but the surface of the particle is still composed of wustite. In Figure 4.08 (bed reduced 85%) more iron has formed and a thin layer of iron is now present on parts of the exterior surface of the particle. The morphology of the progress of reduction as seen in these particles is quite general.

In contrast to this behavior, at temperatures of 840° and 900°C, iron was observed to nucleate on the surface of the particles and grow as nodules. Internal growth of iron also occurred. Figure 4.09 shows a micrograph of a wustite particle reduced at 903°C with nodular growths of iron on its surface. On further reduction iron covers the exterior and

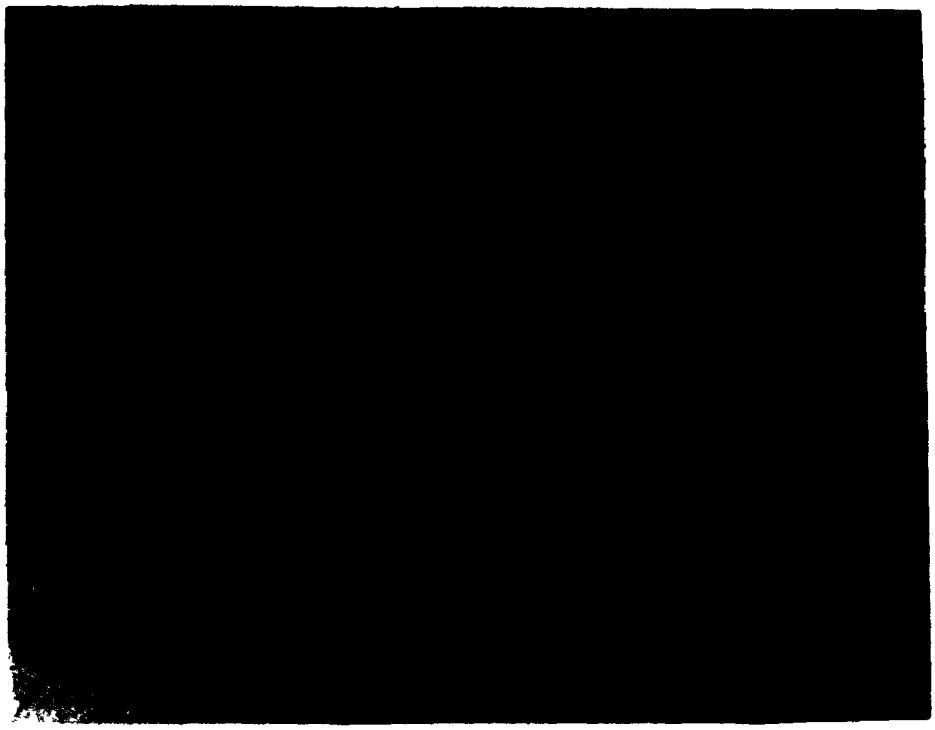

Figure 4.05 Ore Partially Reduced at 680°C, Hematite Light Grey, Magnetite Dark Grey x500

Figure 4.06 Micrograph of Particle From Bed Reduced 40% at 650°C. White Areas Are Iron, Grey Wustite, Black Pores. x1000

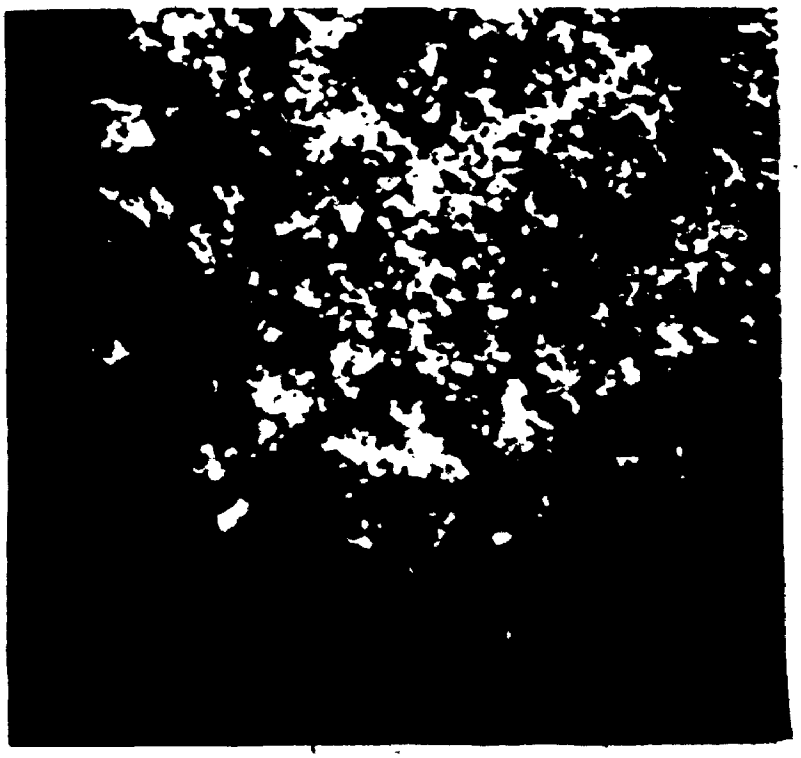

Figure 4.07 Micrograph of Particle From Bed Reduced 70% at 650°C. White Areas Are Iron, Grey Wustite, Black Pores. x1000

Figure 4.08 Micrograph of Particle From Bed Reduced 85% at 650°C. x1000

Figure 4.09 Micrograph of a Wustite Particle Showing Nodular Growths of Iron on the Surface. x1000

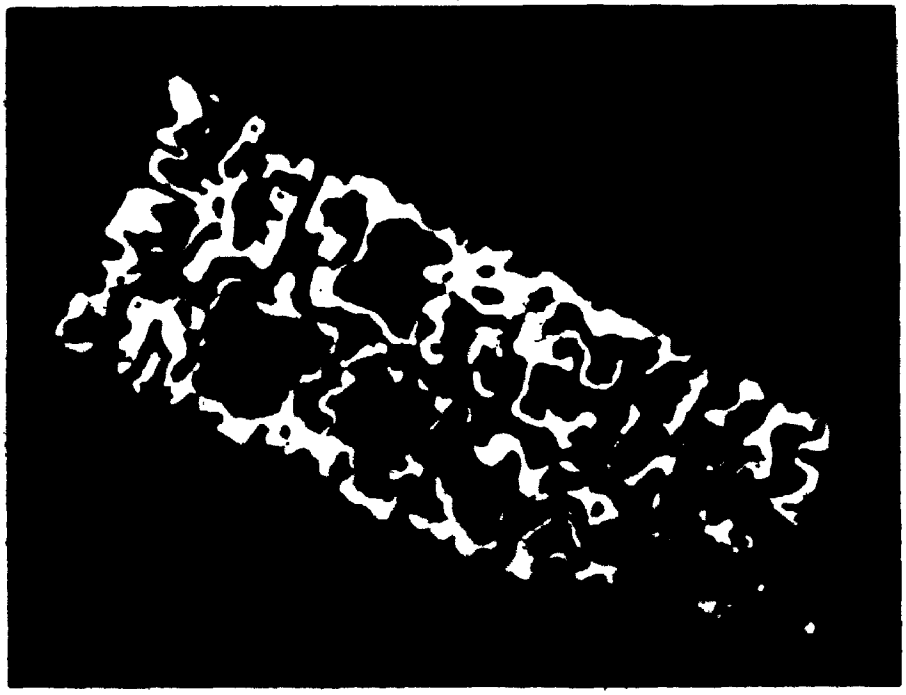

Figure 4.10 Micrograph of a Particle Reduced 40 Minutes at 903°C. x1000

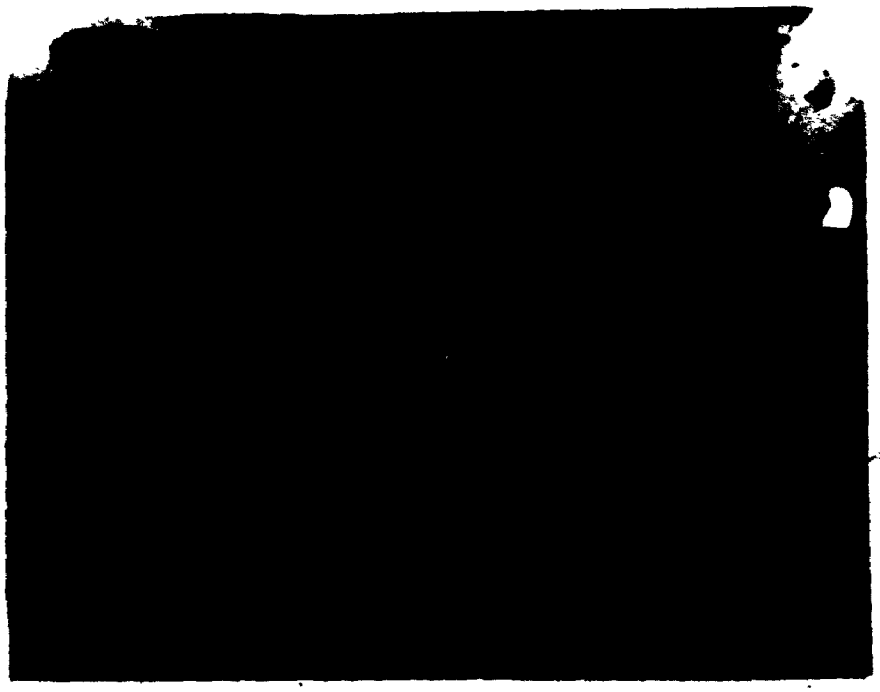

Figure 4.11 Particle Joined by Iron Nodules. Reduced 870°C

interior surfaces of the wustite particles, Figure 4.10.

Additional observations on the reduction morphology were obtained from the experiments used to define the defluidization characteristics of the ore, described previously. In the experiments when bogging occurred the reaction was immediately stopped and the particles examined. Nodules were always found to be present. Lumps of the partially reduced product from bogged beds showed that the particles were often joined to one another by nodules as seen in Figure 4.11. Further work showed that nodules were not formed when bogging did not occur - that is below about 710°C.

Based on these observations it appears reasonable at this stage to tentatively conclude that nodules are the cause of defluidization.

4.1.4 Reduction Kinetics

A typical percentage reduction (obtained by collecting the water from the reaction) versus time plot is shown in Figure 4.12 for a temperature of 684°C when no defluidization occurred. During the initial steep slope hematite is reduced to wustite. In the linear region between about 33 and 90% reduction, wustite is reduced to iron. In these two steps the rate controlling factor is the rate of supply of hydrogen. After about 90% reduction when the curve is no longer linear the reduction of wustite to iron continues but the rate controlling step is changing.

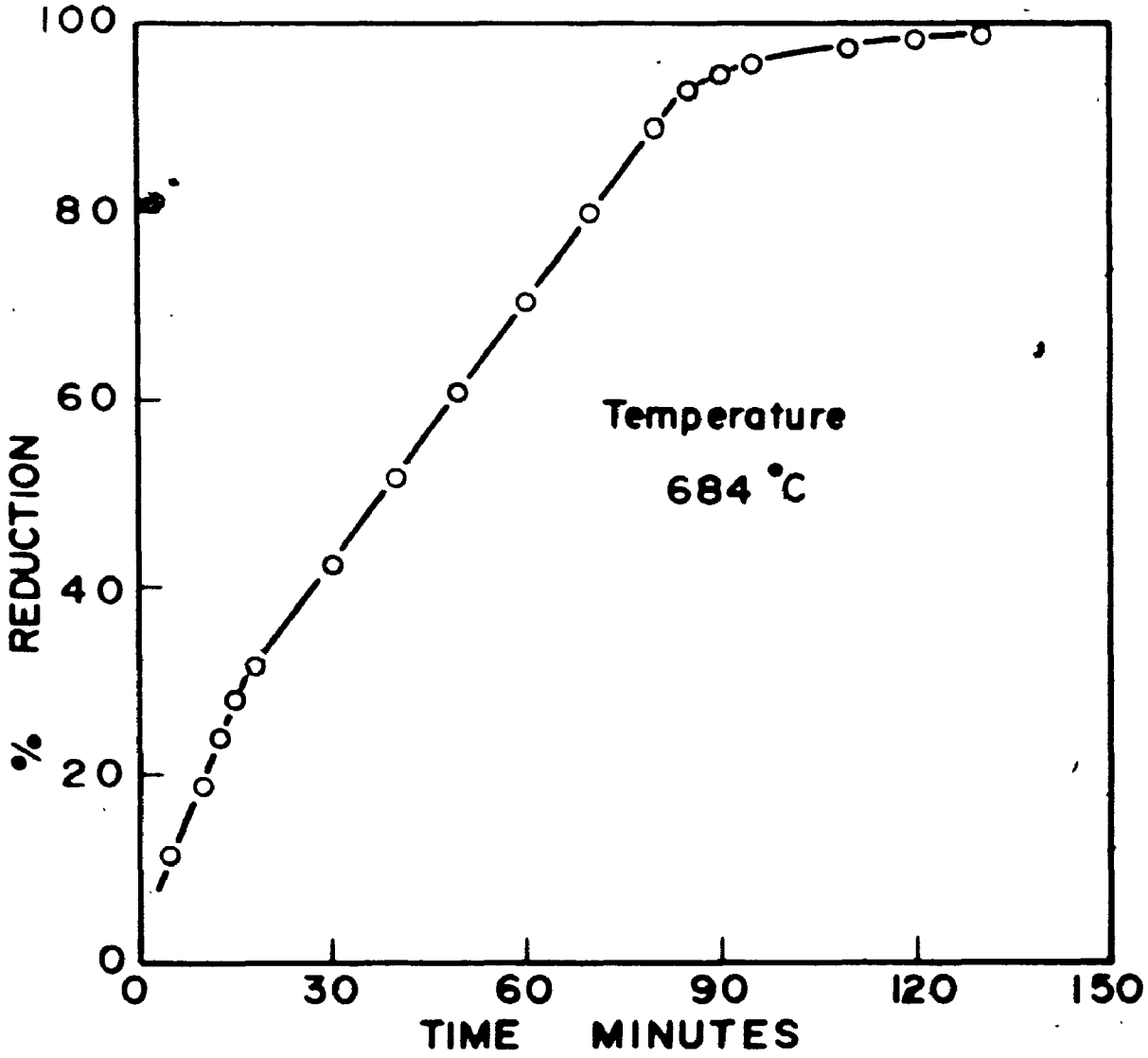

Figure 4.12 Typical % Reduction as a Function of Time Curve

As the bed defluidized at the higher temperatures complete data to the end of the reaction could not be obtained. However Figure 4.13 shows the effect of temperature on the reaction rate up to 30% reduction.

It was found that the different particle sizes used did not alter the reduction rate significantly.

4.1.5 Minimum Fluidization Velocity Measurements

To determine the effect of nodules on the quality of fluidization when the sticking of particles is not a factor, the minimum fluidization velocity was measured at room temperature for

(1) the unreduced ore

(2) ore reduced at 650°C ten minutes beyond iron nucleation (when no nodules are present)

(3) ore reduced ten minutes beyond iron nucleation at 820° (The bogged bed was cooled, broken up and sieved; nodules were present.)

The pressure drop across the bed was measured as a function of nitrogen flowrate. The results are presented in Figure 4.14. In this figure the pressure drop due to the frit (measured in a separate experiment with no bed present) has been subtracted from the total pressure drop. The minimum fluidization velocity, V_{mf}, may be calculated from the value of the gas flow rate at which the inclined and horizontal

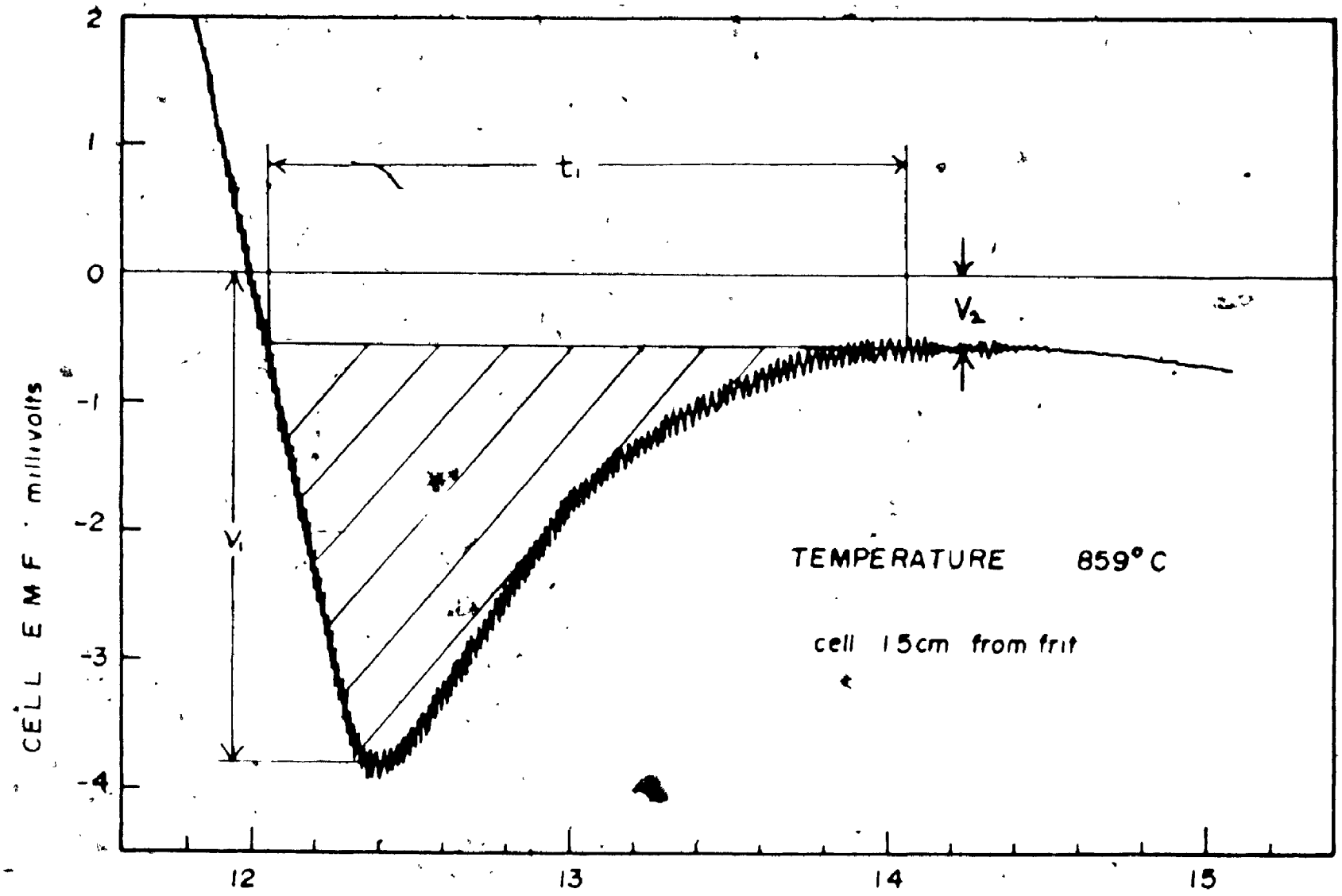

Figure 4.16 Voltage-Time Curve in Region of Iron Nucleation at 859°C

parts of the graph intersect.

Figure 4.14 shows that fluidization begins at volume flow rates of 1033, 830, and 1630 ml/minute of nitrogen, (V_{mf} = 3.5, 2.8, 5.5 cm/sec), for the ore, non-nodular bed and nodular bed respectively.

The results show that nodular particles are considerably more difficult to fluidize than non-nodular particles. However it should be noted that this is not the direct cause of bogging. The V_{mf} of nodular particles is about twice as high as non-nodular but the gas velocity employed, at for example 700°C, was 15 cm/second of hydrogen almost four times greater than the measured V_{mf} of 4.1 cm/second of hydrogen at that temperature.

4.1.6 The Variables Flowrate and Bed Height

A fluidized bed is operated at a flowrate higher than the minimum fluidization velocity, but lower than a value that causes excessive entrainment of particles in the exit gas. In a small diameter bed, such as the one used in this work, slugging (the growth of bubbles to the sides of the bed before they reach the surface) occurs at high gas flows. Slugging modifies the mass flow and causes large bed expansions which could not be tolerated with the experimental apparatus used. The usable range of flowrate was therefore quite small.

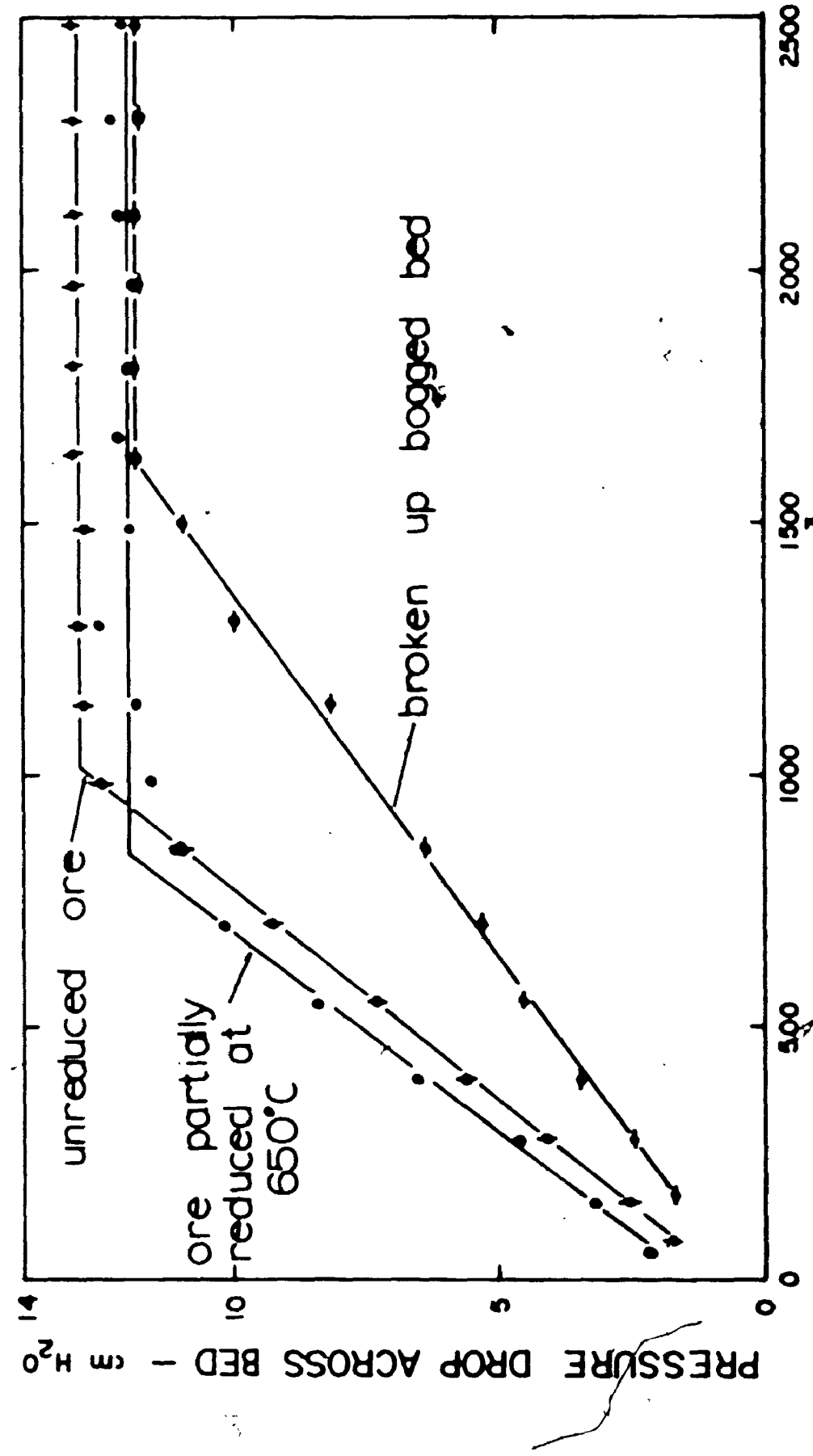

Figure 4.14 Determination of the Minimum Fluidization Velocity

In experiments reported so far a flowrate of 20 ml/second of hydrogen was used. Experiments conducted with a flowrate of 10, 15 and 25 ml/second at 680, 750 and 800°C did not show a very significant change in the defluidization characteristics of the ore. In terms of percentage reduction, at flowrates below 20 ml/second the bed tended to defluidize a little sooner than reported earlier and a little later with the higher flowrate. This is consistent with the fact reported previously that increasing the flowrate directly after bogging, refluidized the bed only for a short time.

Bed weight also had little or no effect above a charge of 20 g. Experiments performed at 680 and 750°C with bed weights of 20, 30, 50 and 100 g showed the same reduction morphology and defluidization phenomena as reported previously for a bed weight of 80 g. However with a charge of 5 or 10 g of ore the reduction morphology proved different, iron nucleating and growing throughout the particle including at and near the surface at both temperatures. Nodules were not observed. At later stages iron often covered the surface so that cross-sectioned specimens showed a thin iron rim around a fine iron and wustite mixture core. Defluidization occurred at 750°C but not at 680°C. With a bed weight of 15 g the reduction morphology was between that just described and that described previously for a bed weight of 80 g.

It was decided that bed weights of less than 40 g were not representative of a normal fluidized bed reduction

process, as the particles are reduced so quickly (residence times in a commercial reactor would probably be measured in hours) and attention was concentrated on a 80 g bed weight.

4.1.7 Reduction Morphology and Kinetic Studies Using the Solid State Cell and Sampler

To obtain samples from the bed during reduction at precisely known points in the reduction sequence so that the interesting reduction morphology could be further studied, the apparatus described in section 3.3 was developed.

The information obtained from the solid state cell will first be described. A bed weight of 80 g was again used.

A typical voltage versus time graph obtained from the zirconia cell with its end (i.e. measuring point) 2.5 cm from the silica frit distributor of the fluidized bed is shown in Figure 4.15 for a temperature of 680°C. The cell is initially measuring the oxygen potential of the nitrogen and the voltage reading drops sharply as hydrogen is let into the reactor. The voltage then rises to a short lived plateau as hematite is reduced to magnetite. After about 2-1/2 minutes the voltage and therefore the water concentration drops rapidly and levels out to another plateau during which magnetite is reduced to wustite. Ten minutes after the start of the reaction the curve begins to drop slowly as the particles in the bed are converted completely to wustite and through the wustite phase field. The measured oxygen potential

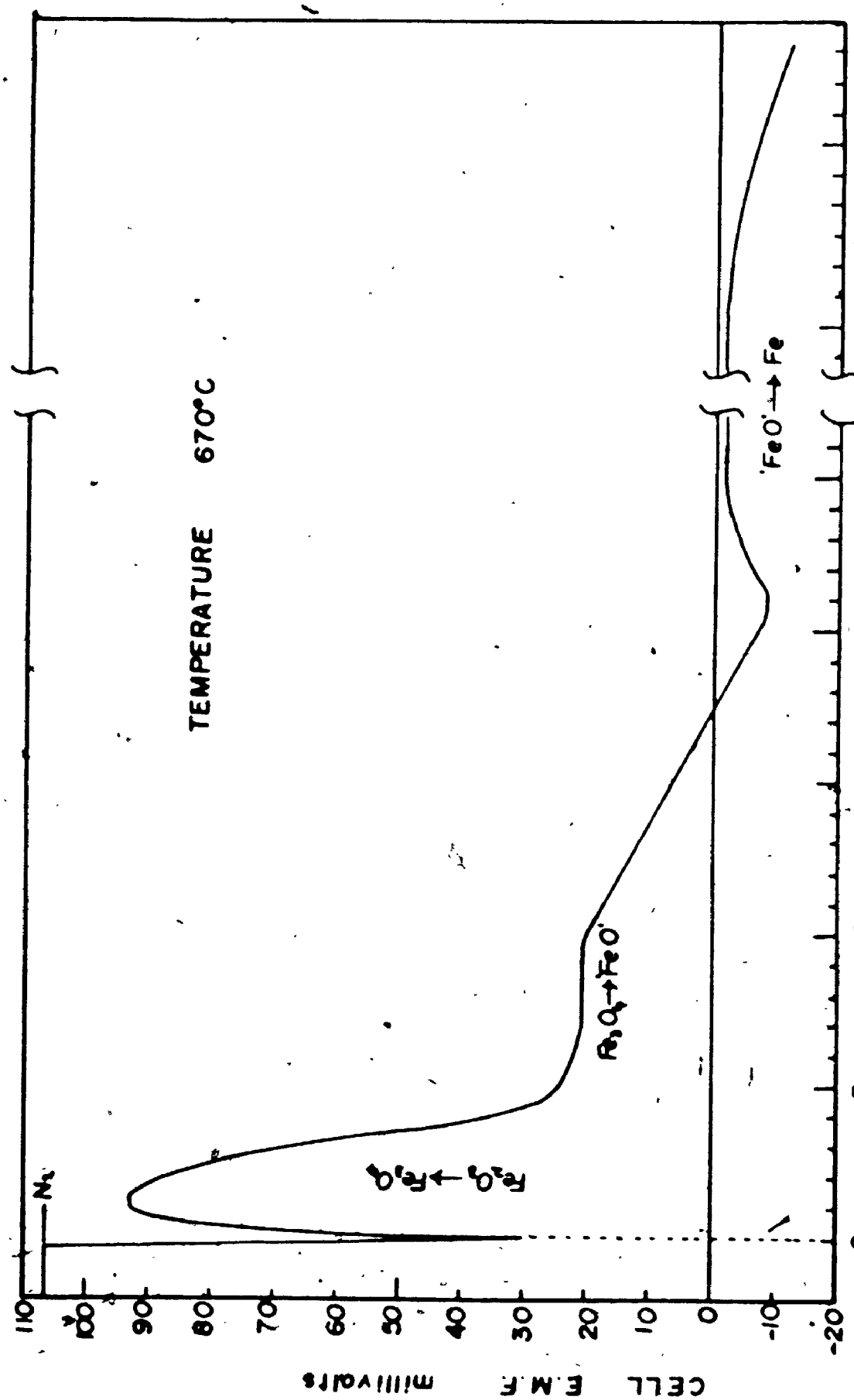

Figure 4.15 Voltage-Time Graph Obtained From Zirconia Cell

of the gas drops below the equilibrium wustite/iron oxygen potential, (zero volts) to a certain minimum value, then returns quickly at first and then more slowly towards the equilibrium potential. Shortly after this minimum in the curve, examination of samples of the ore showed that iron was nucleating. This region of the voltage-time curve (see shaded area of Figure 4.16) will be called the iron nucleation stage, i.n.s., for easy reference. Briefly it is believed the minimum is due to an incubation period associated with iron nucleation, but this will be more fully discussed in Chapter 5. The amount of iron in the particles increases as the oxygen potential stays constant just on the reducing side of the Fe/FeO equilibrium. After about 65 minutes from the start of the reaction the oxygen potential falls away from the Fe/FeO equilibrium.

It will be seen from Figure 4.16 that the cell voltage was not completely steady. Bubbles passing through the bed, which would be expected to contain a greater porportion of hydrogen than the gas immediately around the particles, caused rapid fluctuations, of the order of 1/3 and 1 mV at 859 and 680°C respectively, from the mean reading. When defluidization occurred the fluctuations ceased. The voltage-time curve shown in Figure 4.16 shows that defluidization occurred shortly after the end of the i.n.s. at 859°C.

Samples taken from the bed confirmed the reduction morphology described previously and provided further

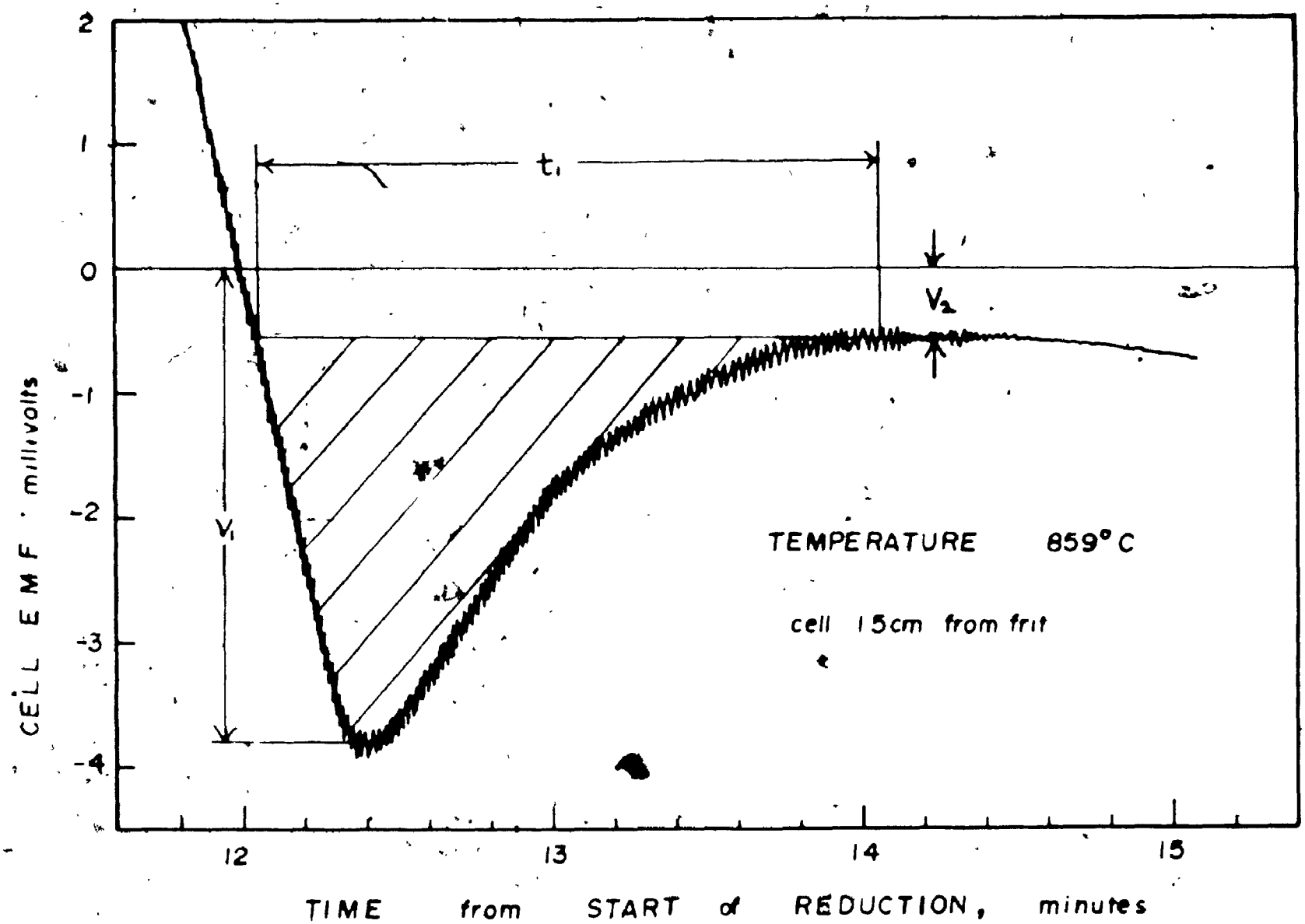

Figure 4.16 Voltage-Time Curve in Region of Iron Nucleation at 859°C

These two factors, the abnormal morphology of iron nucleation and the absence of sticking of fully reduced particles at high temperature, led to the idea that the surface of the ore particles may be coated by a film of impurities. Hence the experimental program continued with a search for such a coating and the results are described in the next section.

4.2 Impurity Film

4.2.1 Impurity Film on As-received Ore

As reported in Chapter 3 the ore concentrate was washed in a water fluidized bed prior to reduction. The purpose of this treatment was to eliminate the dust from the reduction apparatus. However such washing appeared to remove only the larger clinging particles from the ore particles. Figures 4.18, 4.19, 4.20 show the surface of washed particles as they appear in the light microscope and scanning electron microscope (S.E.M.). A film of small particles remains on the surface. Repeated washings with vigorous stirring failed to remove this film.

The film could be removed by washing the ore in various acids. Concentrated hydrochloric acid was very effective but produced many large etch pits. To avoid this the ore was washed in a 50% hydrofluoric acid solution when no pitting could be observed under high magnification.

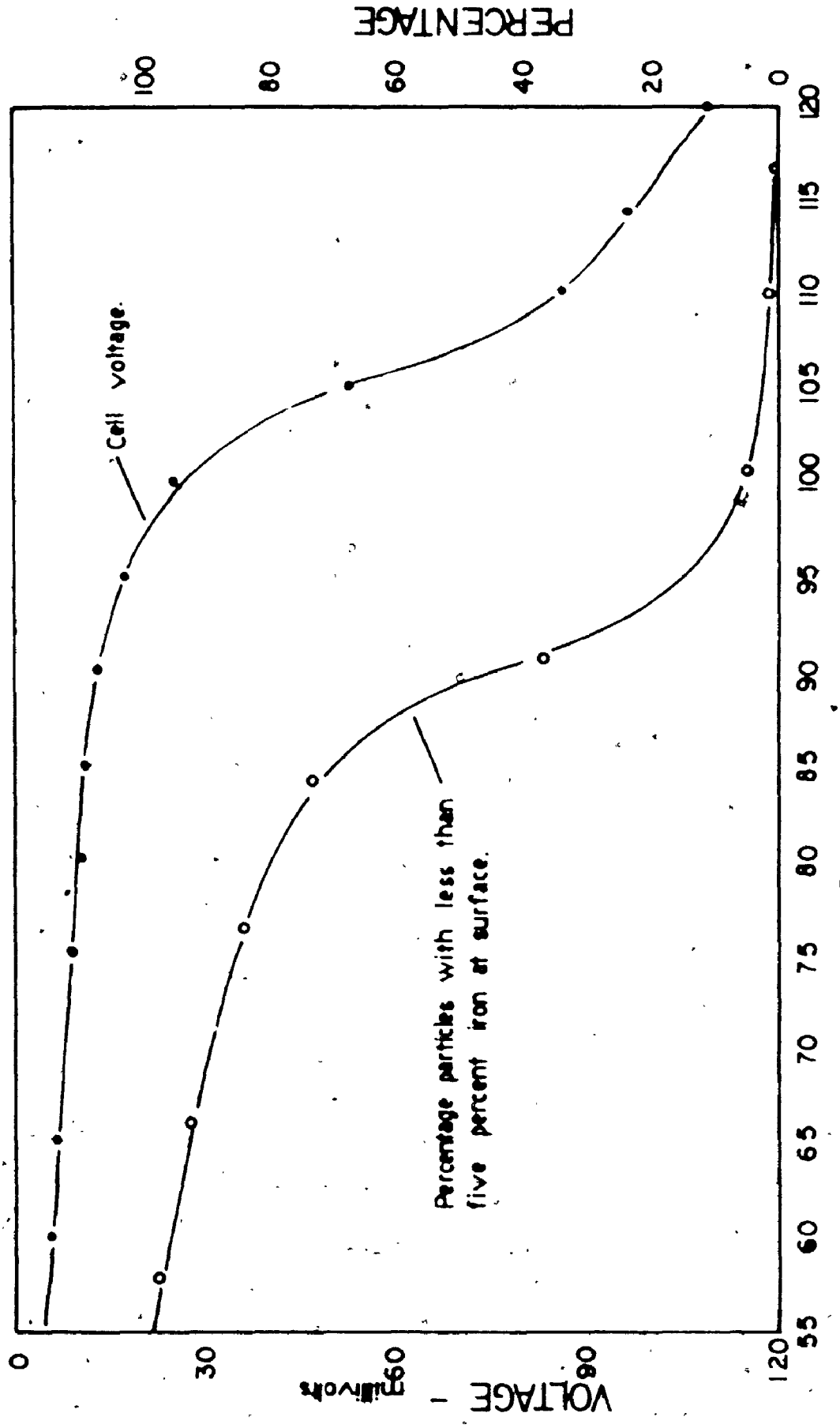

Figure 4.17 Relation Between Cell Voltage-Time Curve and Amount of Iron at Surface of Particles

The apparatus has been described in section 3.4.

In the previous section a voltage-time curve obtained from the solid state cell during a fluidized bed experiment at 680°C was described. Initially the present experimental program simulated this curve (from the magnetite/wustite plateau onwards) so the particles in the platinum boats were reduced at 680°C as if fixed in the bed at the measuring point of the cell. This was accomplished by heating or cooling the water bath and monitoring the voltage of the cell. (At other temperatures the corresponding voltage-time curve was utilized). The platinum boats were lowered at intervals during the reduction.

Experiments at 650 and 680°C showed that iron nucleated and grew inside the particles similar to the behaviour observed below 710°C during fluidized bed reduction. However the number of growing iron areas observed was smaller. At 760 and 810°C the iron grew internally and at the surface as nodules. Qualitatively the number of nodules observed per particle was smaller than during fluidized bed reduction. It was established however that increasing the reduction potential of the gas slightly (about 5 mV in zirconia cell terms at 810°C) increased the number of nodules such that the particles' appearance was similar to particles reduced in the bed at the same temperature.

Other experiments showed that when iron was formed at high reducing potentials (e.g. 50 mV with respect to the

Fe/FeO equilibrium at 680°C) it quickly covered the surface of the particles producing a morphology similar to that described previously for very small bed weights (section 4.1.6).

These results, although sparse due to time considerations, are thought important as they show that in an 80 g bed the average particle behaves as if reduced at a oxygen potential not very far removed from the equilibrium Fe/FeO oxygen potential.

4.1.9 Discussion of the Reduction and Defluidization Characteristics of As-received Ore

In this section a brief discussion of the reduction and defluidization behaviour of the as-received ore is given. A fuller discussion follows later.

From the kinetic data and reduction morphology observations it is clear that each oxide is fully reduced to the next lower intermediate oxide before being further reduced. When the whole bed was quickly cooled at some stage in the reduction and the particles examined, little variability in the state of reduction between particles was observed.

The tentative opinion that nodules are the cause of defluidization was expressed in section 4.1.3. This view is supported for the following reasons.

(1) Defluidization only occurs when nodules are present on the particles.

(2) Metallographic examination shows nodule growth is the beginning of iron formation and occurs after the bed has been reduced about 33% at temperatures above 710°C. It is at this point in the reduction that defluidization of the bed takes place or begins to take place.

(3) Further, reduction experiments with H_2/N_2 mixtures, as expected, slowed the reaction rate. The quite sudden defluidization observed when pure hydrogen was used as the fluidizing gas, was then replaced by gradual defluidization which, however, proceeded to the same extent and occurred over the same few percent reduction.

(4) Metallographic examination showed that the particles were often joined to one another by nodules.

(5) The minimum fluidization velocity, V_{mf}, at room temperature of the nodular iron particles has been shown to be about twice as high as the V_{mf} for non-nodular particles. Nodules, therefore, have quite a large effect on the fluidizability of the bed, and their growth can be expected to decrease significantly the degree of fluidization. This is not however the direct cause of bogging as a fluidizing velocity about four times greater than the minimum fluidization velocity at temperature was used.

The work reported so far has brought to light two surprising facts. First, the growth morphology of iron in the porous wustite particles observed below 710°C. As reported in Chapter 2 iron oxide pellets often reduce topochemically, while the work of Turkdogan and Vinters[31], shows that providing the particles are small and rather porous uniform internal reduction may be expected to occur. The reduction morphology reported here differs from both of these extremes. Iron nucleated within the particles and only became visible at or near surface at a high degree of metallization. It has been shown that this is not due to the fact that reduction was taking place in a fluid bed.

Secondly, the fact that particles reduced completely at temperatures below 710°C, could then be kept fluidized at much higher temperatures for extended periods appeared strange. Due to the reasons given above nodules were thought to be the cause of bogging because of high adhesive properties of the iron phase, not simply because nodules increase the voidage of the bed and therefore decrease its fluidizability. Ore particles fully reduced at low temperatures would then be expected to stick to one another at high temperatures and cause defluidization. That iron particles should stick to iron particles at higher temperatures was demonstrated when a bed of powder metallurgy grade iron powder, of similar particle size as the ore, was fluidized by hydrogen and the temperature slowly raised; defluidization occurred at 550°C.

These two factors, the abnormal morphology of iron nucleation and the absence of sticking of fully reduced particles at high temperature, led to the idea that the surface of the ore particles may be coated by a film of impurities. Hence the experimental program continued with a search for such a coating and the results are described in the next section.

4.2 Impurity Film

4.2.1 Impurity Film on As-received Ore

As reported in Chapter 3 the ore concentrate was washed in a water fluidized bed prior to reduction. The purpose of this treatment was to eliminate the dust from the reduction apparatus. However such washing appeared to remove only the larger clinging particles from the ore particles. Figures 4.18, 4.19, 4.20 show the surface of washed particles as they appear in the light microscope and scanning electron microscope (S.E.M.). A film of small particles remains on the surface. Repeated washings with vigorous stirring failed to remove this film.

The film could be removed by washing the ore in various acids. Concentrated hydrochloric acid was very effective but produced many large etch pits. To avoid this the ore was washed in a 50% hydrofluoric acid solution when no pitting could be observed under high magnification.

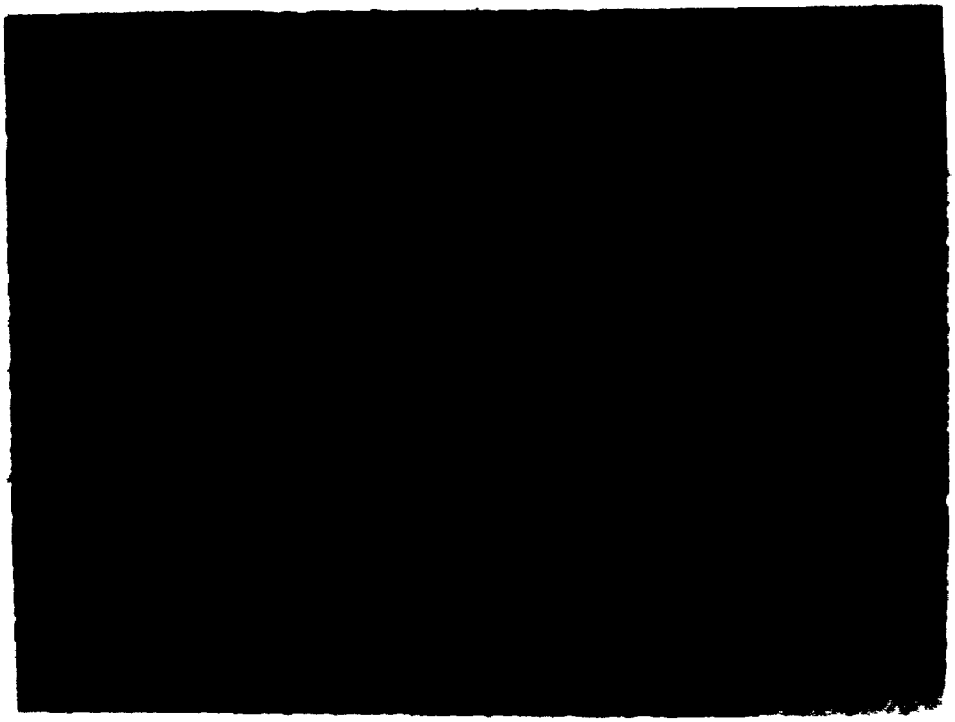

Figure 4.18 Washed As-Received Ore Particles x250

Figure 4.19 Scanning Electron Microscope Picture of Washed As-Received Ore Particle x1500

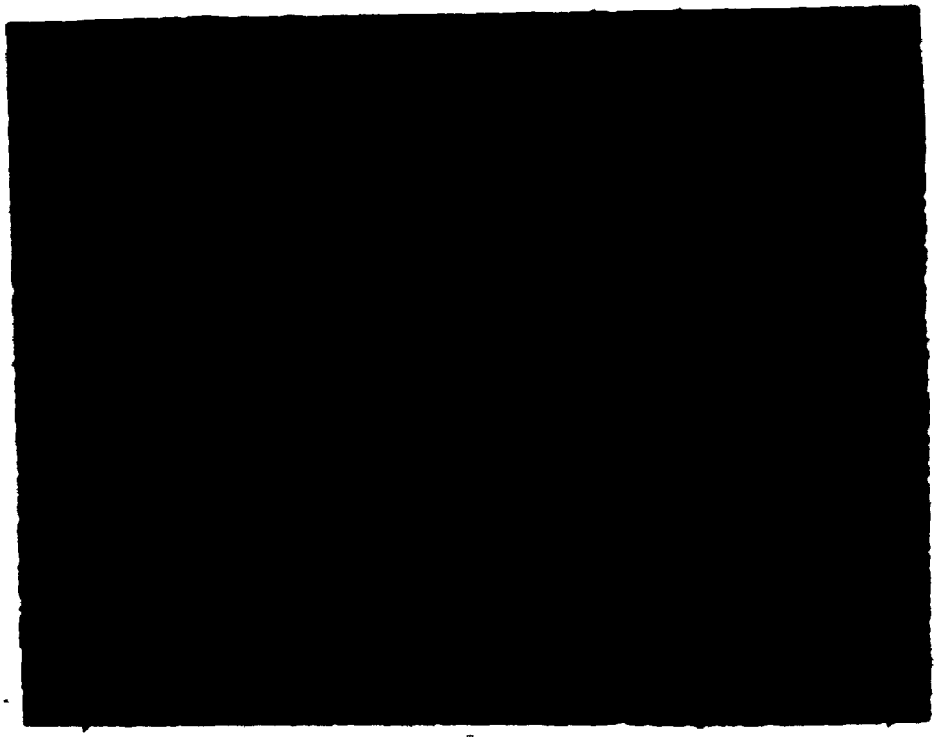

Figure 4.20 Scanning Electron Microscope Picture of Surface of Washed As-Received Ore Particle x15000

The procedure adopted was as follows. The washed ore was placed in a polyethylene beaker and just covered with a 50% HF solution and allowed to stand for ten minutes. The solution was then poured off and the ore thoroughly washed with water. Particles cleaned in this manner are shown in Figures 4.21, 4.22. Ore cleaned in this way will be termed "clean ore".

4.2.2 Analysis of Impurity Film

The material entrained during the water washing in a fluidized bed was reddish-brown in colour and up to this point was believed to be mainly hematite dust produced by the crushing and grinding necessary to beneficiate the ore and produce the concentrate.

The entrained particles were allowed to settle on to a glass slide. X-ray diffraction patterns were then obtained using a G.E. XRD-5 unit. The small particles were found to consist mainly of hematite, silica, talc and various clays.

A more detailed study showed that samples taken at the beginning of washing consisted mainly of talc, hematite, and silica. Later samples consisted mainly of hematite, silica clay minerals. Samples of solution taken after vigorous stirring of the washed ore contained comparatively large quantities of clay and silica.

Figure 4.21 Ore Cleaned in HF Solution x250

Figure 4.22 Scanning Electron Microscope Picture of Surface of Ore Cleaned in HF Solution x1500

To obtain better identification of the clays present in the film, water containing the impurities in suspension was centrifuged through a porous ceramic slab. Clay minerals occur in flake-shaped units and this produces an aggregate orientation of the flakes which enchances the basal reflections[97]. Complete identification of the clay minerals present was not possible but the presence of smectite (montmorillonite) was definitely established as its basal spacing of 14.1 A increased to 17.1 A on treating with ethylene glycerol[98]. The other clay minerals have been tentatively identified using a table given by Brindley as muscovite and chlorite. They appear in parenthesis in Table 4.1 which lists the x-ray diffraction peaks of a typical sample and their identification. No quantitative analysis was attempted.

Dissolving the impurity film from a weighed amount of ore, weighing after drying and then repeating the procedure to obtain a blank, showed that the impurity film was about 0.5% by weight of the ore.

A semi-quantitative spectrographic analysis of the as-received ore gave the following results, accurate to ± a factor of 3:- Ti 0.02%, Cu 0.02%, Al 0.3%, Si 0.1%, Mg 0.007% and Mn 0.07%.

2 OF/DE 2

TABLE 4.01

X-ray Diffraction Data From Impurity Film

Chromium Radiation

Peak Position 2θ	d Spacing	Relative Intensity	Identification	d Spacing*	Relative Intensity*
9.1	14.1	30	Smectite	14-15	100
9.25	14.2	20	(Chlorite)	13.6-14.3	30-100
12.8	10.27	5	-	-	-
13.15	9.98	15	(Muscovite)	9.9-10.1	100
13.95	9.35	80	Talc	9.2-9.4	90
18.55	7.10	30	(Chlorite)		
26.55	4.98	20	(Muscovite)	5.0	90
27.35	4.84	10	-	-	-
28.05	4.72	15	(Chlorite)	4.7-4.8	90
28.35	4.67	10	Talc	4.6-4.7	60
31.8	4.18	25	Quartz	4.21	70
36.25	3.68	11	Hematite	3.67	70
37.3	3.58	11	-	-	-
37.7	3.54	20	(Chlorite)	3.52-3.58	100
40.3	3.32	100	Quartz	3.35	100
43.1	3.11	95	Talc	3.11	100
50.20	2.69	60	Hematite	2.69	100
54.15	2.52	30	Hematite	2.51	80
54.7	2.49	10	Talc	2.47-2.48	60
55.85	2.44	15	Quartz	2.45	30
60.0	2.289	7	Quartz	2.285	30
62.55	2.205	10	Hematite	2.201	70
70.08	1.994	35	(Chlorite)	1.99-2.01	20-80
75.6	1.867	6	Talc	1.87	50
76.95	1.840	10	Hematite	1.835	70
83.85	1.713	6	-	-	-
85.05	1.693	15	Hematite	1.688	80

*Reference (99).

investigation of various heat treatments of clean ore particles covered with alumina, before reduction. Table 4.03 lists the different heat treatments, the reduction temperature and any defluidization that occurred.

In all experiments, iron was observed to have nucleated uniformly throughout the particle including at the surface as nodules. Evidently the annealing treatment produced a superior coating as defluidization did not occur at 680°C and was partially stopped at 750°C.

4.4.4 Other Coatings

Magnesium oxide, MgO: The coverage obtained was good and the bed remained fluidized for 33 minutes (bed reduced 60%) after iron nucleation at 670°C. At 780°C the bed defluidized 2 minutes after iron nucleation began. Iron nucleated and grew internally and as nodules at both temperatures.

Carbon: The results for carbon coatings are similar to those for MgO. The bed remained fluidized for 35 minutes (bed reduced 62%) after iron nucleation at 670°C but bogged shortly after iron nucleation when reduced at 780°C.

Titanium dioxide, Manganese dioxide: Coatings of these compounds were ineffective, the bed defluidizing about 5 minutes after iron nucleation at 670°C.

TABLE 4.02

Electron Microprobe Analysis

		counts in 30 seconds			counts Al / counts Si
		Aluminum	Silicon	Manganese	
water	(1)	6263	1782	490	2.9
washed	(2)	8662	2358	571	2.8
ore	(3)	16617	4413	717	2.7
particles	(4)	5233	1137	477	2.2
	(5)	4437	955	434	2.2
	(6)	7543	1856	1516	2.5
	(7)	9670	2445	582	2.6
Background		717	90	292	
clean	(1)	773	57	323	
ore	(2)	956	103	223	
particles	(3)	911	99	318	
	(4)	857	96	328	
water	(1)	7012	2349	418	2.8
washed	(2)	11243	3998	385	2.7
particles	(3)	5561	1769	384	2.9
reduced 98%	(4)	6232	2222	408	2.6

Ore reduced at higher temperatures showed complete uniform internal reduction, i.e. iron nucleated and grew uniformly throughout the bulk of the particle. Nodules formed on particles reduced at 650°C and above, their number decreasing but their apparent final size increasing the higher the temperature. Figure 4.25 shows a particle reduced 10 minutes beyond iron nucleation at 680°C. A large number of small nodules are visible. Figure 4.26 shows the larger nodules obtained at 820°C.

4.3.3 Discussion of Reduction Behavior of Clean Ore

Comparing the reduction morphology of the as-received and clean ore, the major difference is the growth of iron uniformly throughout the clean ore particles above about 640°C. With the as-received ore this only fully occurs above about 740°C, while below about 710°C iron is apparently prevented from nucleating and growing at and near the surface of the particles. The occurrence of defluidization of beds of clean ore at 595°C led to the investigation of the reduction morphology at low temperatures which proved to be topochemical below about 620°C. This in turn prompted investigation of the as-received ore at these low temperatures. Particles of as-received ore also proved to reduce almost topochemically at 620°C except once again iron was not apparent in large quantities on the surface of the particles until metallization was nearing completion. However at 600°C iron was observed

At 630°C the bed bogged in two stages, the first stage occurring about 10 minutes after the finish of the iron nucleation stage.

At 660, 680, 700 and 720°C the bed defluidized in two steps, defluidization beginning at the end of the i.n.s.

Between 750 and 840°C the bed defluidized usually in one step shortly after the end, or sometimes a little before the end of the i.n.s.

4.3.2 Reduction Morphology of Clean Ore

The reduction morphology observed before iron nucleation was similar in all respects, at all temperatures, to that previously described for the as-received ore.

At a temperature of 595°C iron nucleated and grew predominantly at or very near the surface of the particles, Figure 4.23. Internal nucleation of iron occurred only to a small extent and could often be associated with cracks in the particle. Particles taken from the bed showed continued reduction in a topochemical mode. Figure 4.24 shows a micrograph of a typical particle reduced for 80 minutes. The particle has a wustite core and an outer iron layer.

At 630°C iron nucleated at the surface and also more extensively inside the particle. Iron at the surface sometimes appeared as being raised above the surrounding wustite giving the appearance of bumps.

Figure 4.23 Clean Ore Reduced 35 Minutes at 595°C Showing Iron Growth Near Surface of Particle. x500

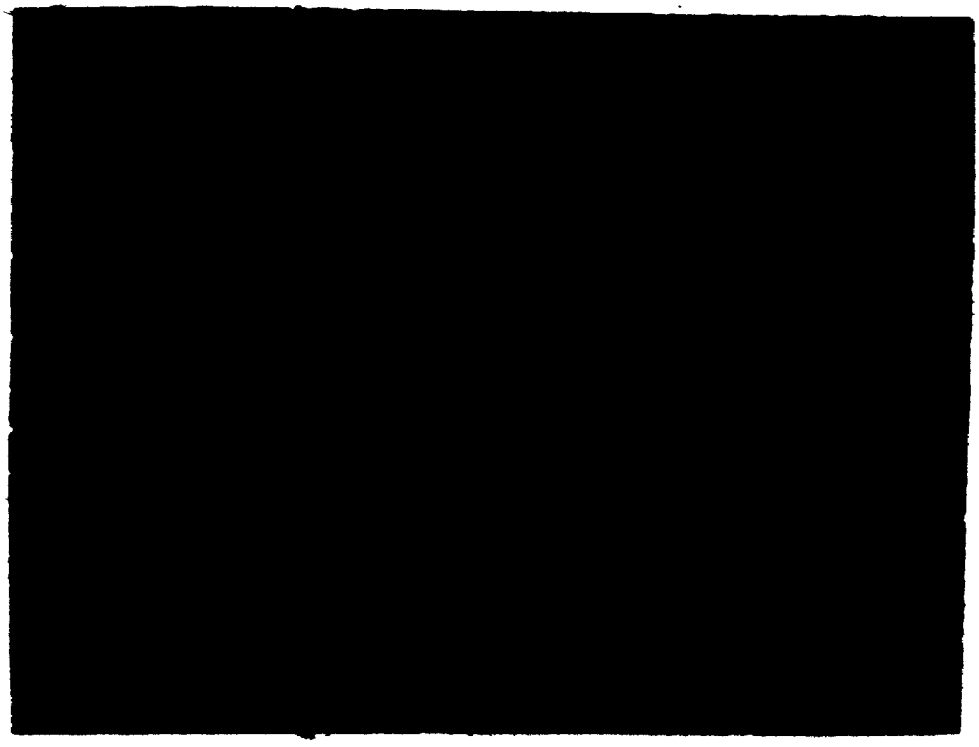

Figure 4.24 Clean Ore Reduced 80 Minutes at 595°C. x500

Ore reduced at higher temperatures showed complete uniform internal reduction, i.e. iron nucleated and grew uniformly throughout the bulk of the particle. Nodules formed on particles reduced at 650°C and above, their number decreasing but their apparent final size increasing the higher the temperature. Figure 4.25 shows a particle reduced 10 minutes beyond iron nucleation at 680°C. A large number of small nodules are visible. Figure 4.26 shows the larger nodules obtained at 820°C.

4.3.3 Discussion of Reduction Behavior of Clean Ore

Comparing the reduction morphology of the as-received and clean ore, the major difference is the growth of iron uniformly throughout the clean ore particles above about 640°C. With the as-received ore this only fully occurs above about 740°C, while below about 710°C iron is apparently prevented from nucleating and growing at and near the surface of the particles. The occurrence of defluidization of beds of clean ore at 595°C led to the investigation of the reduction morphology at low temperatures which proved to be topochemical below about 620°C. This in turn prompted investigation of the as-received ore at these low temperatures. Particles of as-received ore also proved to reduce almost topochemically at 620°C except once again iron was not apparent in large quantities on the surface of the particles until metallization was nearing completion. However at 600°C iron was observed

(a)

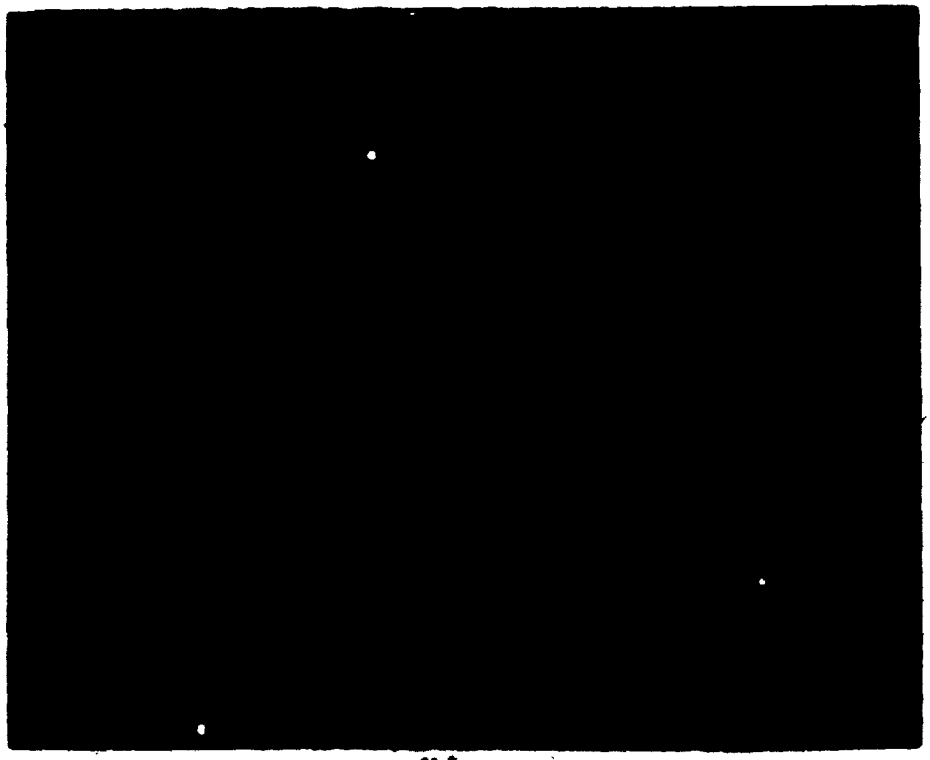

(b)

Figure 4.25 Scanning Electron Microscope Pictures of Particle Reduced at 680°C Showing Nodules of Iron
(a) x750 (b) x2500

Figure 4.26 Scanning Electron Microscope Picture of Particle Reduced at 820°C Showing Iron Nodules. x3000

at the surface shortly after the beginning of metallization and quickly covered the surface.

The defluidization of HF ore at 595°C shows that the iron phase is inherently sticky and that nodules are not necessary for defluidization to occur. This confirms the previous tentative idea that an impurity film was preventing, at certain temperatures, defluidization of the as-received ore. In addition the impurity film appears responsible for the difference in reduction morphology.

To investigate these phenomena further, the experimental program continued along two lines. First, clean ore was coated with various compounds in an effort to improve its defluidization behavior and to attempt to find the ingredient in the slime film responsible for the reduction morphology and the superior defluidization behavior of the as-received ore. Secondly, ores from other sources and reagent grade particles were investigated.

4.4 Particle Coatings

It was recognized that, although the major elements in the slime film were (besides hydrogen and oxygen) silicon and aluminum, smaller amounts of other elements, which could be the active ingredient of the slime film, were present. The spectrographic analysis, reported earlier, identified a number of these elements.

Preliminary experiments showed that the coating material must cover the ore particles extremely well before any improvement in the defluidization characteristics could be expected. This dictated that the coating material be in a very finely divided state, and that the method of application lead to good coverage. The method adopted (which has been described in Chapter 3) is similar to the method used to add bentonite to ore concentrates before balling.

4.4.1 Clay Coatings

The clays bentonite (the term bentonite is used to signify a clay containing predominantly smectite) and kaolinite produced good coatings on clean ore particles.

Both bentonite and kaolinite prevented defluidization at temperatures of 650 and 680°C. Cross-sectioned specimens obtained during reduction at these temperatures showed iron had nucleated inside the particles, nodules were absent, and that a band of wustite around the edge of the particles did not reduce until the reaction was nearing completion. This is similar to the reduction morphology of the water washed ore.

Unfortunately it was not found possible to reduce the clay covered particles at higher temperatures. The beds defluidized while heating up in nitrogen around a temperature of 720°C.

4.4.2 Silica Coatings

Three different sources of silica were used to coat the particles.

Crushed fused quartz (particle size 0.5-2 μm) did not stop defluidization at 680°C. However some particles appeared to have unreduced wustite rims after the bed had been reduced 60%. This promising trait prompted the use of more finely divided silica.

The use of colloidal silica led to excellent coverage of the particles, but the bed defluidized on heating up in nitrogen around 600°C. This may have been due to impurity additions (e.g. NaOH) used to stabilize the colloid.

The third source of silica used was fumed silica. This was prepared by decomposing silicon tetrachloride vapour in an oxy-hydrogen flame. The liquid silicon tetrachloride, contained in a conical flask, was heated on a hot plate and the vapour allowed to escape through a 1/16" internal diameter silica tube. A oxy-hydrogen burning torch held across the path of the issuing vapour, decomposed it to SiO_2 and HCl by the reaction

$$SiCl_4 + 2H_2O \rightarrow SiO_2 + 4HCl$$

The product was collected in an inverted four litre beaker. The particle size of the silica produced by this method is in the range 0.007-0.05 μm[101].

Fumed silica gave excellent coatings, and no defluidization of beds of clean ore particles covered with this material occurred during reduction up to the highest temperature investigated, 840°C. Nodules were not observed to grow, in general, at any temperature in the range 630 to 840°C. At high temperatures iron nucleated deep inside the particles and appeared to grow towards the surface. After a certain amount of metallization, therefore, the particles have a essentially unreduced shell of wustite around the outside (Figure 4.27 reduced 58% at 780°C). In one experiment the bed was kept fluidized for five hours at 840°C after the particles were fully reduced and no bogging was observed.

4.4.3 Alumina Coatings

The coverage obtained with 0.05 μm alumina was very good. However during reduction the bed bogged 9 minutes and 3 minutes after nucleation of iron at 670°C and 780°C respectively. Nodules were observed piercing the alumina coating after reduction at both temperatures.

The work of Fuwa and Ban-Ya[102] which showed that swelling of iron oxide pellets during reduction (which, as will be discussed later, may be associated with iron growing as nodules) is not observed with alumina or silica containing pellets, and the possibility that alumina could be made to produce the same reduction morphology as silica, prompted

(a)

(b)

Figure 4.27 Silica Coated Particles Reduced 58% at 780°C Showing a Essentially Unreduced Rim of Wustite At Their Surfaces. (a) x500 (b) x1000

investigation of various heat treatments of clean ore particles covered with alumina, before reduction. Table 4.03 lists the different heat treatments, the reduction temperature and any defluidization that occurred.

In all experiments, iron was observed to have nucleated uniformly throughout the particle including at the surface as nodules. Evidently the annealing treatment produced a superior coating as defluidization did not occur at 680°C and was partially stopped at 750°C.

4.4.4 Other Coatings

Magnesium oxide, MgO: The coverage obtained was good and the bed remained fluidized for 33 minutes (bed reduced 60%) after iron nucleation at 670°C. At 780°C the bed defluidized 2 minutes after iron nucleation began. Iron nucleated and grew internally and as nodules at both temperatures.

Carbon: The results for carbon coatings are similar to those for MgO. The bed remained fluidized for 35 minutes (bed reduced 62%) after iron nucleation at 670°C but bogged shortly after iron nucleation when reduced at 780°C.

Titanium dioxide, Manganese dioxide: Coatings of these compounds were ineffective, the bed defluidizing about 5 minutes after iron nucleation at 670°C.

TABLE 4.03

Alumina Coatings

Run	Heat Treatment	Reduction Temp.	Remarks
187	None	670°C	bogged
201	None	780°C	bogged
218	held 'FeO' 2 hrs. 780°C	780°C	bogged
218a	held Fe_3O_4 2 hrs. 780°C	780°C	bogged
218b	held Fe_3O_4 2 hrs. 870°C	680°C	bogged
227	held Fe_2O_3 5 hrs. 1000°C	680°C	no bogging
240	held Fe_2O_3 2 hrs. 1000°C	680°C	no bogging
242	held Fe_2O_3 2 hrs. 1000°C	750°C	defluidized slowly
243	held Fe_2O_3 2 hrs. 1000°C	830°C	bogged

Calcium oxide: Defluidization occurred shortly after iron nucleation at 670 and 780°C.

The work of Bleifuss[103] suggests that calcium in the oxide lattice produces large iron nodules on reduction. To see if this phenomenon could be observed CaO covered ore was annealed for various times and temperatures at the magnetite and wustite stages. On reduction at 670 or 780°C no difference in the size or number of nodules, compared to those formed on clean ore reduced at these same temperatures, could be detected.

4.4.5 Discussion of Coatings

The results obtained using fumed silica coatings on clean ore particles suggest that the silica in the slime film may be responsible for the observed reduction morphology of the as-received ore. Only silica (besides the clay coatings), of the compounds studied, changed the reduction morphology of the clean ore. The clays used contain silicon in their lattice but in addition there was evidence from x-ray diffraction studies that free silica was present mixed with the clay. This is often the case[104].

The coating results in general show that anything that prevents iron-iron contact will lessen the tendency for beds to defluidize. In addition they show that complete prevention of bogging is difficult if nodules grow and pierce the coating.

As silica coatings prevent nodule growth and provide a good barrier, stopping iron-iron contact, they prevent defluidization very effectively.

4.4.6 Further Experiments Involving Silica Coated Clean Ore

In this section further experiments involving silica coated HF ore are reported, which were performed to learn more about the way in which silica modifies the reduction morphology.

In a reduction experiment the temperature of the bed was raised to the reduction temperature and one hour allowed for the temperature to stabilize before the reaction was started. If beds were kept at the reduction temperature for longer times before beginning the reduction it was found that the unreduced wustite rim, when measured after a constant percentage reduction of the bed at a particular temperature, increased in size. The size of the rim was measured under the microscope at a magnification of 1000x using a calibrated graticule. Two readings were made diametrically opposite each other for each particle and a total of 100 particles measured. The average value was then calculated. The average rim size so obtained is plotted against annealing time in Figure 4.28 for a temperature of 680°C and a total reduction time of 47 minutes (bed reduced 58%).

The as-received ore gave the same results as the silica covered clean ore. This is further evidence that the active

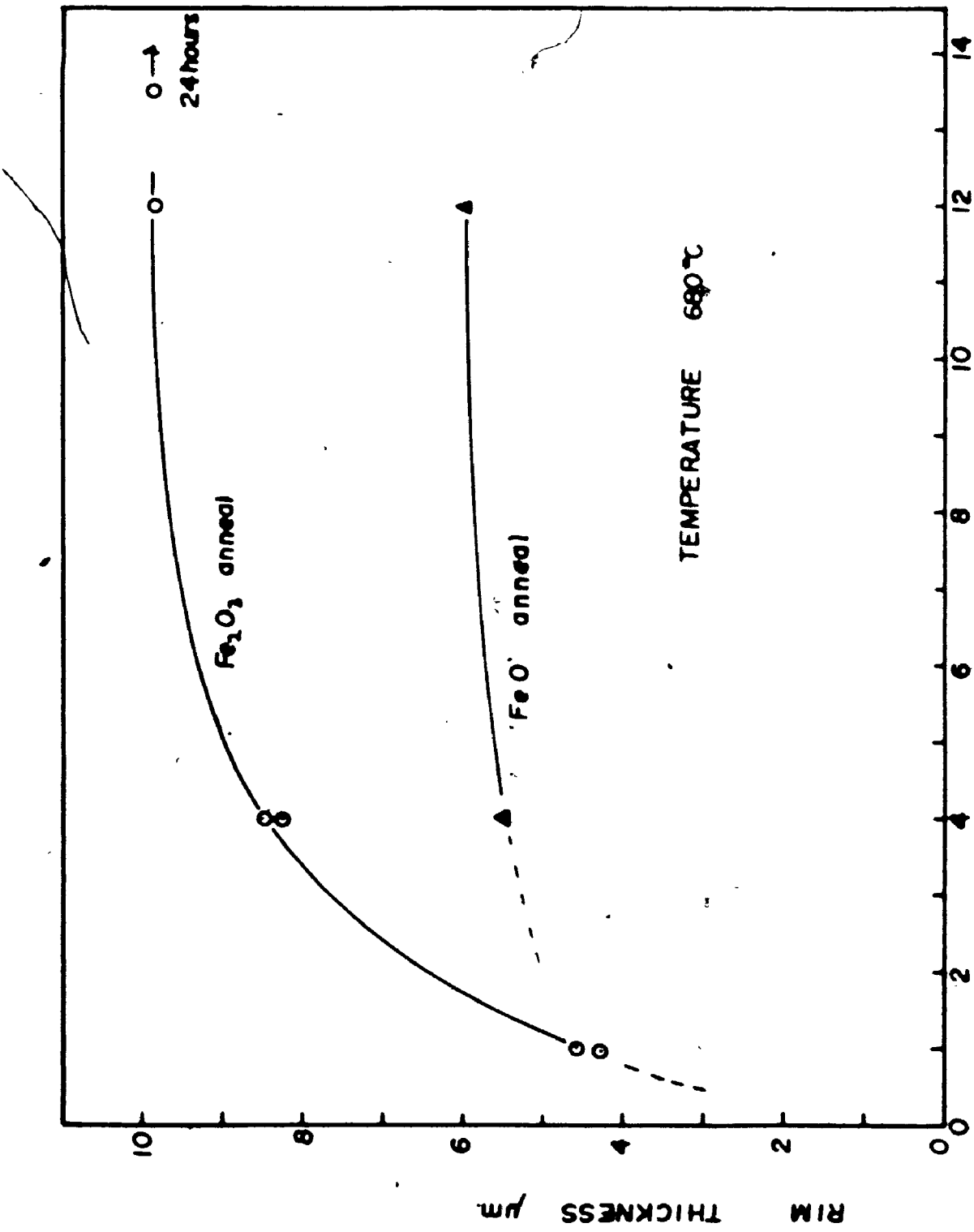

Figure 4.28 Relationship Between Rim Thickness and Annealing Time at 680°C

ingredient of the slime film is silica.

Results were also obtained (Figure 4.28) for annealing the silica coated clean ore at the wustite stage. The results include the effect of the one hour at temperature as hematite necessary to stabilize the temperature. With this treatment the increase in rim thickness with time is much smaller. Similar results were obtained when the bed was held at temperature as magnetite.

In one experiment a bed of clean ore was reduced to wustite, cooled, the particles silica coated and then reduction continued at 680°C. Nodular growth in general did not occur but the unreduced rim was small and irregular. It is thought good coverage of the particles was not obtained due to the friable nature of the wustite particles which tended to break up while the coating was being applied.

Increasing the temperature of reduction, while keeping the holding time at temperature before reduction and percentage reduction constant at one hour and 58% respectively, also increased the rim size. The results are plotted in Figure 4.29.

The results presented in this section will be discussed in Chapter 5.

4.5 Reduction and Defluidization Behavior of Reagent Grade Fe_2O_3 and Other Ores

It was recognized early in the experimental program that the behavior of pure hematite particles should be investigated

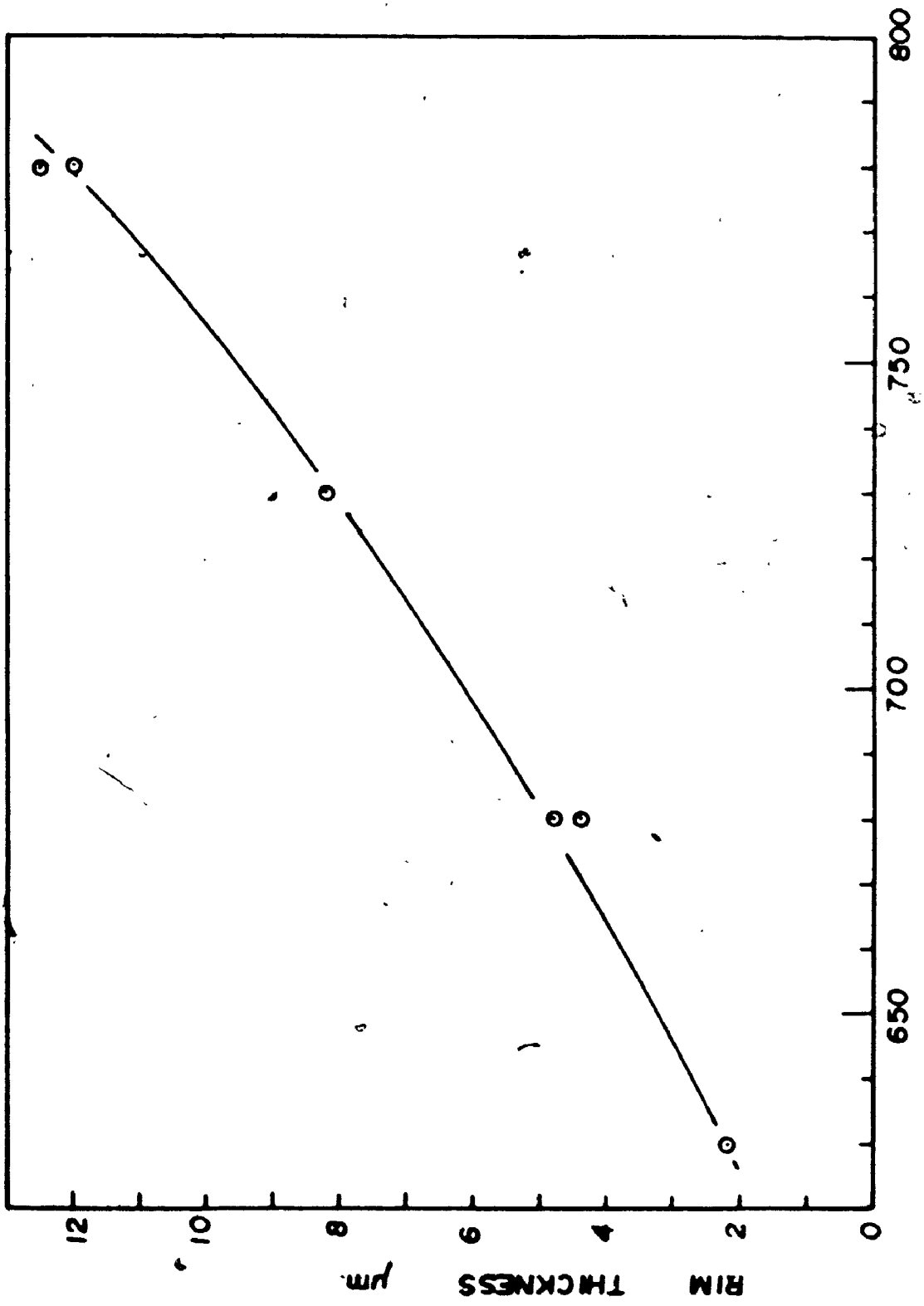

Figure 4.29 Relation Between the Rim Thickness and Reduction Temperature

to ascertain that the reduction behavior of the ore was not peculiar to this particular ore. The method of preparing reagent grade particles has already been described. The crushing of the pellets (which was done manually using a mortar and pestle) to obtain the required particle size wasted much material. Obtaining an 80 g charge for a single reduction experiment was therefore a lengthy process and only ten reduction experiments using reagent grade particles were carried out.

The reduction behavior of two other ores, a Carol Lake hematite concentrate, which according to Gray and Maak[90] has a severe tendency to bog during reduction, and a Australian goethite ore ($Fe_2O_3.H_2O$), were investigated to see if the principles found so far could be generalized to include other ores. In particular the effect of silica coatings was of interest.

Beds of reagent grade hematite particles reduced isothermally in the temperature 650-840°C behaved similarly to clean washed ore. Iron nucleated and grew both as nodules and uniformly throughout the particles at all temperatures and the bed defluidized. Figure 4.30 shows a cross-section of a particle reduced at 680°C. Beds of silica coated particles were reduced at 680 and 780°C, and no defluidization was observed. Growth of nodular iron did not, in general, occur. However the unreduced wustite rim observed after the bed had been reduced 60% was very small especially at 780°C when compared

Figure 4.30 Reagent Grade Fe_2O_3 Particle Reduced at 680°C Showing Uniform Internal Reduction and Iron Nodules x1000

Figure 4.31 Australian goethite Ore Reduced 730°C Showing Growth of Iron Nodules x500

to silica coated clean particles after similar treatment. This is thought to be due to the very porous nature of the reagent grade particles and will be discussed later.

The Carol Lake hematite appeared similar to HF ore under the microscope except that the particles were less angular. Its reduction and defluidization behavior proved very similar to the HF ore, and no differences were detected. This applies also to beds of silica coated particles reduced at 680 and 780°C.

The Australian goethite ore defluidized at 730 and 780°C but not completely at 680°C during reduction. At 680°C the quality of fluidization, after the beginning of iron formation, decreased slowly and continued to do so after the reaction was essentially complete. At all temperatures iron was observed to grow uniformly throughout the particles but nodules were only apparent at 730 and 780°C (Figure 4.31). Once again fumed silica coatings prevented nodule growth and defluidization at 680 and 780°C.

4.6 Solid State Cell Results

4.6.1 Effect of Reduction Temperature on the Measured Oxygen Potential

Examples of cell voltage versus time curves for three different temperatures are shown in Figure 4.32 (cell 2.5 cm from frit). Data to the end of reduction for the two highest temperatures was made possible by silica coating clean ore

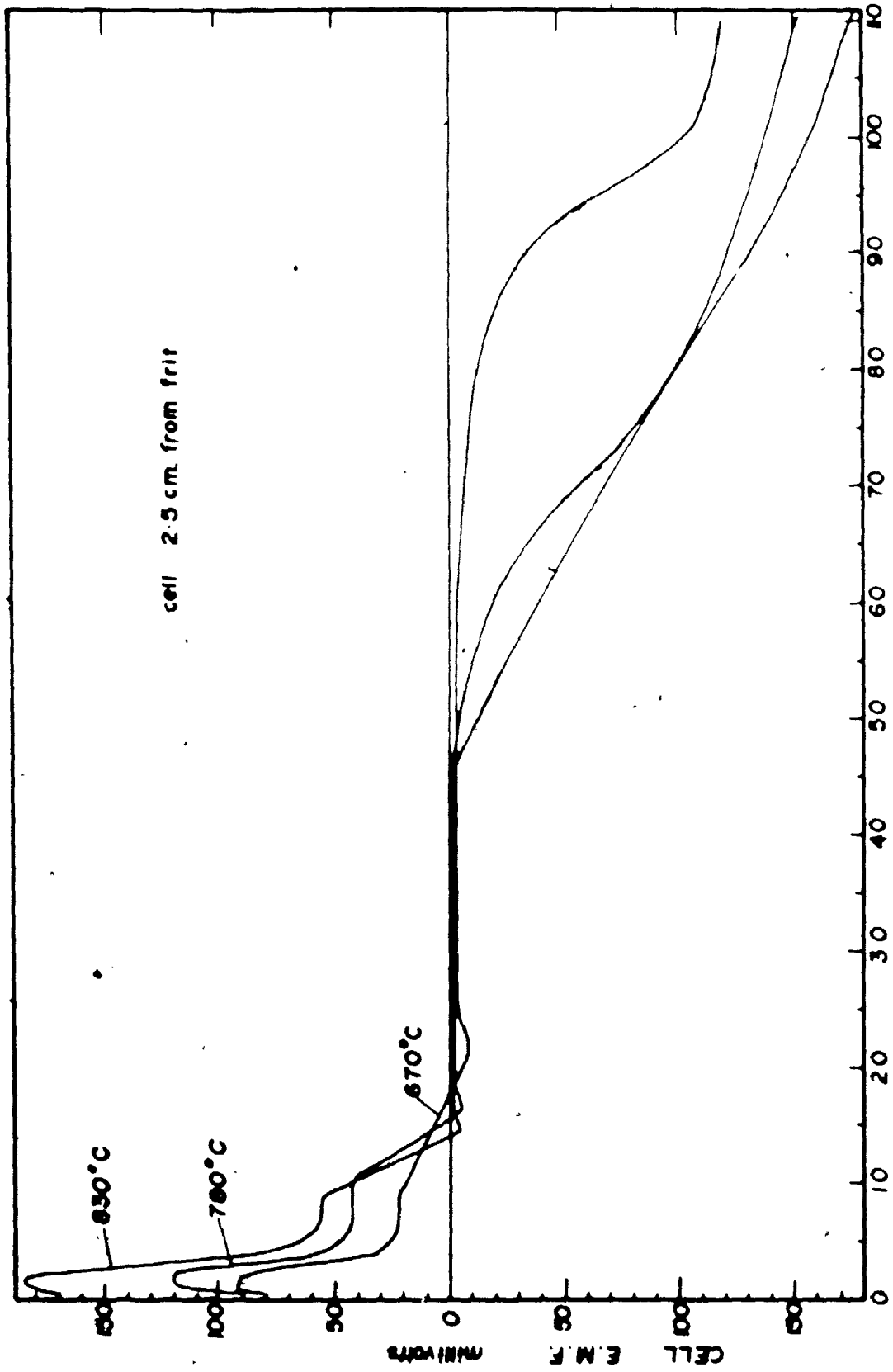

Figure 4.32 Cell Voltage-Time Curves at 670, 780 and 830°C

particles. Using the thermodynamic data given by Charette and Flengas[105] for the wustite/iron equilibrium

$$Fe + \frac{1}{2} O_2 = FeO$$

$$G_T = -62,952 + 15.403T\ (°K) \pm 100 \text{ calories/mole}$$

and the data given by Kubaschewski, Evans and Alcock[106] for the reaction

$$H_2 + \frac{1}{2} O_2 = H_2O$$

$$G_T = -57,250 + 4.48T \log T - 2.21T \pm 300 \text{ calories/mole}$$

the graphs were converted to a plot of water concentration versus time shown in Figure 4.33, using a simple computer program. The program also summed the area under the curve at 30 second intervals. Using this data and the known hydrogen flowrate approximate graphs of percentage reduction versus time can be constructed, Figure 4.34. Errors arise from:-

(1) the reduction is not complete at the measuring point,

(2) an amount of gas passes through the bed in the bubble phase which is richer in hydrogen than that between the particles which is monitored by the cell. (As described earlier bubbles passing the

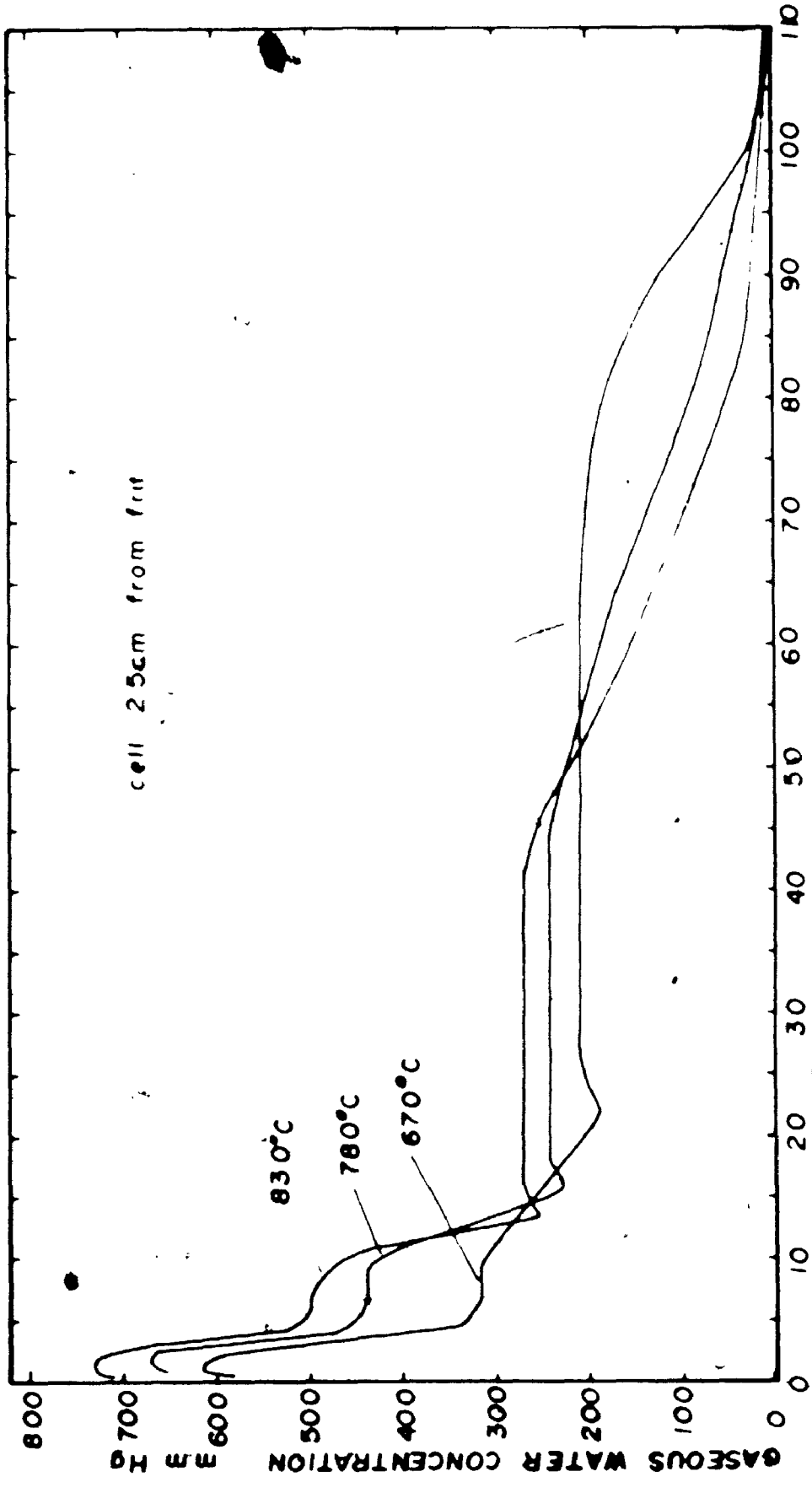

Figure 4.33 Gaseous Water Content - Time Curves For 670, 780 and 830°C

cell created a fluctuation on the otherwise steady voltage reading).

Considering (1), by comparing curves obtained at 680°C for cell positions 2.5 and 6.5 cm from the frit, calculations show that the reaction is about 93% complete 2.5 cm from the frit. The graphs are presented in the form water produced (below the cell) versus time, Figure 4.34. These graphs, once again are not strictly correct because of (2) but in turn show that (2) is small in the following way. An 80 g bed of ore produces about 27 g of water if fully reduced. If (2) is large this would increase substantially the calculated amount of water. At the same time (1), the fact that the reaction is not complete at the measuring point of the cell, should decrease the calculated amount. In fact the graphs shown in Figure 4.34 indicate a final value of about 27 g indicating that as (1) is small (2) is also. That is the composition of the gases in the bubble phase, with the flow-rate used and at least at and above 680°C, are only slightly more reducing than the gas that passes between the particles.

The same conclusion was reached by calculating the minimum throughput of hydrogen for 85% reduction (before gas phase control is lost) using the calculated equilibrium concentration of water for each step of the reduction and comparing it to the observed hydrogen throughput necessary to produce 85% reduction.

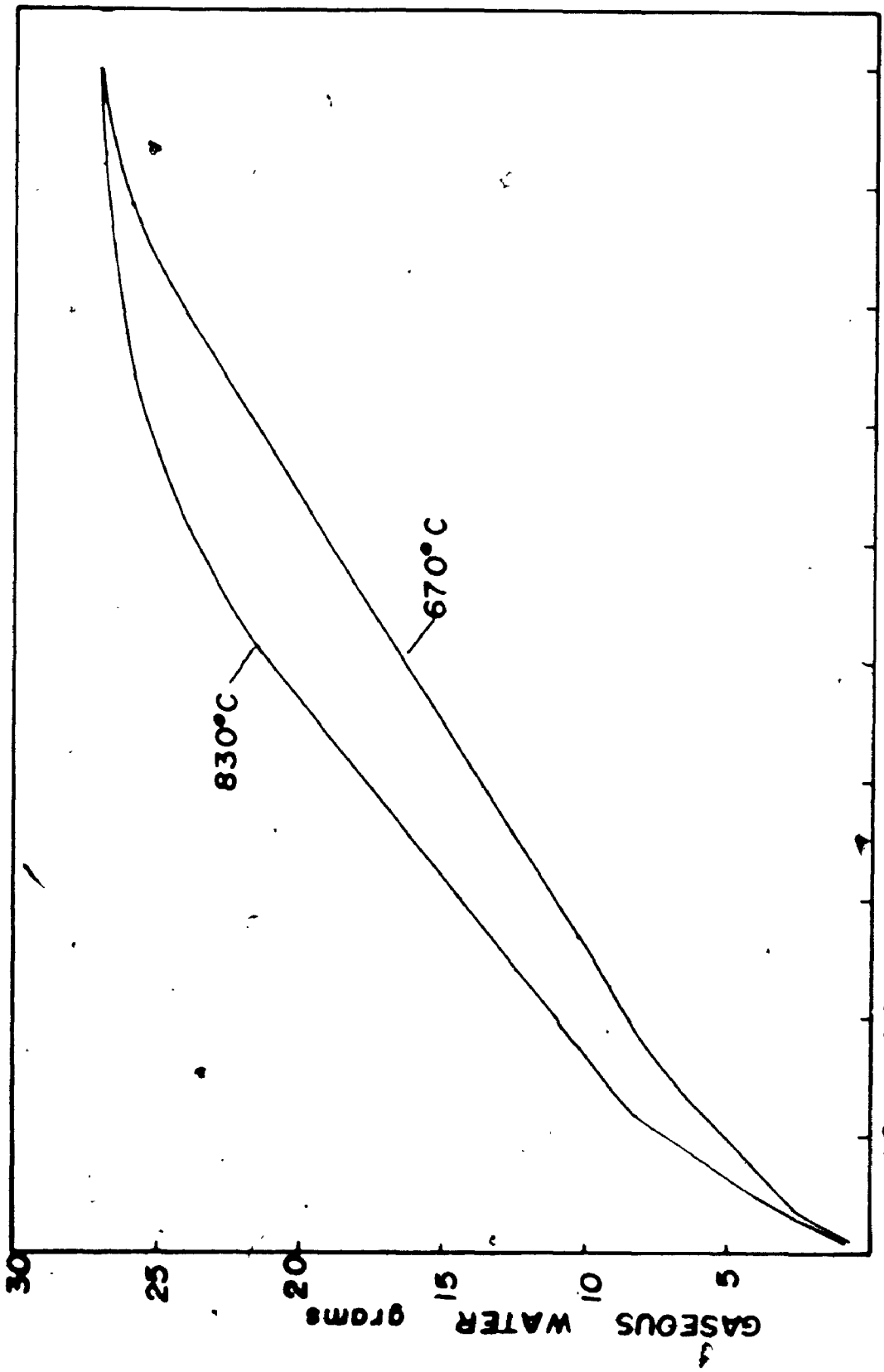

Figure 4.34 Cumulative Water Produced-Time Graphs Calculated From Cell Voltage

Two noteworthy points are evident in the graphs of Figure 4.34. First the curves distinctly show the change in reduction rate for the reactions hematite to magnetite, magnetite to wustite unlike the graphs obtained by plotting the water collected from the reaction against time. Second the graphs show only a small deviation from a smooth curve during the iron nucleation stage.

The voltage-time relationships showed that the rate of reduction of hematite to magnetite, over the temperature range 650-840°C, was independent of temperature. An interesting feature of the curves is their behavior during iron nucleation. Figure 4.35 shows the voltage-time relationships during iron nucleation (i.e. the i.n.s.) for a number of different temperatures. Figure 4.36 shows that the maximum voltage, v_1, reached below the Fe/FeO equilibrium (zero volts), during the i.n.s. increases markedly with decreasing reduction temperature. The time taken for the curve to level out to a horizontal line, $t_{1,}$ (see Figure 4.16) is plotted against reduction temperature in Figure 4.37.

4.6.2 Experiments Influencing the Voltage-Time Minima

The minima in the voltage-time curves have been associated with the nucleation of iron and possible reasons for their occurrence are discussed in Chapter 5. It was thought that the nucleation and growth of iron deep inside particles might be expected to influence the shape of the minima,

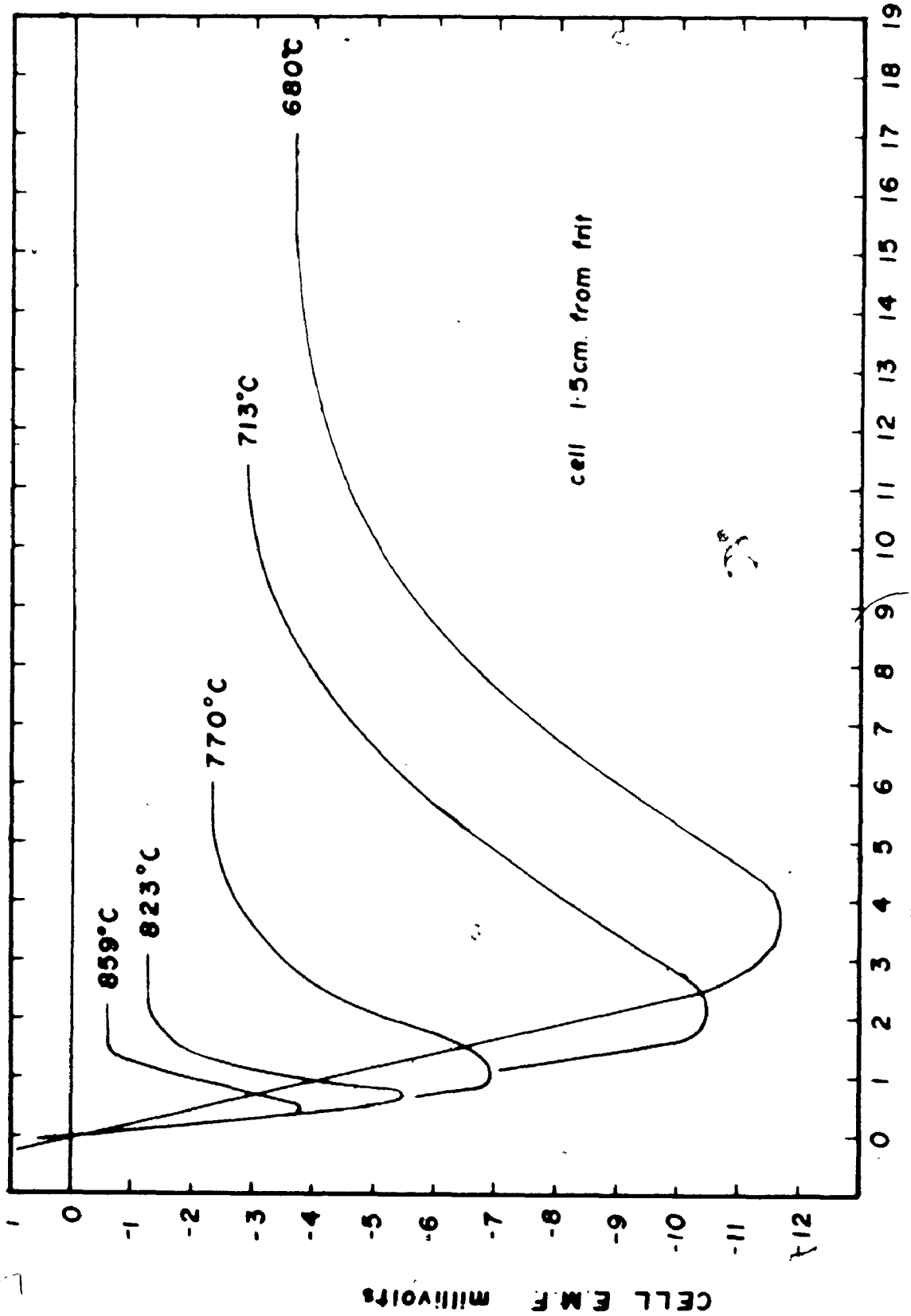

Figure 4.35 Voltage-Time Curves During Iron Nucleation at Different Temperatures

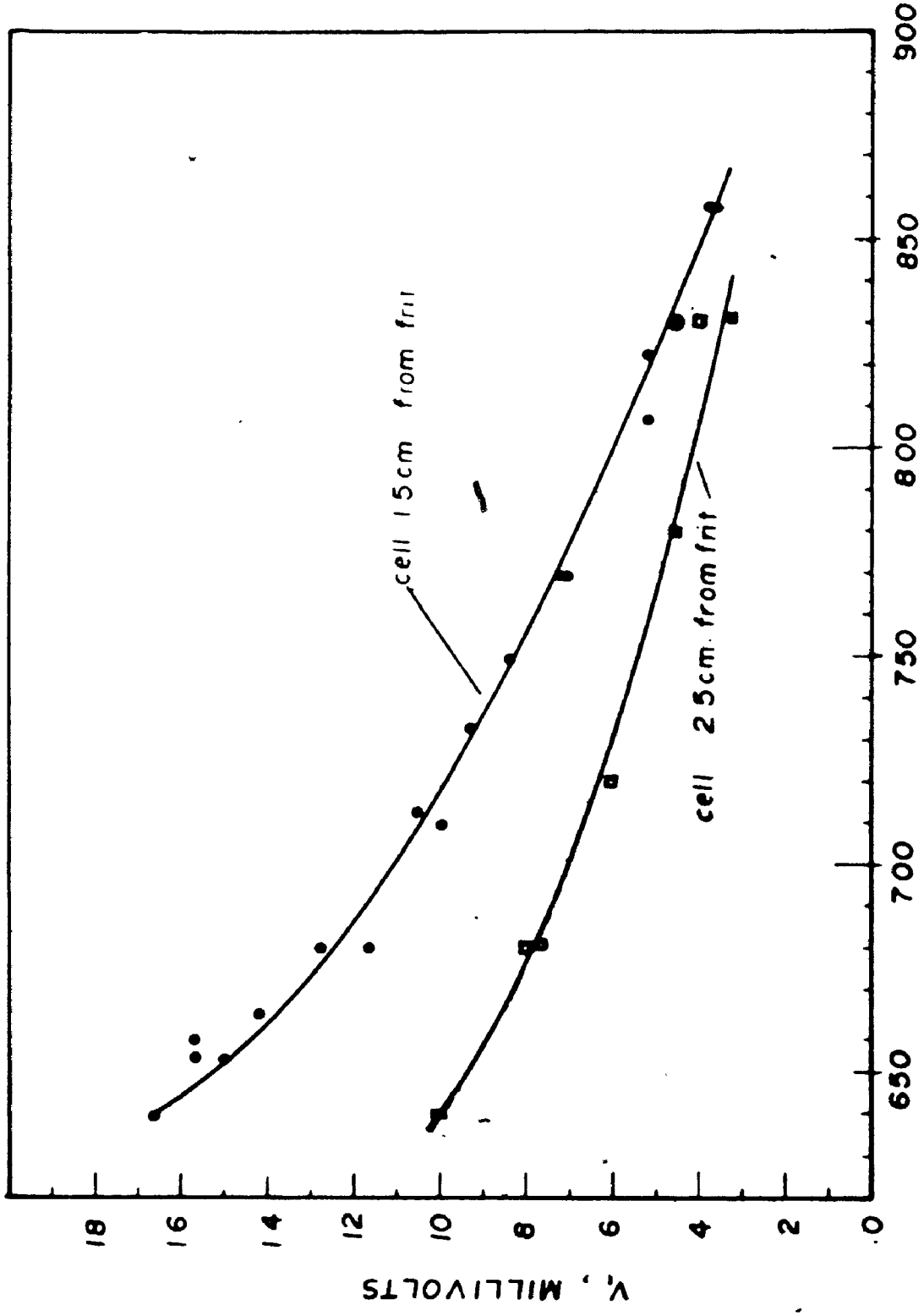

Figure 4.36 Maximum Cell Voltage, V_1, Below Fe/FeO Equilibrium Voltage During Iron Nucleation Stage at Different Reduction Temperatures

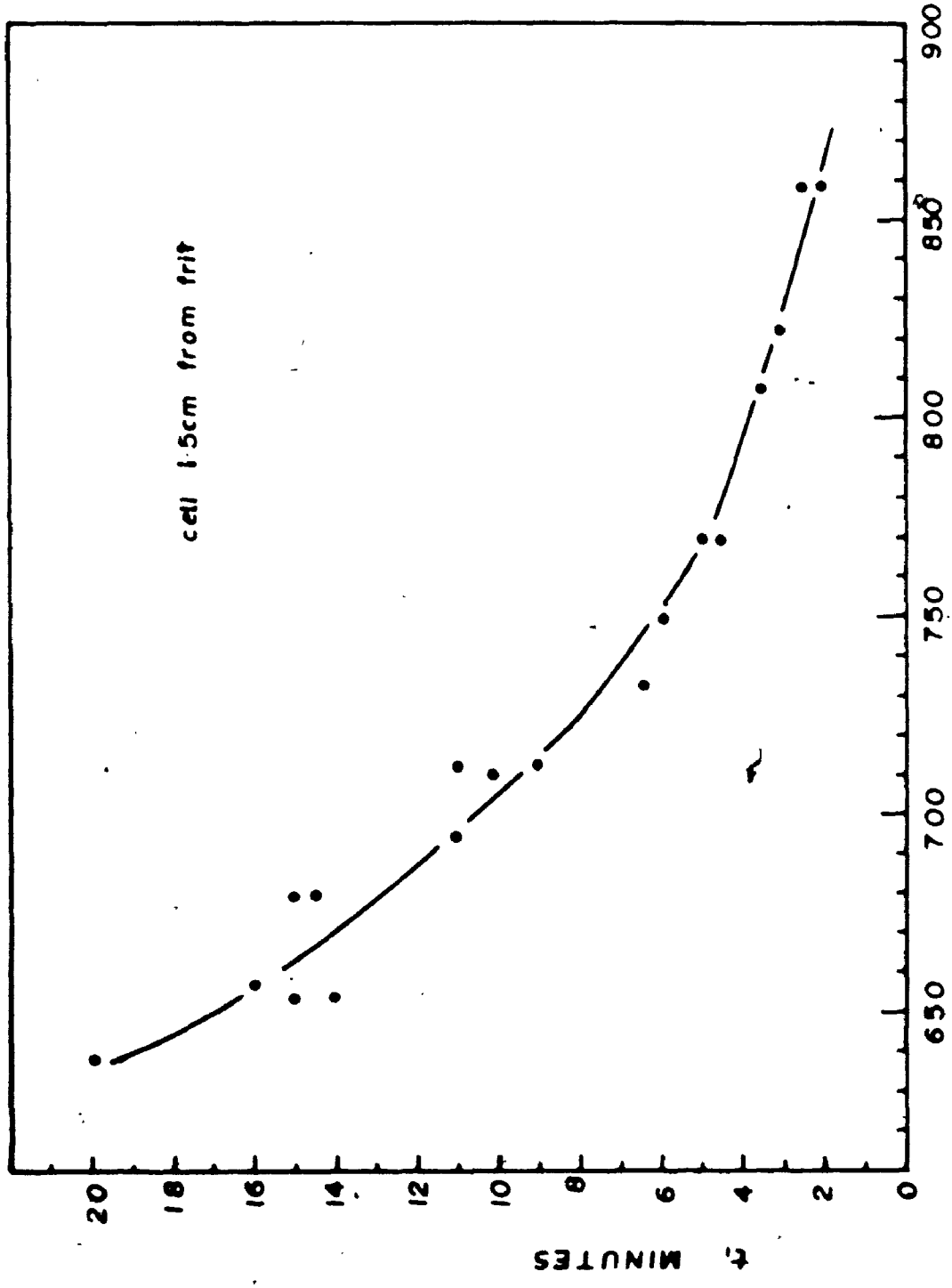

Figure 4.37 Time, t_1, For Cell Voltage To Adopt a Constant Value (see Figure 4.16) after Iron Nucleation

Comparing voltage-time curves obtained using clean ore and silica coated clean ore (and also the as-received ore reduced at 680°C with other beds annealed before reduction at the same temperature, when iron was observed to grow deeper inside the particles), this was not found to be the case. The curves, in general, were similar to within ± 1 mV and this, in turn, is similar to the reproducibility of any certain curve. It was of interest to determine what would change the shape of the minima and two series of experiments were carried out for this purpose.

(1) Annealing: Batches of ore reduced to wustite at 670°C were annealed for 90 minutes at a higher temperature, the temperature adjusted again to 670°C and the reduction continued. The voltages v_1 and v_2 increased with annealing temperature (Figure 4.38).

(2) Two Temperature Experiments: When batches of ore were reduced at temperatures above 670°C to wustite, and then further reduced at 670°C, large increases in v_1 and v_2 occurred. Figure 4.39 shows this phenomenon for a number of initial reduction temperatures.

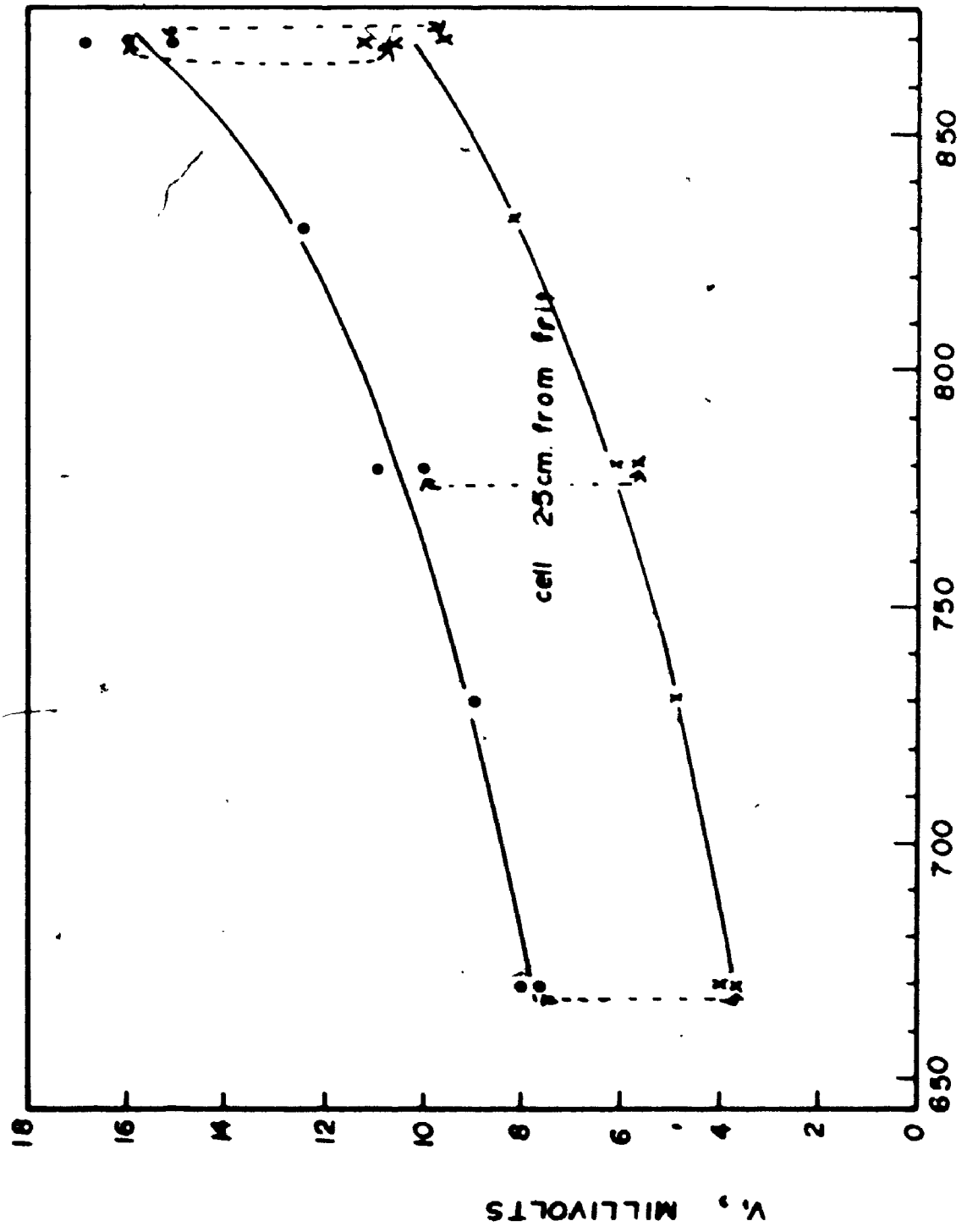

Figure 4.38 Relationship Between V_j and Annealing Temperature

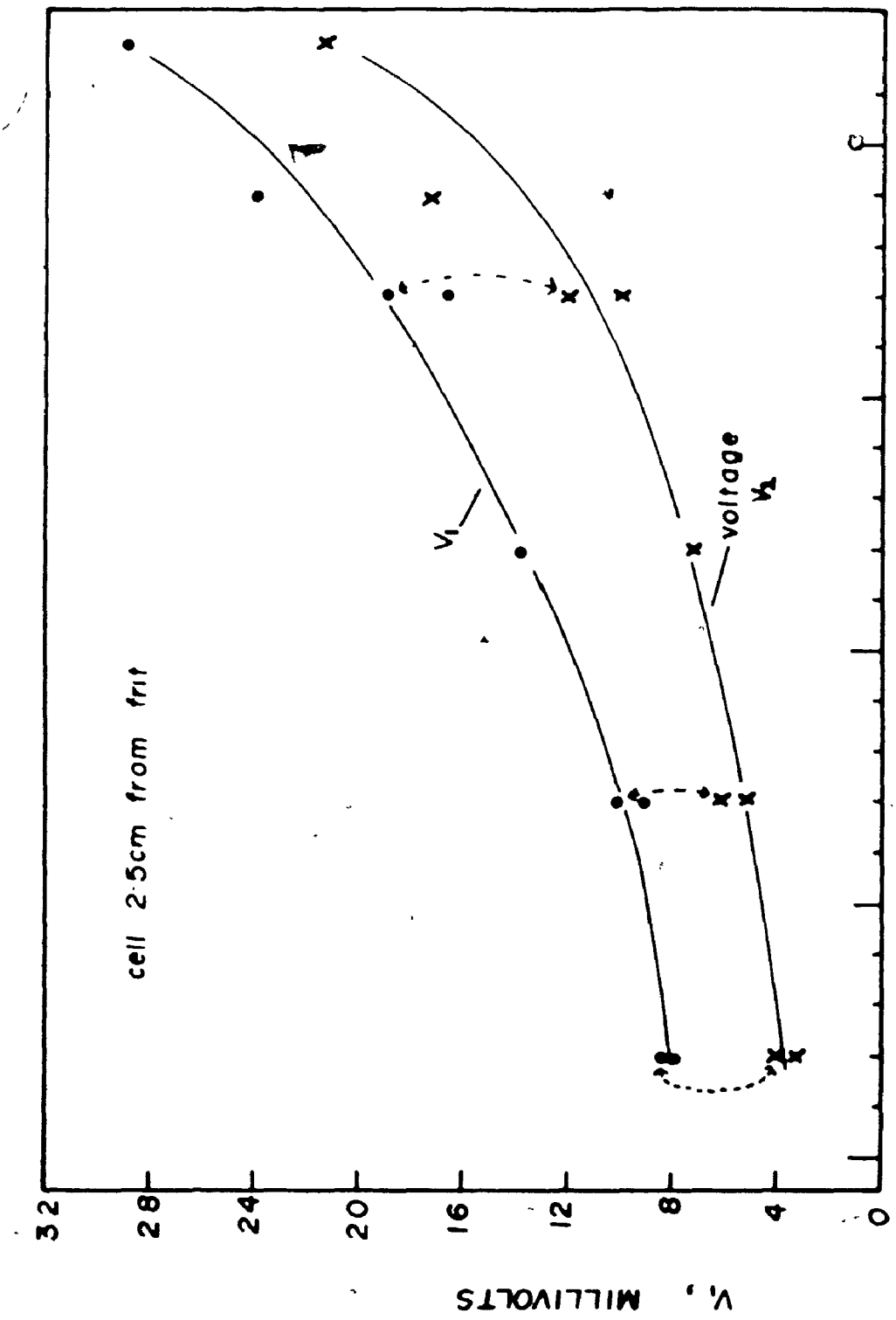

Figure 4.39 Relationship Between V_1, V_2 and Pre-Reduction Temperature

CHAPTER 5

DISCUSSION

5.1 Defluidization Phenomena

In section 4.1.9 a number of factors were presented which indicated that iron nodules caused defluidization of the as-received ore above about 710°C. In the light of the work described subsequently it is clear that this simple statement is still valid but that its simplicity masks the complete truth.

Using clean ore when the composition of the particles in the bed was essentially hematite, or magnetite, or wustite, it was determined that there was no tendency towards defluidization at temperatures up to 900°C (the highest temperature investigated). When iron is present at the surface of the particles, on the other hand, defluidization can occur at much lower temperatures. For example clean ore defluidized completely at 595°C when reduction was near completion, although nodules did not form. The iron phase alone, therefore, is responsible for sticking and defluidization. The slime film on the as-received ore prevents iron-iron contact and therefore bogging unless nodules grow through the impurity layer and can then stick to one another.

The above interpretation together with the observed reduction morphology of the as-received ore below 710°C, leads to an explanation of the results of the two temperature reduction experiments presented in section 4.1.2. In these experiments ore was partially reduced at 630°C and then further reduced at 790 or 870°C. If the ore was pre-reduced sufficiently past the iron nucleation stage at 630°C, no new nucleation of iron, particularly as nodules, occurred at 790°C, even though an unreduced wustite shell exists at the surface. The iron phase grows to the outside of the particles and the slime film remains intact at the surface preventing sticking and defluidization. Similar comments apply when the final reduction temperature was 870°C except the tendency towards defluidization was greater and in this case some nodule growth was observed.

The slime film appears to be quite wear resistant as ore fully reduced at 630°C did not show any loss in the degree of fluidization at 790°C during a five hour period of fluidization. Only a small loss of fluidization occurred after 5 hours at a temperature of 870°C.

Although care is needed in extrapolating phenomena from one size reactor and set of conditions to other sizes and conditions, the present study is believed to show that the tendency for a bed to defluidize will be greater shortly after iron nucleation (due to iron nodule growth) or will increase as the degree of metallization increases (due to increasing

iron surface area). Most workers find bogging a problem at high metallization as discussed in section 2.3.4. However the observation of Hyde[82] and Whalley[91] who found the tendency towards bogging was greatest when the bed was 20-50% reduced may be explained by nodule formation. Gray and Maak[90] also attributed defluidization to the growth of iron nodules, as they found that pre-reducing ore at low temperatures, when an iron layer but no nodules are formed on the particles, allowed fluidized reduction to the end of metallization at high temperatures. Without a pre-reduction treatment the bed defluidized.

Ezz[66] found defluidization occurred at a higher percentage reduction the more impure the ore and expressed the opinion that this was due to gangue diminishing iron-iron contact. The beneficial effect of a small amount of gangue if in the form of a slime film on the particles is apparent from the present work. On the other hand Bhat and Whitehead[63] determined that a silica to ore ratio of 3 to 1 was needed, if the silica particle size was similar to the ore particle size, to avoid defluidization at 800°C. The importance of the physical nature of gangue present may help to explain the results of Brown et al[83] who found that a simple chemical analysis of ten different ores did not reveal their susceptibility to defluidization.

5.2 Particle Coatings

First attempts to coat clean ore particles to influence the defluidization behavior of beds of ore showed that the coverage had to be excellent before any effect became discernable. An interest in simulating the slime film and the presence of clays in this film, led to the examination of clay coatings. Clays proved the easiest materials to work with, the coverage obtained being excellent in each case. This particularly applies to bentonite, and has been observed and discussed by Grim[107] in connection with moulding sands.

As reported before bentonite and kaolinite covered particles behaved similar to the as-received ore at 680°C and below. Nodules did not grow and bogging was prevented. Unfortunately clay covered particles could not be heated above about 720°C in nitrogen without the bed defluidizing. Observation showed no apparent reason for this but it may be due to the decomposition of the clay mineral structure. For example Furlong[108], using an electron microscope, has observed that spots of liquid (probably siliceous) are expelled from smectite clays, starting around 600°C and increasing in number to 850°C.

The later finding that silica is responsible for the reduction morphology of the as-received ore below 710°C poses the question as to how the clays also produce the same morphology. X-ray diffraction studies showed the clays used

contained free silica. Silica may also form when the clay decomposes on heating (for example kaolinite, after the loss of its 'OH lattice water' around 525°C, adopts a near amorphous state which may be considered an intimate mixture of SiO_2 and Al_2O_3 [109]). In addition the clay may simply play the same role as silica, a point which is discussed later.

Using fused quartz ground to a particle size of less than 3 μm, the preliminary experiments with silica suggested it alone was responsible for the reduction morphology observed with the as-received ore below 710°C. However the coverage was poor and only a small number of particles showed the sought-for reduction morphology. Nodules grew on most particles and the bed defluidized above about 650°C. The excellent coverage obtained with fumed silica and the resulting reduction morphology and ability to prevent defluidization at 840°C, already described, again emphasizes the importance of coverage.

The results of experiments with other coatings show only a slight improvement in the defluidization characteristics of beds of ore. This is thought to be due to the prevention, to some extent, of iron-iron contact. Unlike silica coatings they do not change the morphology of reduction, and heat treatments aimed at causing a change proved unsuccessful. Probably the variable results obtained with these coatings reflect the degree to which the particles were covered.

5.3 Relation to Other Work

Pellets made from certain ores have been observed to undergo 'catastrophic swelling'[103] during reduction. Early work[110] suggested a number of reasons for this phenomena but recent research has shown that the growth of fibrous iron from wustite is probably responsible[102,103]. It has also been shown that calcium[103,111] and sodium[112,113] additions promote the growth of large nodules, while silica and alumina prevent swelling[102]. The importance of nodules in this work leads to the idea that pellets of ores observed to undergo abnormal swelling may also be highly susceptible to defluidization during reduction.

5.4 Reduction Kinetics

For the greater part of the reduction the reaction is gas phase controlled, i.e. controlled by the rate of supply of the reducing gas. The rate data, obtained from water collection, for the steps hematite to wustite (Figure 4.13) and for the greater part of wustite to iron (Figure 5.1) show relatively small increases with increase in temperature. This reflects the increase in chemical utilization of the gas due to more favourable thermodynamic equilibrium at higher temperatures. This is in agreement with the results of other workers[63,64,66,71].

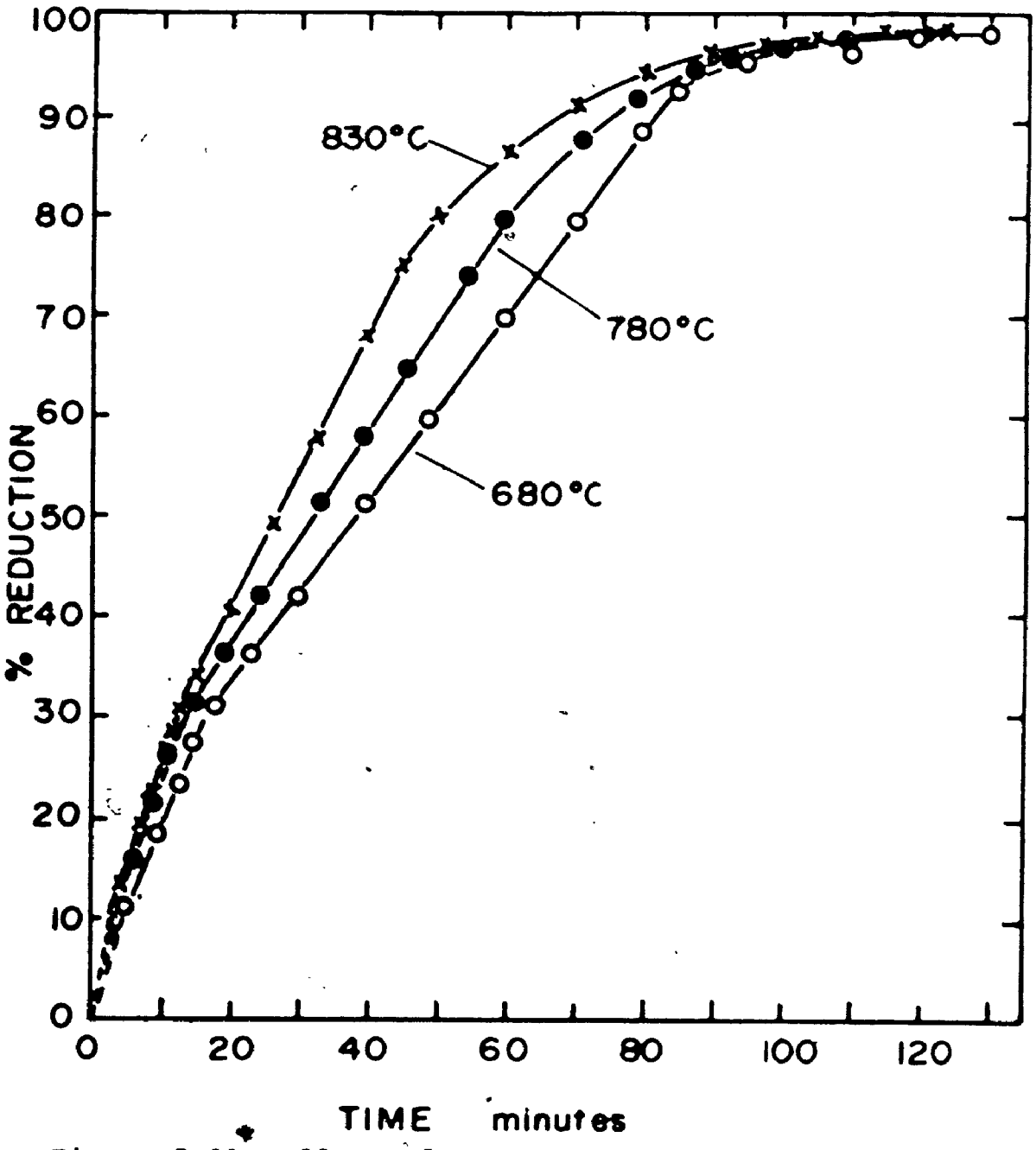

Figure 5.01 Effect of Temperature on the Reaction Rate (Data Obtained From Water Collection)

For the last part of the reduction of wustite to iron the rate controlling step changes. During this stage metallography reveals the particles to be mostly iron with wustite "islands". These islands appear to be completely surrounded by dense iron, suggesting access of reducing gas through pores is limited. Lien et al[29] have suggested that the rate controlling step in the reduction of such islands of wustite is oxygen ion diffusion in the iron.

In agreement with other authors[68,71], the change in the rate controlling step appears to occur at a lower percentage reduction the higher the reduction temperature (Figure 5.1). Feinman and Drexler[71] attributed this phenomena to the sintering and collapse of the internal pore structure, so reducing the effective diffusivity of reactant and product gases within the iron layer. In the present work, observable pores grew less in number but apparently larger in diameter as the reduction temperature was increased, so isolating islands of wustite earlier in the reduction.

Solid State Cell

The results obtained from the solid state cell allow a more detailed discussion of the reduction kinetics.

Solid state cells are well suited for operation in a fluidized beds as the temperature of a fluidized bed is usually very uniform due to the good mixing of the particles. In addition the heat requirements for an exothermic or

endothermic reaction can be transmitted efficiently due to the fluidized bed's good heat transfer characteristics, without fear of a substantial temperature difference between the bed and cell. This is a necessary requirement for precise voltage readings. For example near the Fe/FeO equilibrium oxygen potential calculation shows that a temperature difference of 3°C would produce (neglecting thermal e.m.f.s. which are known to be small[114]) a voltage reading in error by about 1 mV. The temperature in the cell was always within 2°C of that in the bed except after the occurrence of defluidization when the temperature of the bed suddenly rose and temperature gradients were formed.

If during the reduction of wustite to iron the gas flow was turned off and time allowed for temperature gradients to dissipate, the voltage of the cell was usually found to be within 0.2 mV of zero. Larger voltages indicated excessive thermal e.m.f.s. or faulty contacts and the results were discarded.

The change in water concentration with time during reduction obtained from the voltage of the cell, suggests that the bed of ore completely or substantially reduces to the next lower oxide before reducing to the next lowest one again. This was confirmed metallographically and by x-ray diffraction studies, as reported before, and is in agreement with the work of Bhat and Whitehead[63].

In Figure 5.02 the concentration of gaseous water vapour in thermodynamic equilibrium with Fe_2O_3/Fe_3O_4, Fe_3O_4/Fe_xO, and Fe_yO/Fe is plotted against composition for a temperature of 830°C. The similarity between this diagram and the experimental water concentration-time curves is apparent. The gas utilization at some point in the bed, when the reaction is proceeding at a finite rate, is somewhat less, as shown schematically by line AB. The difference between the two values of gas utilization represents the driving force (to overcome the various resistances to the reaction as discussed in section 2.2.1) for the reaction at that point. The equilibrium lines can be thought of as the gas utilization at zero reduction rate.

Some of the interesting features of the emf-time curves will now be described and discussed. When the bed, fluidized by nitrogen, had attained a steady temperature, the fluidizing gas was quickly changed to hydrogen and the oxygen potential, as shown in Figure 4.15 fell quickly from its initial high value in nitrogen and then increased as the reduction of hematite to magnetite gained momentum. This behavior suggests the reaction is autocatalytic. The time from the start of the reaction to when the gas utilization was a maximum proved independent of temperature and the same if the initial atmosphere was nitrogen or argon.

As reported previously the reduction of hematite to magnetite occurred, using the same flowrate, during the same

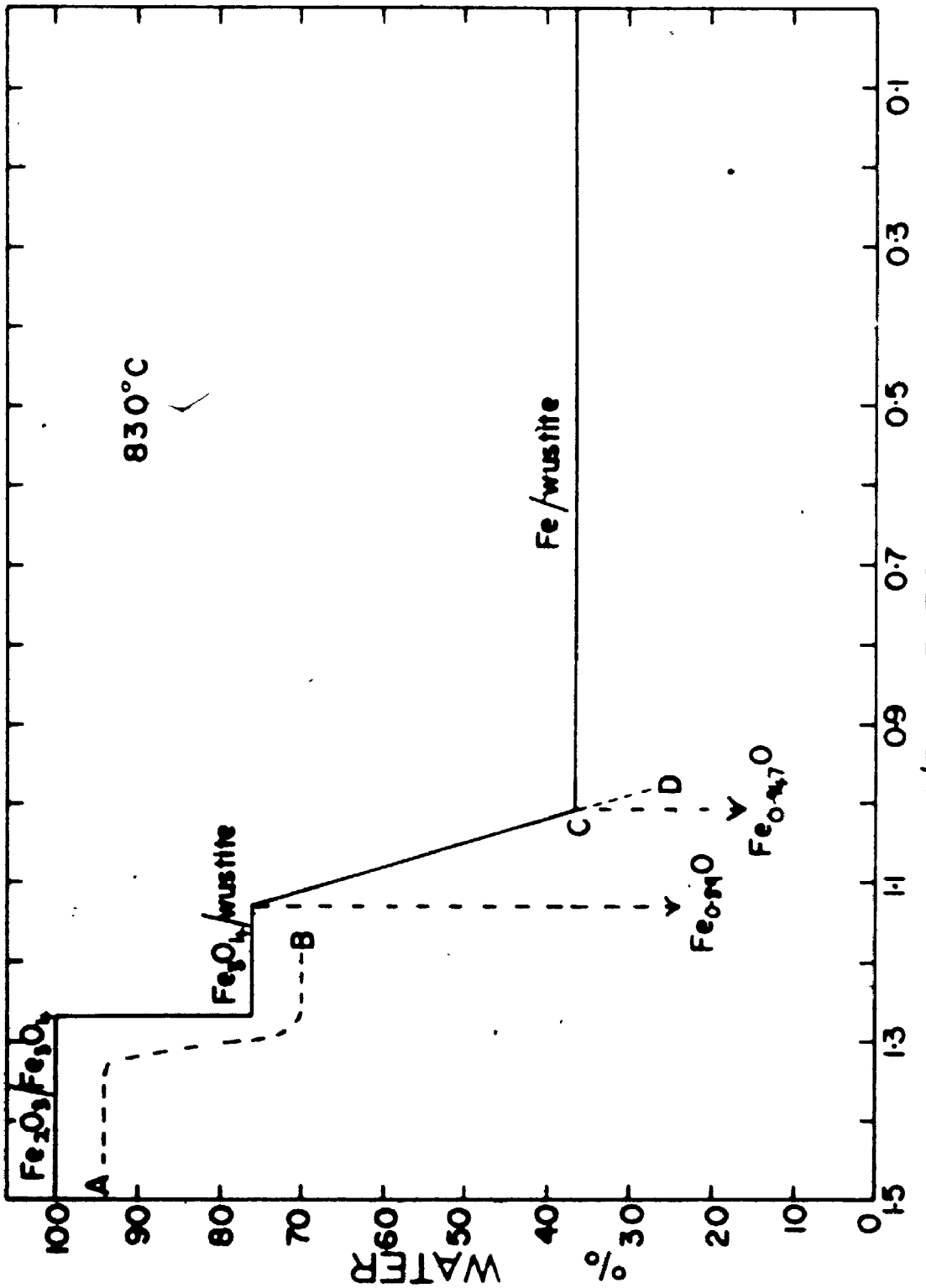

Figure 5.02 % Gaseous Water in H_2/H_2O Mixtures in Equilibrium With the Oxides of Iron at 830°C

time interval at all temperatures. Figure 4.33 shows that the water concentration reached in the gas was equivalent to a partial pressure of about 730, 670, and 615 mm of Hg at temperatures of 830, 780 and 680°C, 2.5 cm from the gas distributor. When the measuring point of the cell was 6 cm, from the frit a value of approximately 745 mm of Hg was obtained for all three reduction temperatures (about 98% of the equilibrium concentration).

After the hematite/magnetite plateau the oxygen potential dropped smoothly to the magnetite/wustite plateau. No minima occurred in the curves (as observed at the beginning of the wustite to iron reaction) as wustite formed from magnetite. Following the completion of the last mentioned reaction the oxygen potential decreases slowly toward the Fe/FeO equilibrium oxygen potential as wustite is reduced through its phase field. After the 'iron nucleation stage', which is to be discussed presently, wustite is reduced to iron during the next long plateau. The drop in oxygen potential when this reaction nears completion has been identified with the reduction of isolated "islands of wustite" as described previously.

5.4.1 Iron Nucleation

The minima in the voltage time curves, as iron nucleates will now be discussed. The observance of an incubation period at the start of a reaction or phase transformation is common.

In the present case there appear to be at least three possible causes for the observed minima.

(1) A supersaturation of wustite with respect to iron is needed to form iron nuclei.

(2) The rate of oxygen removal from wustite may be increased if iron is present. That is the reaction is autocatalytic.

(3) As iron forms the particles become more porous, decreasing the values of the various resistances to the reaction and increasing the rate.

Before discussing these points, a further experiment is described. In Figure 5.03 two experimental e.m.f.-time curves are shown representing the gas phase composition (or gas utilization) at points 6 cm and 2 cm from the gas distributor (curves 1 and 2 respectively), obtained during a single reduction experiment at 670°C. (Curve 1 was obtained by attaching a second external electrode to the cell at the required position). As the curves approach their minima they become further apart from each other and from curve AB. Line AB represents the average oxygen potential of the wustite particles in the bed. The three points X, Y and Z defining this line are experimental points obtained by stopping the reduction in three separate experiments (as this disturbs the temperature and the concentration gradients within the

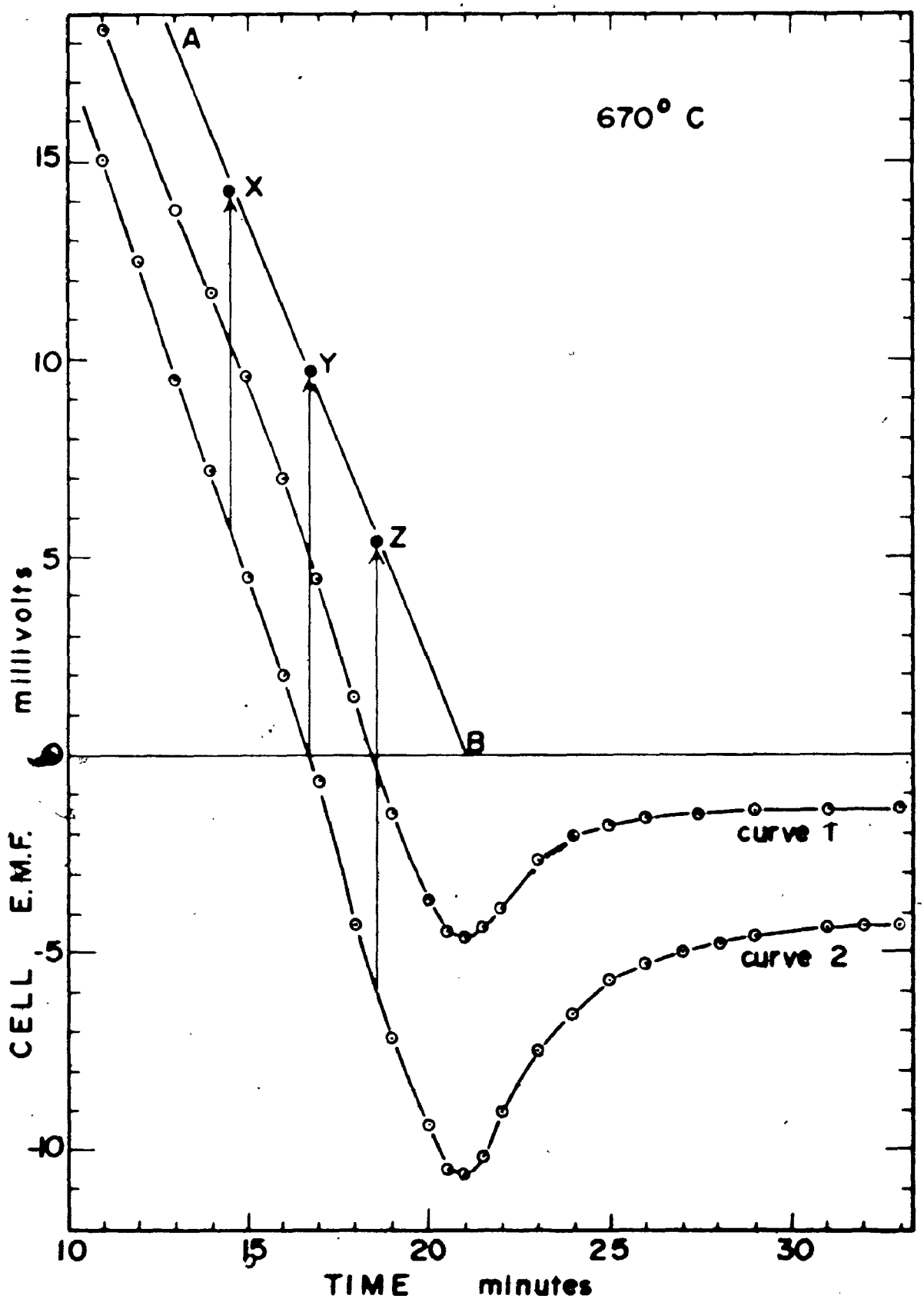

Figure 5.03 Cell Voltage-Time Curves in Region of Iron Nucleation for Two Cell Positions

particles) and allowing time for equilibrium to be attained.

If the minima in the curves are due to the necessity of a supersaturation of wustite with respect to iron for iron nuclei to form, the rate of iron nucleation would be expected to be the greatest at the minima. (Samples taken from the bed about 4 minutes after the minima at 680°C showed the majority of particles had very small 'spots' of iron. Some further reduction and growth is necessary after nucleation for the nuclei to obtain a observable size). To conclude that a supersaturation has been detected the minima would have to occur after point B (where curve AB intersects the line drawn at zero millivolts) in time, as B represents the time at which the average composition of the particles corresponds to the equilibrium Fe/FeO oxygen potential. The required supersaturation decreases the oxygen activity of the wustite and therefore the phase boundary reaction rate[115] and gas utilization. The drop in the maximum possible gas utilization is schematically shown by line CD in Figure 5.02. Such a supersaturation is, of course, required by nucleation theory. Wagner[33] was able to measure the amount of supersaturation required for silver nucleation during the reduction of silver sulphide by monitoring the silver activity. The curves obtained by him are very similar in appearance to those under discussion.

The point B in Figure 5.03 approximately coincides with the minima in time but the results are not accurate enough to determine if, in reality, this is the case.

An autocatalytic reaction[5] is a possible cause of the minima in the curves. Engell[116] expressed the opinion from work he reviewed that "the removal of oxygen (from wustite) is apparently very much quicker if the wustite surface is in contact with iron", and that this may be due to catalysis of the phase boundary reaction at the point of contact of the iron and wustite. The increased rate of the phase boundary reaction after nucleation of iron may therefore increase the gas utilization and so produce the observed minima.

Engell[115] and Kohl and Engell[117] interpreted the increase in reaction rate at the start of the reduction of wustite to iron at temperatures in the range 800-1050°C as due to an increase in surface area. It is thought that this is unlikely to explain the minima in the present case as iron growth has only just begun and the increase in porosity of the already porous particles must be small.

The above discussion implies that it is not possible to distinguish between causes (1), (2), and (3) above (although (3) is not considered a likely cause) from the experimental results. Further work would be required to clearly resolve this question.

When reduction at 670°C was stopped in the wustite phase field and the particles annealed at a higher temperature, the magnitudes of v_1 (e.m.f. at which the minimum occurred) and v_2 (e.m.f. after the i.n.s., see Figure 4.16) on continuing the reduction at 670°C were increased

(Figure 4.38), above their values for isothermal reduction at 670°C. The increasing value of v_2 with annealing temperature indicates the resistance to the reduction of FeO to Fe increases with annealing temperature, i.e. the rate of the phase boundary reaction solid state or gaseous diffusion has been decreased. In principle annealing could effect all three resistances by decreasing the available surface area, decreasing the porosity and the non-equilibrium defect structure of the wustite particles. In addition v_1 appears to increase faster with annealing temperature than v_2. The difference observed, $(v_1 - v_2)$, about 4 mV for no anneal and 6 mV after annealing at 870°C is perhaps not to be considered outside experimental error, but the trend is apparent. An interpretation of the trend is difficult as the exact cause of the minima is unknown, but as discussed in section 2.2.3 Boetticher, et al[41] have demonstrated that similar annealing treatments lengthens the observed incubation period. These authors believe this is due to the observed decrease in stored lattice energy hindering, further, iron nucleation.

When beds of ore were reduced to wustite above 670°C and then further reduced to iron at 670°C, v_2 was increased substantially (Figure 4.39). The increase was greater the higher the pre-reduction temperature. The decreased reducibility of the particles, in this case, must be attributed to the observed less porous nature of the particles formed during reduction at the higher temperature.

5.5 Reduction Morphology

5.5.1 Clean Ore

Uniform internal reduction occurred when the clean ore particles were reduced above about 640°C. Below about 620°C nucleation and growth of iron took place at or near the surface of the particles and grew towards the centre. This morphology is fairly consistent with that observed by Turkdogan and Vinters[24] for particles of similar size, except these authors indicate that with decreasing reduction temperature the greater the tendency should be towards uniform internal reduction (for constant particle size). The reason for the difference probably lies in the differing experimental conditions. The above mentioned authors used a fast flow of hydrogen over a relatively small number of hematite particles which had a initial porosity of 31%, while the porosity of the specular hematite used in this work was essentially zero. On reduction significant porosity develops as hematite reduces to magnetite (little or no more porosity forms magnetite is reduced to wustite[4]) but a large difference in porosity of the two starting materials might be expected to exist as iron starts to form in a wustite particle. A relatively porous structure is required for uniform internal reduction to allow good gas penetration.

Qualitatively the number of growing iron areas per particle observed (both as nodules on the surface and internal) increased with decreasing reduction temperature. Remembering

the total reduction rate increases only a small amount with temperature, this is consistent with the fact that more iron nuclei must form the lower the temperature to sustain the reduction as diffusion of iron ions is slower.

It has not been possible to decide from observation whether the iron that grows as nodules on the free surface differs in morphology from iron that grows internally in the particles. It seems reasonable to suppose that at least some of the internal iron nuclei grow as nodules on pore surfaces.

It was pointed out before that Wagner[34] considers the reduction of FeO analogous to the reduction of silver sulphide. In both cases nodules of metal grow. Corish et al[118] showed clearly that silver nodules grown from silver sulphide (by electrochemical reduction) are actually composed of a number of filaments which have coalesced, often leaving a cavity at the centre of the nodule. A similar phenomena may occur in the growth of iron nodules from wustite (see Figure 5.04). In general, however, the iron nodules appeared rounded and smooth but this may be due to iron diffusion smoothing the contact points of the individual whiskers. If nodular ore was held at 850°C, for example, the nodules decreased in height and after two hours were little more than bumps on the surface. (Experiments with the intention of refluidizing a bogged bed of the as-received ore after the nodules had annealed out were unsuccessful. It would appear

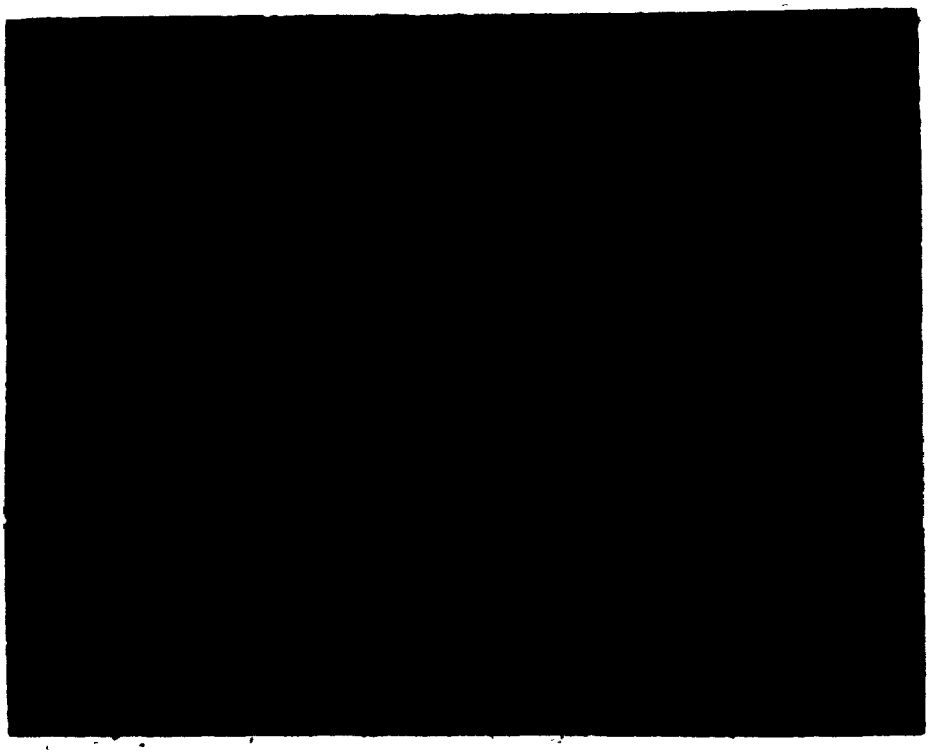

Figure 5.04 Scanning Electron Microscope Picture Suggesting Large Nodules May be Composed of Smaller Iron Nodules. x15000

that the iron-iron contact was consolidated during this time).

5.5.2 As-received Ore and Silica Coated Clean Ore

Iron avoided nucleating at the surface of the as-received ore particles below 710°C and this has been attributed to the slime film. The similar behavior of clean ore and reagent grade Fe_2O_3 silica coated particles suggests silica is the responsible constituent in the slime film. The iron tended to nucleate far from the free surface especially when the reduction temperature was high or if the ore was held at the lower reduction temperatures a few hours before reduction was commenced. Furthermore the iron showed a reluctance to grow to the free surface and an essentially iron free shell persisted around each particle until the later stages of metallization. It appears that silica or silicon is reacting with or diffusing into the iron oxides. As the shell thickness increases substantially with time if the ore is held at temperature as Fe_2O_3 but only a small amount if held as Fe_3O_4 or FeO, it appears SiO_2 or Si is active primarily with Fe_2O_3.

Silicon is essentially insoluble in Fe_2O_3, Fe_3O_4 and FeO[119-121]. However, silica forms fayalite, Fe_2SiO_4, with FeO to some extent at temperatures of 700°C and higher[122]. The occurrence of fayalite in the particles was carefully sought for without success. It was not detected metallographically or by x-ray diffraction studies at any stage of

reduction at any temperature. Furthermore the unreduced rim could not contain fayalite to any extent as the rim was observed to reduce quite quickly and fully as soon as the oxygen potential of the gas phase, as shown by the cell, began to fall away from the Fe/FeO equilibrium potential and it can be shown that fayalite is difficult or impossible to reduce under the conditions used. For example at a temperature of 700°C and using the data of Elliott et al[123] for the standard free energy of formation of fayalite

$$\Delta G^{\circ}_{700°C} = -8,980 \text{ calories/mole}$$

the equilibrium oxygen potential of the reaction

$$Fe_2SiO_4 + 2H_2 \rightleftharpoons 2Fe + SiO_2 + 2H_2O$$

is found to be 8.0×10^{-27}. The Fe/FeO equilibrium oxygen potential is 3.1×10^{-22} at 700°C while the measured oxygen potential of the hydrogen used, at the same temperature, was about 6.0×10^{-25}. Thus fayalite will not be reduced under the conditions used.

It is suggested that when iron nucleates the particles in the bed consist of wustite doped with silicon around the outside. Unfortunately there is little direct evidence that silicon did in fact dissolve in the ore particles. Electron microprobe analysis failed to resolve silicon gradients in

the particles but nor was it really expected that it would as the concentrations involved are suspected to be low (less than 1%). The best evidence for the solution of silicon into the particles is the kinetics of rim formation. A detailed discussion of rim formation is given later but in brief a reasonable value for the diffusion coefficient of Si was deduced from the size of the rim as a function of time and temperature.

The reasons for the presence of the unreduced rim, considered doped with Si, in particles partially reduced to iron may then be one of the following.

(1) The doped wustite is incapable of reducing thermodynamically until the bed adopts a lower oxygen potential throughout its bulk. The doped oxide in the near equilibrium reduction conditions of the fluidized bed is of sufficient lower reducibility to cause the observed reduction morphology. (This argument may be applied to any element not just silicon, subject only to the constraint of having a diffusion coefficient of suitable magnitude).

If the solubility of silicon in wustite is placed at 1% (probably too high) then the activity of the solvent would be expected to follow Raoults Law (i.e. activity FeO = 0.99). Calculation shows the doped wustite would then be less reducible to an extent (in zirconia cell terms) of 0.8 mV at

700°C. This value is too small to support the argument of the above paragraph as is clear from the discussion on the reduction kinetics. (At 700°C the outgoing gas was about 2 mV on the reducing side of the Fe/FeO equilibrium).

(2) Nucleation of iron is hindered in the doped wustite shell. Little comment can be offered but impurities usually aid nucleation[57].

(3) The kinetics of reduction of the doped wustite is slower.

Lien et al[54] working with SiO_2 additions to reagent grade magnetite pellets obtained lower rates of reduction compared to pure magnetite pellets and suggested that silica retards the phase boundary reaction by "poisoning the active wustite sites".

Lahiri[52] has shown that the rate of reduction may be expected to be influenced by impurities which cause a shift in the surface Fermi level of wustite. The adsorption of the reacting gas, its reaction with wustite and the desorption of product gas all involve the transfer of electrons and the rates of these reactions will be influenced by the activity of the electrons, i.e. the surface Fermi level. Lahiri's analysis shows that a slight lowering of the Fermi level will increase the reaction rates significantly if the reactions

are near equilibrium. The Fermi level may be lowered by Group I impurities (assumed to substitute for Fe^{2+}) which increase the concentration of holes in the wustite. Group I impurities, in fact, are observed to increase the reduction rate[51]. Conversely cation impurities of valency three and higher should raise the surface Fermi level and lead to a lower reduction rate. Levin and Wagner[53] found the addition of Cr_2O_3 to FeO did in fact lower the reduction rate in CO/CO_2 mixtures.

Lahiri's hypothesis is considered a possible explanation (and in addition the only one that can be forwarded) for the unreduced wustite shell observed in this work. The cation Si^{4+} increases the Fermi level and decreases the reaction rate to near zero as the reactions are near equilibrium.

5.5.3 Kinetics of Rim Formation

The data obtained (reported in section 4.4.6) concerning the measured rim thickness after a constant % metallization as a function of (a) reduction temperature and (b) after annealing for different times at 680°C before reduction suggests the possibility of evaluating a diffusion coefficient for Si in FeO. It will now be shown that the data is consistent with a diffusion mechanism. The numerical values may be expected to be inaccurate. No attempt was made to obtain the average true rim thickness which is different from the average measured thickness reported.

It was assumed that in a bed of particles (reduced to a constant degree of metallization at different temperatures) iron had grown outwards from the centre of each particle to a constant 'doped' concentration and this was taken as 50% of the maximum concentration. Using Ficks Laws of diffusion applied to a semi-infinite medium and constant diffusivity[124]

$$1 - \text{erf}\left(\frac{x}{\sqrt{D_T t}}\right) = \frac{C - C_o}{C_s - C_o}$$

where C = concentration of solute at distance x from surface

C_o = initial concentration

C_s = concentration at surface

D_T = diffusion coefficient at T°K cm^2/second

t = time in seconds

If $\frac{C - C_o}{C_s - C_o} = 0.5$ then $\frac{x}{\sqrt{D_T t}}$ approximately equals one.

Thus the rim thickness squares, i.e. x^2, plotted against annealing time should yield a straight line. From the data obtained at 680°C (Figure 5.05) only the 1 and 4 hour anneals lie on a straight line passing through the origin. Therefore D_T has been calculated using 1 hour anneals for the different temperatures. The results are tabulated in Figure 5.06 which also shows that log D_T plotted against $\frac{1}{T°K}$ yields a straight line in accordance with the equation

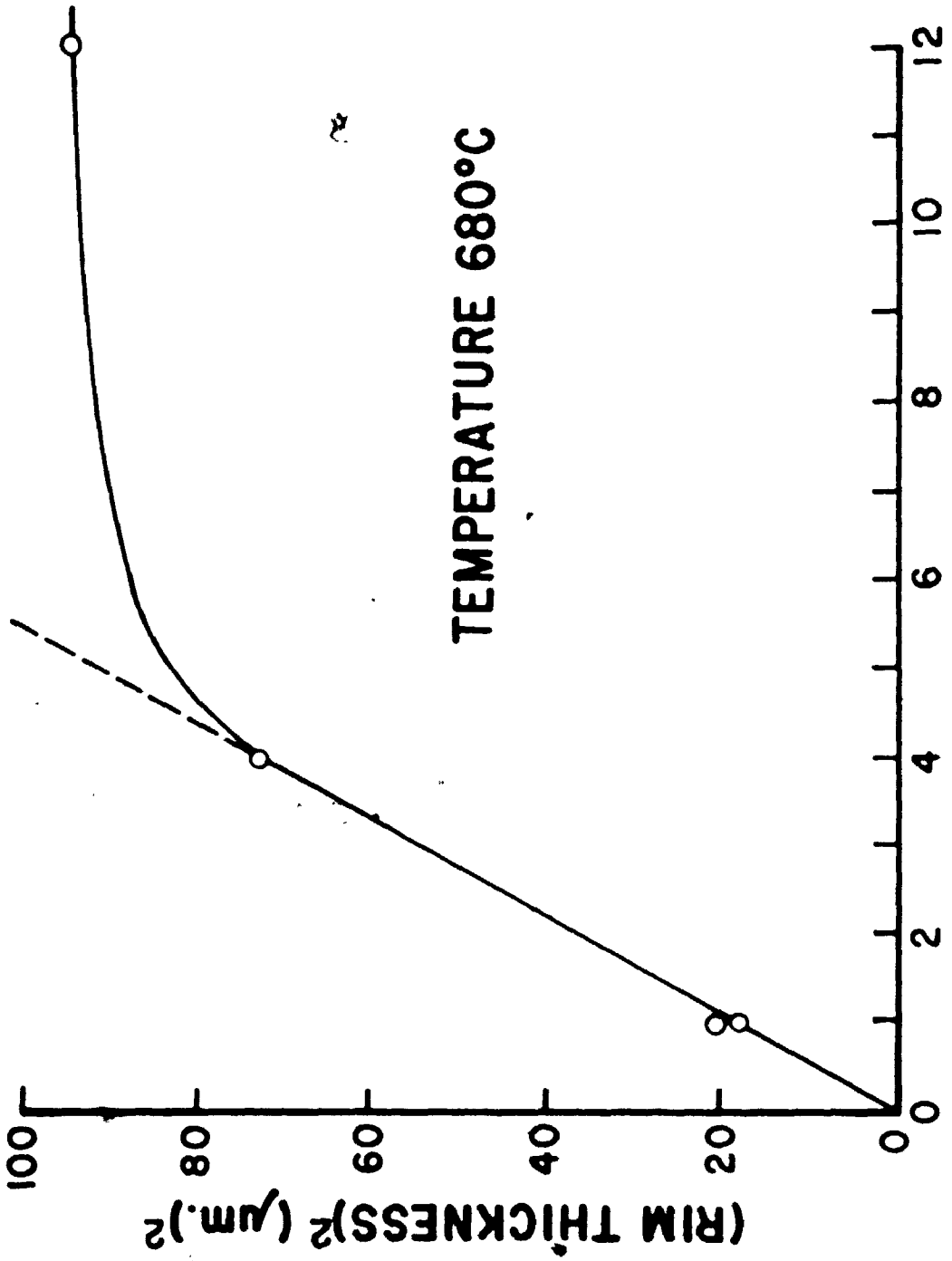

Figure 5.05 Relationship Between the (Rim Thickness)^2 and Annealing Time at 680°C

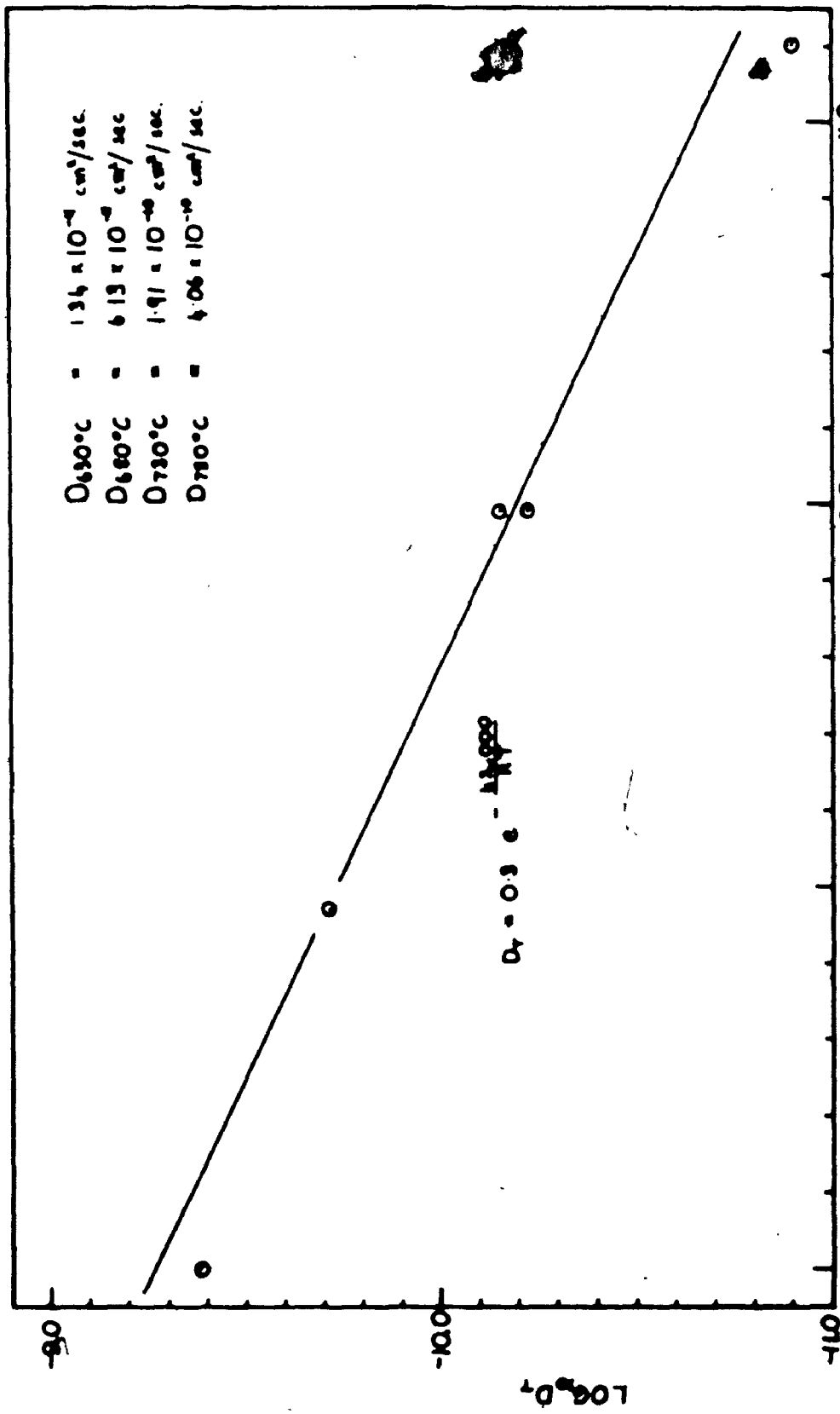

Figure 5.06 Calculated Diffusion Coefficient at 630, 680, 730 and 780°C and $\log_{10} D_T$ versus $1/T°K$

$$\log D_T = -\frac{Q}{2.3RT} + \log D_O \quad \text{(in natural logarithms}$$

$$\ln D_T = -\frac{Q}{RT} + \ln D_O)$$

where Q is the activation energy (calories/mole), R universal gas constant, D_O the frequency factor. The equation of the straight line drawn is

$$D_T = 3.0 \exp(-42{,}000/RT)$$

Experiments were conducted to determine the mode of reduction if the particles were essentially saturated with silica. It was found that annealing silica covered hematite particles at a temperature of 1000°C for 3 hours and then reducing in the temperature range 650-830°C led to uniform internal reduction including nucleation of iron as nodules. The degree of fluidization began to drop after iron nucleation during reduction at temperatures between 650 and 750°C but complete defluidization only occurred at 780°C and 830°C.

If silica is truly responsible for the observed reduction morphology of the as-received ore below 710°C (and it is believed to be), it must be concluded that either insufficient silica is present or the coverage is not good enough to avoid the growth of nodules above about 710°C.

As reported previously silica covered reagent grade particles did not develop unreduced wustite rims comparable in size to silica coated clean ore at 780°C. This is thought

due to the high porosity of the reagent grade particles which prevented, somewhat, diffusion of Si.

CHAPTER 6

CONCLUSIONS AND SUGGESTIONS FOR FURTHER WORK

6.1 Conclusions

Reduction of hematite ore in a fluidized bed proceeds by steps: cne oxide is substantially reduced to the next lower intermediate oxide before this intermediate oxide itself is further reduced.

The iron phase alone was found responsible for defluidization. Iron evidently has greater adhesion or sticking properties than the oxides of iron and defluidization was encountered at temperatures as low as 595°C. The reduction morphology is of importance. Uniform internal reduction of wustite particles occurred above 630°C. Iron nucleates and grows throughout the porous particles and at the surface of the particles in the form of iron nodules. The growth of iron nodules decreases the fluidizability of the bed and causes sticking of particles to one another and therefore defluidization near the beginning of metallization.

The prevention of defluidization by coating the particles with various inorganic chemicals is often thwarted by the growth of nodules which pierce the coating.

A slime coating on the particles of one of the ores studied changed the reduction morphology significantly in a certain temperature range. The growth of iron nodules did not occur and iron-iron contact and therefore defluidization was prevented. The active constituent in the slime film was silica. Particles artificially coated with silica could be fully reduced at 840°C without defluidization occurring. Iron nucleated and grew within the particles reaching the outside surface only near the end of reduction. Evidence that Si is mobile in the oxides of iron has been presented and reasons for the change in reduction morphology discussed.

The use of a solid state cell to monitor the gas phase in the fluid bed proved useful. An anomaly in the gas utilization curves as iron nucleates was detected and has been discussed.

6.2 Suggestions For Further Work

The importance of the reduction morphology during the reduction of wustite to iron in relation to defluidization has been shown. In addition, as discussed previously, the growth of nodules is currently believed to cause abnormal swelling of pellets of iron oxide during reduction. A complete characterization of the reduction morphology should therefore be undertaken. Such a study should include the variables time, rate of reduction, temperature and nature of the reducing gas. The effect of impurities should then be investigated.

The advantages of gangue in the form of slime coatings is apparent from this work. Industrial use of artificial coatings to avoid defluidization is really a question of economics. A coating stage in a fluid bed operation may prove similar to the bentoniting process used in pelletizing iron ore. The investigation of ore covered with various silica containing clays in pilot plant fluid bed appears worthwhile.

REFERENCES

1. Darken, L.S., and R.W. Gurry: J. Am. Chem. Soc., 68, 798, (1946).

2. Kun Li: Blast Furnace, Coke Oven, Raw Mater. Comm. Proc., 19, 153, (1960).

3. Goldschmidt, H.J.: J. Iron Steel Inst., 146, 157P, (1942).

4. Edstrom, J.O.: J. Iron Steel Inst., 175, 289, (1953).

5. Themelis, N.J., and W.H. Gauvin: Bull. Can. Inst. Mining Metallurgy, 55, 444, (1962).

6. Lu, Wei-Kao: Trans. Met. Soc. A.I.M.E., 227, 203, (1963).

7. Lu, Wei-Kao, and G. Bitsianes: Trans. Met. Soc. A.I.M.E., 236, 531, (1966).

8. Levenspiel, O.: 'Chemical Reaction Engineering', John Wiley and Sons, New York, (1962), page 338.

9. St. Clair, H.W.: Trans. Met. Soc. A.I.M.E., 233, 1145, (1965).

10. Seth, B.B.L., and H.U.Ross: Trans. Met. Soc. A.I.M.E., 233, 180, (1965).

11. Spitzer, R.H., and F.S. Manning, and W.O. Philbrook: Trans. Met. Soc. A.I.M.E., 236, 726, (1966).

12. McKewan, W.M.: Trans. Met. Soc. A.I.M.E., 212, 791, (1958).

13. McKewan, W.M.: Trans. Met. Soc. A.I.M.E., 218, 2, (1960).

14. McKewan, W.M.: Trans. Met. Soc. A.I.M.E., 221, 140, (1961).

15. McKewan, W.M.: Trans. Met. Soc. A.I.M.E., 224, 2, (1962).

16. McKewan, W.M.: Trans. Met. Soc. A.I.M.E., 224, 387, (1962).

17. McKewan, W.M.: 'Steelmaking: The Chipman Conference', J.F. Elliott, editor, page 141, The M.I.T. Press, Cambridge, Mass., (1965).

18. Themelis, N.J., and W.H. Gauvin: Trans. Met. Soc. A.I.M.E., 227, 290, (1963).

19. Quets, J.M., M.E. Wadsworth, and J.R. Lewis: Trans. Met. Soc. A.I.M.E., 218, 545, (1960).

20. Udy, M.C., and C.H. Lorig: A.I.M.E. Trans., 154, 162, (1963).

21. Bogdandy, L. von, and W. Janke: Z. Elektrochem., 61, 1146, (1957).

22. Kawasaki, E., and J. Sanscrainte, and T.J. Walsh: A.I.Ch.E. J., 8, 48, (1962).

23. Lu, Wei-Kao, and G. Bitsianes: Canadian Met. Quart., 7, 3, (1968).

24. Turkdogan, E.T., and J.V. Vinters: Met. Trans., 2, 3175, (1971).

25. Warner, N.A.: Trans. Met. Soc. A.I.M.E., 230, 163, (1964).

26. Seth, B.B.L.: Journal I.S.I., 207, 1104, (1969).

27. Gray, N.B., and J. Henderson: Trans. Met. Soc. A.I.M.E., 236, 1213, (1966).

28. Strangway, P.K., and H.U. Ross: Trans. Met. Soc. A.I.M.E., 242, 1981, (1968).

29. Lien, H.O., A.E. El-Mehairy, and H.U. Ross: Journal I.S.I., 209, 541, (1971).

30. Themelis, N.J., and W.H. Gauvin: A.I.Ch.E. Journal, 8, 437, (1962).

31. Turkdogan, E.T., and J.V. Vinters: Met. Trans., 3, 1561, (1972).

32. Bogdandy, L. von, and H.J. Engell: 'The Reduction of Iron Ores', English Edition, Springer-Verlag, Berlin, 1971, page 48.

33. Wagner, C.: J. of Metals, 4, 214, (1952).

34. Wagner, C.: 'Steelmaking: The Chipman Conference', J.F. Elliott, editor, page 19, The M.I.T. Press, Cambridge, Mass., (1965).

35. Schmalzried, H., and C. Wagner: Trans. Met. Soc. A.I.M.E., 227, 539, (1963).

36. Sasabe, M., and K. Goto, and M. Someno: Trans. Iron Steel Institute of Japan, 10, 25, (1970).

37. Volmer, M., and A. Weber: Z. Phys. Chem., 119, 277, (1926).

38. As in (32) pages 81-85.

39. As in (32) pages 165-175.

40. Morawietz, W., and H.D. Schaefer: Arch. Eisenhuttenwesen, 40, 523, (1969).

41. Botticher, H., L.V. Bogdandy, E. Forster, and U. Schierloh: Z. Phys. Chem., 53, 240, (1967).

42. Forster, E., U. Schierloh, and L. Smeets: Arch. Eisenhuttenwesen, 40, 535, (1969).

43. Quoted by H.-J. Engell in (32) page 173.

44. Tigerschiold, M.: J. Iron Steel Inst., 177, 13, (1954).

45. Edstrom, J.O.: Jernkontorets Ann., 142, 401, (1958).

46. Doi, Y., and K. Kasai: Blast Furnace, Coke Oven, Raw Mater. Comm., Proc., 18, 182, (1959).

47. Schenck, R., H. Franz, and H. Willeke: Z. Anorg. Chem., 184, 1, (1929).

48. Seth, B.B.L., and H.U. Ross: Can. Met. Quart., 2, 15, (1963).

49. Mazanek, E., and S. Jasienska: J. Iron Steel Inst., 202, 319, (1964).

50. Strangway, P.K., and H.U. Ross: Can. Met. Quart., 4, 97, (1965).

51. Khalafalla, S.E., and P.L. Weston, Jr.: Trans. Met. Soc. A.I.M.E., 239, 1494, (1967).

52. Lahiri, A.K.: Trans. Indian Inst. Metals, 22, 59, (1969).

53. Levin, R.L., and J.B. Wagner: Trans. Met. Soc. A.I.M.E., 233, 159, (1965).

54. Lien, H.O., A.E. El-Mehairy, and H.U. Ross: Paper presented at the Canadian Inst.Min. Met., Conference of Metallurgists, Windsor, Ont., (1969).

55. Strangway, P.K., H.O. Lien, and H.U. Ross: Can. Met. Quart., 8, 235, (1969).

56. Geiger, G.H., and J.B. Wagner, Jr.: Trans. Met. Soc. A.I.M.E., 233, 2092, (1965).

57. Morawietz, W., and H.D. Schaefer: Arch. Eisenhuttenwesen, 40, 531, (1969).

58. Singh, B., and G.N. Bhat: Brit. Chem. Eng., 12, 242, (1967).

59. As in (32) page 226.

60. Zenz, F.A., and D.F. Othmer: Fluidization and Fluid-Particle Systems, Reinhold Publishing Co., New York, (1960), page 3.

61. Meissner, H.P., and F.C. Schora: Trans. Met. Soc. A.I.M.E., 218, 12, (1960).

62. Renzoni, L.S.: Can. J. Chem. Eng., 47, 3, (1969).

63. Bhat, G.N., and A.B. Whitehead: Australian Inst. Min. Met. Proc., 201, 97, (1962).

64. Feinman, J.: I. & E.C. Process Design and Development Quart., 3, 241, (1964).

65. Meissner, H.P., and F.C. Schora: Trans. Met. Soc. A.I.M.E., 221, 1221, (1961).

66. Ezz, S.Y.: Trans. Met. Soc. A.I.M.E., 218, 709, (1960).

67. Ezz, S.Y., and R. Wild: J. Iron Steel Inst., 194, 211, (1960).

68. Osberg, G.L., and T.A. Tweddle: I. & E.C. Process Design and Development, 5, 87, (1966).

69. Agarwal, J.C., and W.L. Davis, Jr.: Chem. Eng. Prog. Symp. Series, No. 67, 62, 101, (1966).

70. Okura, A., and Wei-Kao Lu: Can. Met. Quart., 8, 325, (1969).

71. Feinman, J., and T.D. Drexler: A.I.Ch.E. Journal, 7, 584, (1961).

72. Langston, B.G., and F.M. Stephens: 'Iron Ore Reduction' proceedings of a symposium Electrothermics and Metallurgy Division of the Electrochemical Society, held in Chicago, May, 1960. MacMillan Co., New York. p. 207.

73. Ezz, S.Y.: Trans. Inst. Min. Metall., 79, 226, (1970).

74. Lubker, R.A., and K.W. Bruland: J. Metals, 12, 321, (1960).

75. Traub, J.W.: Iron Steel Engineer, 37, 167, (1960).

76. Stotler, H.H., and R.A. Lubker: as in (72) page 163.

77. Keith, P.C., H.H. Stotler, and R.J. McMullen: Iron Steel Engineer, 40, 95, (1963).

78. Reed, T.F., J.C. Agarwal, and E.H. Shipley: J. Metals, 12, 317, (1960).

79. Reed, T.F., J.C. Agarwal, and E.H. Shipley: as in (72) page 174.

80. Astier, J.: Skillings' Mining Review, 60, No. 11, 1, (March 11, 1972).

81. Anonymous: Skillings' Mining Review, 59, No. 45, 8, (November 6, 1971).

82. Hyde, R.W.: as in (72), page 189.

83. Brown, J.W., D.L. Campbell, A.L. Saxton, and J.W. Carr, Jr.: J. Metals, 18, 237, (1966).

84. Fine, M.M.: Skillings' Mining Review, 59, No. 9, 1, (February 27, 1971).

85. Bogdandy, L. von: as in (32), page 268.

86. Winzer, D.: as reported by L. von Bogdandy in (32), page 258.

87. Yamamichi, Y.: Tetsu to Hagané Overseas, 3, 296, (1963).

88. Jolley, G.B.: U.S. patent 3,251,677.

89. Mayer, F.X., and D.S. Roberts: U.S. patent 3,320,050.

90. Gray, C.F., and R.O. Maak: U.S. patent 3,368,884.

91. Whaley, T.H.: U.S. patent 3,295,956.

92. Bailey, G.W.: U.S. patent 3,341,322.

93. Johnson, C.A., and T.M. Engle: U.S. patent 3,227,546.

94. Schenck, H., W. Wenzel, and H.D. Butzmann: Arch. Eisenhuttenwesen, 33, 211, (1962).

95. Sterling, E.: U.S. patent 3,062,639.

96. Rapp, R.A., and D.A. Shores: 'Techniques of Metal Research', Vol. IV, part 2, R.F. Banshah editor, John Wiley and Sons, New York, (1970), page 123.

97. Grims, R.E.: 'Clay Mineralogy', 2nd Edition, McGraw-Hill, New York, (1968), page 128.

98. MacEwan, D.M.C.: 'X-ray Identification of Clay Minerals', G.W. Brindley editor, Mineralogical Society of Great Britain Monograph, (1961), pages 86-137.

99. Brindley, G.W.: as in (98), facing page 19.

100. Taggart, A.F.: Handbook of Mineral Dressing, John Wiley and Sons, New York, (1967), page 15-04.

101. Maher, P.K.: Kirk-Othmer 'Encyclopedia of Chemical Technology' John Wiley and Sons, New York, Volume 18, page 67.

102. Fuwa, T., and S. Ban-Ya: Trans. Iron Steel Inst. Japan, 9, 137, (1969).

103. Bleifuss, R.L.: Trans. Soc. Mining Engineers A.I.M.E., 247, 225, (1970).

104. MacEwan, D.M.C.: as in (98), page 307.

105. Charette, G.G., and S.N. Flengas: J. Electrochemical Soc., 115, 796, (1968).

106. Kubaschewski, O., and E. LL. Evans, and C.B. Alcock: 'Metallurgical Thermochemistry', Pergamon Press, London, (1967), page 424.

107. Grim, T.E.: 'Applied Clay Mineralogy', McGraw-Hill, New York, (1962), page 179.

108. Purlong, R.B.: 'Clays and Clay Minerals', proceedings of the 15th Conference on Clays and Clay Minerals, Pergamon Press, (1967), pages 87-101.

109. Richardson, H.M.: as in (98), page 85.

110. Bogdandy, L. von: as in (32), page 421.

111. Ende, H., K. Grebe, and S. Thomalla: Stahl und Eisen, 91, 815, (1971).

112. Ende, H., K. Grebe, S. Thomalla, and E.E. Hofmann: Stahl und Eisen, 90, 667, (1970).

113. Wenzel, W., and H.W. Gudenau: Stahl und Eisen, 90, 689, (1970), and following discussion pages 694-697.

114. Someno, M., and G. Ito: Trans. Met. Soc. A.I.M.E., 245, 1662, (1969).

115. Engell, H.-J.: as in (32), page 168.

116. Engell, H.-J.: as in (32), page 80.

117. Kohl, H.K., and J.-J. Engell: Arch. Eisenhuttenwesen, 34, 411, (1963).

118. Corish, J., and C.D. O'Brian: J. Material Sc., 6, 252, (1971).

119. Levin, E.M.: 'Phase Diagrams for Ceramists', M.K. Reser, editor, American Soc. Metals, Ohio, (1964).

120. Darken, L.S.: J. Am. Chem. Soc., 70, 2046, (1948).

121. Smeltzer, W.W., L.A. Morris, and R.C. Logani: Can. Met. Quart., 9, 513, (1970).

122. Baldwin, B.G.: Jorn. Iron Steel Inst., 177, 312, (1954).

123. Elliott, J.F., M. Gleiser, and V. Ramakrishna: 'Thermochemistry for Steelmaking', Vol. 2, Reading (Mass.)/ London, (1963).

124. Darken, L.S., and R.W. Gurry: 'Physical Chemistry of Metals', McGraw-Hill, New York, (1953).

125. Spitzer, R.H., F.S. Manning and W.O. Philbrook: Trans. Met. Soc. A.I.M.E., 236, 1715, (1966).